Singlet Fission

Millicent B. Smith[†] and Josef Michl[*,†,‡]

Department of Chemistry and Biochemistry, University of Colorado, 215 UCB, Boulder, Colorado 80309-0215, United States, and Institute of Organic Chemistry and Biochemistry, Academy of Sciences of the Czech Republic, Flemingovo námçstí 2, 166 10 Prague 6, Czech Republic

Received August 13, 2010

Contents

1. Introduction

In the following we provide a comprehensive review of singlet fission in organic materials. We first sketch an outline of the underlying theory and then turn to molecular crystals, aggregates, neat and dispersed conjugated polymers, and dimers (isolated molecules containing two covalently coupled chromophores). Because the review forms a part of a thematic issue dedicated to solar energy conversion, our focus throughout is on a specific ultimate goal, namely, the design of a system that could be useful in an actual solar cell.

Singlet fission is a process in which an organic chromophore in an excited singlet state shares its excitation energy with a neighboring ground-state chromophore and both are converted into triplet excited states (Figure 1).[1,2] The two chromophores can be of the same kind ("homofission") or of different kinds ("heterofission"). In principle, the sharing of excitation energy could be more extensive, resulting in the formation of more than two triplet states, but this has never been observed as far as we know.

Josef Michl was born in 1939 in Prague, Czechoslovakia. He received his M.S. in Chemistry in 1961 with V. Horák and P. Zuman at Charles University, Prague, and his Ph.D. in 1965 with R. Zahradník at the Czechoslovak Academy of Sciences, also in Prague. He left Czechoslovakia in 1968. He did postdoctoral work with R. S. Becker at the University of Houston, with M. J. S. Dewar at the University of Texas at Austin, with J. Linderberg at Aarhus University, Denmark, and with F. E. Harris at the University of Utah, where he stayed and became a full professor in 1975 and served as chairman in 1979−1984. In 1986−1990 he held the M. K. Collie-Welch Regents Chair in Chemistry at the University of Texas at Austin, and subsequently moved to the University of Colorado at Boulder. He now shares his time equally between his research groups at Boulder and in Prague, Czech Republic, where he works at the Academy of Sciences. He is a Fellow of the American Chemical Society and a member of the U.S. National Academy of Sciences, the American Academy of Arts and Sciences, the Czech Learned Society, and the International Academy of Quantum Molecular Science. Dr. Michl's current research interests are the photophysics of solar cells; organic photochemistry; nanoscience, especially new ways of attaching molecules to metal surfaces and preparing artificial surface-mounted molecular rotors; chemistry of lithium, boron, silicon, and fluorine; and use of quantum chemical and experimental methods for better understanding of molecular electronic structure. He has been the Editor of *Chemical Reviews* since 1984.

* To whom correspondence should be addressed.
[†] University of Colorado.
[‡] Academy of Sciences of the Czech Republic.

10.1021/cr1002613
Published on Web 11/01/2010

Millicent Smith received her B.A. in chemistry in 2002 from Tufts University. In 2007 she earned her Ph.D. in physical chemistry from Columbia University under the supervision of Professor Louis Brus. Her graduate work included the synthesis and characterization of nanocrystalline barium titanate. She is currently a postdoctoral fellow in the group of Professor Josef Michl at the University of Colorado at Boulder. Her current research focuses on the photophysics of singlet fission chromophores.

A somewhat similar process, involving the successive emission of two longer-wavelength photons after excitation by absorption of a single higher-energy photon, is known for inorganic chromophores, especially rare earth ions, under the name quantum cutting.[3−5]

The multiple exciton generation process known in quantum dots of inorganic semiconductors and reviewed elsewhere in this thematic issue[6] may also have a related physical origin even though it occurs within a single but much larger "chromophore" in which singlet and triplet excitations have nearly identical energies and are not readily differentiated. This is particularly true in the presence of heavy elements and strong spin−orbit coupling, where the spin quantum number is not even approximately meaningful. In spite of the obvious differences between singlet fission in organic materials and multiple exciton generation in quantum dots, certain features of the theoretical treatment of the former given in section 2 are related to one of the theories proposed for the latter.[7] Unlike singlet fission, multiple exciton generation in quantum dots inevitably faces stiff competition with conversion of electronic energy into vibrational energy followed by vibrational cooling.

We review only the literature dealing with organic chromophores (singlet fission), from the time of the initial discovery of the phenomenon to the present day. An extensive review of the subject appeared in 1973,[1] and the most recent update we are aware of is found in a 1999 book chapter.[2]

1.1. Singlet Fission

Singlet fission is spin-allowed in the sense that the two resulting triplet excitations produced from an excited singlet

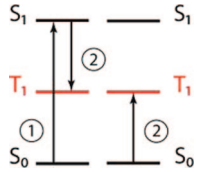

Figure 1. Singlet fission: (1) The chromophore on the left undergoes an initial excitation to S_1. (2) The excited chromophore shares its energy with the chromophore on the right, creating a T_1 state on each.

are born coupled into a pure singlet state. Singlet fission can therefore be viewed as a special case of internal conversion (radiationless transition between two electronic states of equal multiplicity). Like many other internal conversion processes, it can be very fast, particularly in molecular crystals. There, when it is isoergic or slightly exoergic and the coupling is favorable, the transformation occurs on a ps or even sub-ps time scale, competing with vibrational relaxation and easily outcompeting prompt fluorescence. Only excimer formation and separation into positive and negative charge carriers appear to have the potential to be even faster under favorable circumstances.

In the absence of any interaction between the two triplets, the singlet ^{1}(TT), triplet ^{3}(TT), and quintet ^{5}(TT) states that result from the nine substates originating in the three sublevels of each triplet would have the same energy. In reality, there will be some interaction and the ^{1}(TT), ^{3}(TT), and ^{5}(TT) states will not be exactly degenerate. As long as they are at least approximately degenerate, they will be mixed significantly by small spin-dependent terms in the Hamiltonian, familiar from electron paramagnetic resonance spectroscopy (EPR). In organic molecules that do not contain heavy atoms, these terms are primarily the spin dipole−dipole interaction, responsible for the EPR zero-field splitting, and the Zeeman interaction if an outside magnetic field is present. Hyperfine interaction with nuclear magnetic moments, responsible for the fine structure in EPR spectra, is also present but is weaker. In molecular crystals, where triplet excitons are mobile, its effect averages to zero if exciton hopping is fast on the EPR time scale. Spin−orbit coupling is present as well, but in molecules without heavy atoms it is weak and is normally negligible relative to the spin dipole−dipole and Zeeman interactions.

The nine eigenstates of the spin Hamiltonian are not of pure spin multiplicity. The wave function of the initially formed pure singlet state ^{1}(TT) is a coherent superposition of the wave functions of these nine sublevels, and their ultimate population will reflect the amplitude of the singlet ^{1}(TT) wave function in each one. As long as the states resulting from singlet fission are of mixed multiplicity, the overall process can also be viewed as a special case of intersystem crossing (radiationless transition between two electronic states of different multiplicities).

There is an interesting difference between intersystem crossing induced by singlet fission, primarily as a result of the existence of spin dipole−dipole interaction, and the much more common intersystem crossing induced by spin−orbit coupling. Unlike the spin−orbit coupling operator, which connects singlets only with triplets, the spin dipole−dipole interaction is a tensor operator of rank two, and it has nonvanishing matrix elements between singlets and triplets, as well as between singlets and quintets. Therefore, singlet fission has the potential for converting singlets into both triplets and quintets efficiently, thus expanding the Jablonski diagram as shown in red in Figure 2. Excited quintet states of organic chromophores with a closed-shell ground state have never been observed to our knowledge. In the singlet fission literature they are usually dismissed as too high in energy, but this need not be always justified.

Why is it, then, that singlet fission has remained relatively obscure, and all textbooks and monographs dealing with organic molecular photophysics show a version of the

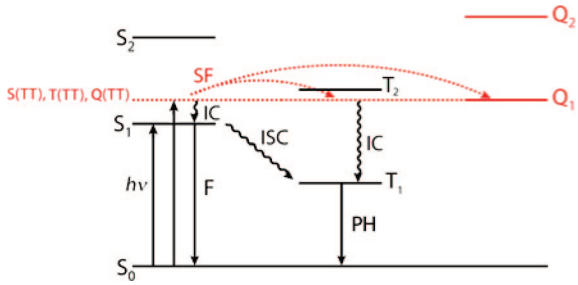

Figure 2. Expanded Jablonski diagram with the singlet fission (SF) process shown in red. F, fluorescence; IC, internal conversion; ISC, intersystem crossing; PH, phosphorescence.

Jablonski diagram shown in black in Figure 2, in which singlet fission is absent? In our opinion, the answer has four parts:

(i) Singlet fission does not occur in single small-molecule chromophores, at least not at the usual excitation energies, and is constrained to multichromophoric systems, because there have to be at least two excitation sites to accommodate the two triplet excitations (although "a pair of very strongly singlet-coupled triplets" is one of the ways to represent certain states of a single conjugated chromophore, such as the $2A_g$ state of 1,3-butadiene, a radiationless transition to such a state is not normally viewed as singlet fission but as ordinary internal conversion; the distinction becomes blurred in very long polyenes, cf. section 2.2.2). The two chromophores can be in the same molecule, but they do not need to be. All initial observations were performed on molecular crystals, in which the two triplet excitations reside on different molecules.

In principle, singlet fission in single-chromophore molecules could be observed in solutions of chromophores whose fluorescence lifetime is long enough and ground state concentration high enough for diffusive $S_1 + S_0$ encounters to be frequent, but we are not aware of studies of this kind. There is a single report[8] that provides some indirect evidence that singlet fission might take place via an intermediate $S_1 + S_0$ interaction when tetracene radical cations and radical anions annihilate during a solution electrochemiluminescence experiment.

(ii) Favorable energetics are encountered very infrequently. In most organic molecules, twice the triplet excitation energy $2E(T_1)$ exceeds the lowest singlet excitation energy $E(S_1)$ significantly, and singlet fission from a relaxed S_1 state does not take place without considerable thermal activation. It can occur rapidly only from a higher singlet S_n or a vibrationally excited S_1, but then it must compete with internal conversion and vibrational equilibration, both of which are fast. It is a tribute to the speed with which singlet fission can occur that it has been observed even under these circumstances, albeit in a low yield.

(iii) The interaction between the chromophores apparently needs to satisfy a demanding and not widely known set of conditions before singlet fission will take place rapidly. For instance, as we shall see below, it occurs rapidly in a tetracene crystal but very slowly in covalent linearly linked tetracene dimers. When the coupling is too strong, the system (e.g., 1,3-butadiene, viewed as a combination of two ethylene chromophores) effectively becomes a single chromophore, the energy splitting between the ^{1}(TT), ^{3}(TT), and ^{5}(TT) levels is large, and it is not useful to think of the two triplet excitations as more or less independent. Although the resulting singlet electronic state may have considerable "doubly excited character", and conceivably might show some propensity toward a simultaneous double electron injection, it is more likely to behave as any other singlet excited electronic state. Then, singlet fission (in this example, $1B_u$ to $2A_g$ transformation via a conical intersection) becomes just another example of ordinary internal conversion.[9−11]

(iv) It need not be easy to detect singlet fission even when it does take place. Unless the yield of the triplets exceeds 100%, it is natural to assume first that they were formed by ordinary spin−orbit induced intersystem crossing. If the triplets diffuse apart rapidly, as they can in molecular solids and conjugated polymers, they may be observed. If not, they may destroy each other by triplet−triplet annihilation, usually forming an excited singlet or a higher excited triplet, but annihilation could also result in the ground state singlet, the lowest triplet, or even an excited quintet.

1.2. A Brief History

Singlet fission was first invoked in 1965[12] to explain the photophysics of anthracene crystals. It was then used in 1968[13] to account for the strikingly low quantum yield of fluorescence of tetracene crystals, and the proposal was proven correct in 1969[14,15] by studies of magnetic field effects. Increasingly sophisticated theories[16−18] emphasized the close relation of singlet fission to the inverse phenomenon, triplet−triplet annihilation, and ultimately accounted for magnetic field effects on both of these phenomena quantitatively. This and related work on molecular crystals was summarized in 1971[19] and 1975.[20] A definitive review was published in 1973[1] and updated in 1999.[2] In the mid-1970s, the chapter was more or less closed, although occasional publications on the subject continued to appear in subsequent years. A certain revival of interest and a burst of publications were prompted by discoveries of singlet fission in new types of substrates. In 1980[21] it was observed for a carotenoid contained in a bacterial antenna complex (carotenoids can be viewed as oligomeric analogues of polyacetylene), and in 1989[22] it was observed in a conjugated polymer. Still, the phenomenon has remained relatively obscure even within the organic photophysical and photochemical community.

1.3. Relation to Photovoltaics

The current wave of interest that prompted a request for the present review can be dated back to 2004,[23,24] when it was suggested that the little known phenomenon of exciton multiplication by singlet fission could actually find a practical use in improving the efficiency of photovoltaic cells. A parallel and presently significantly larger effort attempts to exploit multiple exciton generation in quantum dots of inorganic semiconductors.[6] The organic and the inorganic materials offer different advantages. For instance, the former contain no poisonous elements, whereas the latter promise better long-term stability.

The case for using singlet fission in a solar cell is based on a quantitative analysis[25] that showed that the Shockley-Queisser limit[26] of about 1/3 for the efficiency of an ideal single-stage photovoltaic cell would increase to nearly 1/2 in a cell whose sensitizer is capable of quantitative singlet fission, provided that the two triplets resulting from the absorption of a single photon of sufficient energy are sufficiently independent of each other to produce charge

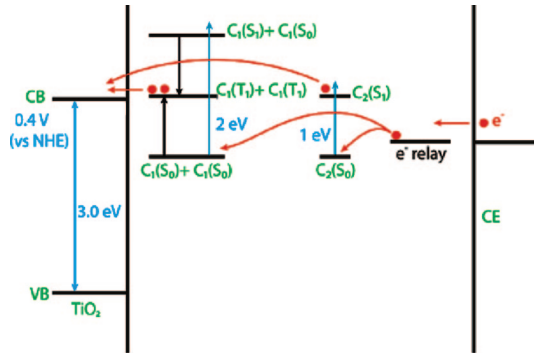

Figure 3. Dye-sensitized solar cell that uses a singlet fission sensitizer (C_1) in conjunction with a conventional sensitizer (C_2). The C_1 sensitizer comprises the top layer of the cell and absorbs light above 2 eV. The C_2 sensitizer absorbs the remaining light between 1 and 2 eV. CB, conduction band; VB, valence band; CE, counterelectrode; NHE, normal hydrogen electrode.

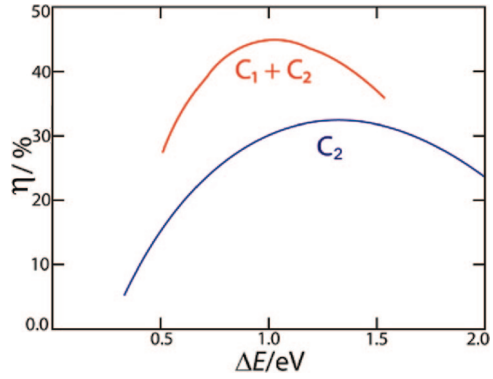

Figure 4. Schematic sketch of theoretical efficiency as a function of the S_0-T_1 band gap for a singlet fission solar cell defined in Figure 3 (red) and a conventional dye-sensitized solar cell (blue).

carriers separately and quantitatively (Figure 3). The ideal efficiency of such a singlet fission cell is shown schematically as a function of the S_0-T_1 band gap in Figure 4, assuming a 200% yield of charge carrier pairs per photon. The optimal location of the S_0-S_1 absorption edge is ~2 eV, with the triplet energy at ~1 eV, but minor deviations from these values would have little effect. In the derivation of the optimum efficiency value close to 1/2, it was assumed that the layer doped with singlet-fission capable sensitizer absorbing at 2 eV and above would be immediately followed by a layer of an ordinary sensitizer capable of absorbing photons of energies between 1 and 2 eV and generating a single electron and hole per photon. It is then arguable whether the assembly can still be called a single junction cell, but because no current matching is necessary, even if it is viewed as a double junction cell, it would be one of a particularly simple kind.

There would be an intrinsic advantage to the use of triplets for electron or hole injection, since back electron transfer to yield the ground state would be spin-forbidden. The longer lifetime of the triplet would provide more opportunity for charge separation but also more opportunity for quenching, for example, by charge carriers.

A sensitizer capable of singlet fission needs to contain more than one excitation site. While the use of covalent dimers or oligomers in dye sensitized solar cells is similar to the already well established use of individual molecular dyes,[27−29] the injection of charges from molecular crystals, aggregates, or polymers is likely to present challenges. This is at least partially due to the fact that single molecules can be more easily specifically and covalently bound to oxide surfaces, securing efficient electron transfer and charge collection. The difficulty with crystals is that they would need to be extremely small in order to be useful as semiconductor sensitizers. Nanocrystalline semiconductor films used in photovoltaic cells, such as TiO_2, typically have a porosity of ~50% and a grain size in the range of 10−80 nm,[29] and charge transfer to the macroscopic electrode occurs by grain-to-grain hopping. For efficient charge injection into the semiconductor and its further transfer to electrode, the sensitizer nanocrystals probably should be significantly smaller than the semiconductor grains on which they are adsorbed. In this respect, work with flat or bulk heterojunctions may be easier.

At present, the proposed use of singlet fission is at the stage of fundamental research. Even if one disregards entirely all possible practical problems that have not been addressed, such as cost and long-term stability in sunlight, basic molecular engineering problems remain. These challenges include matching energy levels appropriately for fast yet low-potential-loss charge separation and transfer, and preventing premature charge injection from the short-lived originally excited singlet state while assuring efficient charge injection from the long-lived triplet excited state.

At an even more fundamental level, it appears sensible to divide the problem of finding a useful singlet fission system into three parts. (i) Which chromophore should be used to maximize the rate of singlet fission while minimizing the rate of the reverse process and also meeting other conditions such as a high absorption coefficient at all energies above the onset of absorption, which needs to be located near 2 eV? (ii) How should neighboring chromophores be coupled into pairs or higher aggregates? Relatively strong coupling is needed if singlet fission is to be very fast. (iii) How should we ensure independent behavior of the two resulting triplets that would permit them to undergo two independent charge separation steps, avoiding the danger that the hole (or electron) left behind after the first injection step will quench the remaining triplet before the second injection can take place? The quenching of triplets by spin 1/2 particles is well known and tends to be fast. Relatively weak coupling is obviously needed.

Assuring a coupling that is simultaneously strong to ensure fast singlet fission and weak to allow the triplets to move apart or act as if they were far apart sounds like magic. However, although it has not been demonstrated, it appears that in this case there is a chance that one may actually be able to have one's cake and eat it, too (section 2.3).

Work on the problem has barely begun. Of the three fundamental tasks, the first has received attention in the literature.[30,31] As a result, some theoretical guidance toward chromophore structures likely to be efficient in singlet fission is available (section 2.2.1). Although it has already been put to use,[32] as will be seen below, very few organic materials have been examined so far. Little has been published[33] on the second task, optimization of chromophore coupling for fast singlet fission (section 2.2.2). At the moment, neat (pure) solid materials and aggregates are the only ones for which highly efficient singlet fission with triplet yields up to 200% has been demonstrated, and they need

Chart 1. Structures Considered in This Review

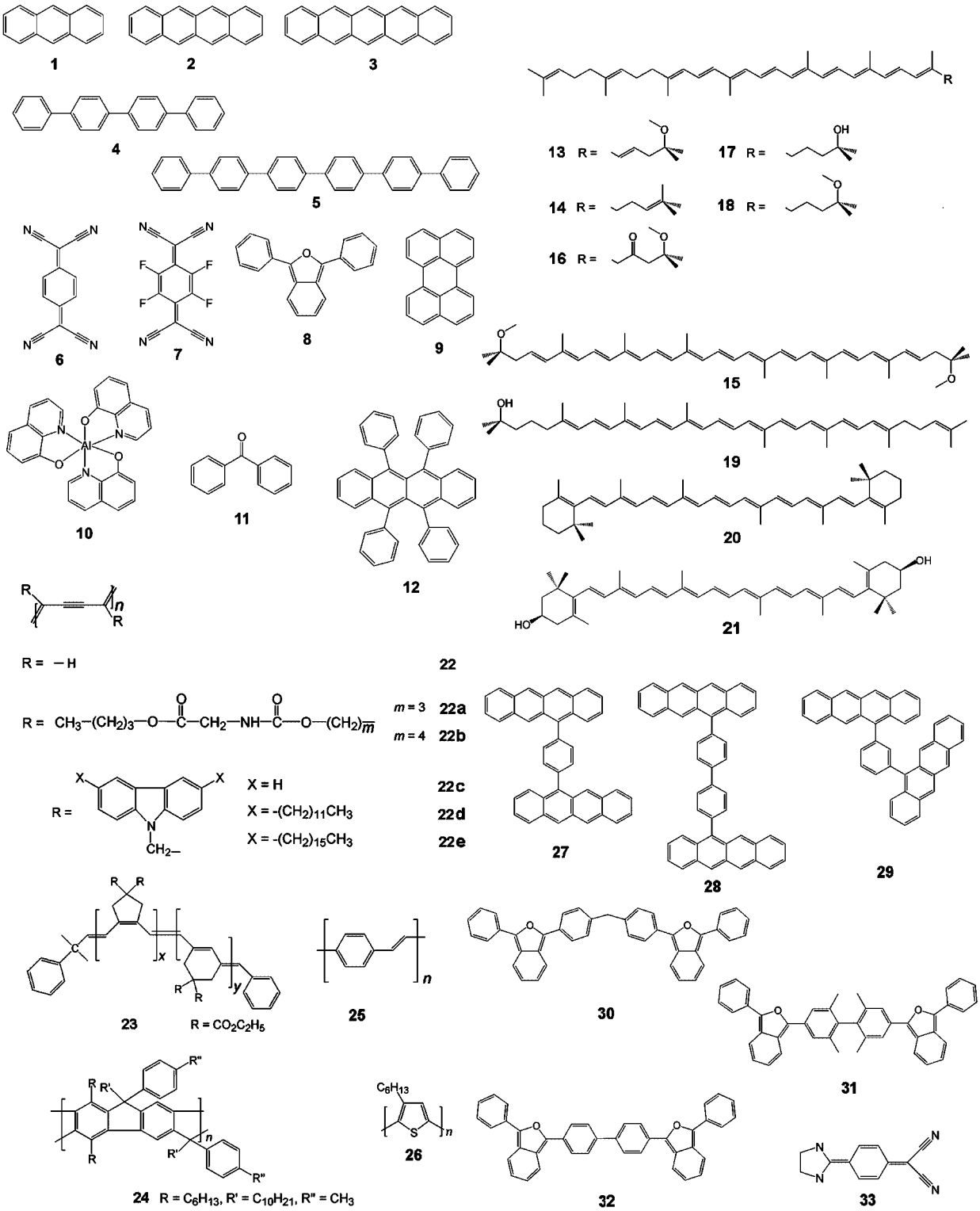

not be ideal in certain kinds of applications, e.g., as sensitizers. It is not known with certainty why molecules of the covalent dimer type that have been tried so far are either inefficient or total failures, and a rationalization is proposed in section 2.2.2. We are not aware of published theoretical work dedicated to the third subject, chromophore coupling optimized for efficient triplet separation, but a phenomenological rate constant for this process has been determined experimentally for several crystals (section 3). When it comes to practical molecular design of interchromophore coupling, the second and the third task are clearly inseparable.

Much more theoretical and experimental work is needed, and it is hoped that it will be stimulated by the present review. The chances for a practically useful singlet fission solar cell may be small, but the payoff would be substantial.

1.4. Molecular Structures

The molecular structures **1**−**33** considered in this review have been collected in Chart 1.

2. Theory

2.1. Basics

In the simplest approximation, the steady-state kinetics of singlet fission and of the reverse process of triplet fusion (annihilation) are described by two rate constants, traditionally called γ' and γ_S, respectively.

$$S_0 + S_1 \underset{\gamma_S}{\overset{\gamma'}{\rightleftharpoons}} T_1 + T_1 \quad (1)$$

The rate constants γ' and γ_S nominally describe an equilibrium dictated by the free energies of the initial state $S_0 + S_1$ and the final state $T_1 + T_1$ and are related through the equilibrium constant defined by these energies, taking into account that the latter is favored by a statistical factor of 9.[34]

A more detailed but still oversimplified kinetic scheme for the conversion of an excited singlet state of a chromophore into two triplet states located on adjacent chromophores and their possible subsequent dissociation in a molecular crystal contains four rate constants. It is traditionally written as[16−18]

$$S_0 + S_1 \underset{k_2}{\overset{k_{-2}}{\rightleftharpoons}} {}^1(TT) \underset{k_1}{\overset{k_{-1}}{\rightleftharpoons}} T_1 + T_1 \quad (2)$$

where the "correlated triplet pair" ^{1}(TT) is defined somewhat vaguely as a combination of two triplet states on adjacent molecules whose spin functions are coupled into a pure singlet. More correctly, the wave function of this singlet state is thought of as a coherent superposition of the wave functions of the nine sublevels that result from the combination of two triplets and that are not pure spin states. It represents the hypothetical final outcome of the first of the two steps into which the singlet fission process is artificially divided for convenience, and in which only the electrostatic Hamiltonian $\mathscr{H}_{el}$ is allowed to act. Simultaneously, it represents the starting point for the second step, in which the spin Hamiltonian $\mathscr{H}_{spin}$, exciton diffusion, and decoherence mechanisms are allowed to act. The interconversion of ^{1}(TT) with the initial state $S_0 + S_1$ is described by the rate constants k_{-2} and k_2, and its interconversion (diffusive in a crystal) with the final state $T_1 + T_1$ is described by the rate constants k_{-1} and k_1. It is common to refer to the ratio $\varepsilon = k_2/k_{-1}$ as the branching ratio, since it reflects the probability that ^{1}(TT) returns to S_1 instead of proceeding to $T_1 + T_1$. The qualitative description given here is a considerable oversimplification, because at short times the nine levels of the final state are coherent and their time development needs to be described by density matrix formalism (the Johnson−Merrifield model).[17] In time they lose coherence and become kinetically independent, but their behavior cannot be described with four rate constants.

The Hamiltonian describing a pair of chromophores contains a part that describes each individual chromophore in isolation and a part describing their interaction. When using eq 2, we start with eigenstates of the isolated chromophores as the initial diabatic excited singlet state (one chromophore singlet typically in its excited state S_1 and the other in its ground state S_0) and allow the interaction Hamiltonian to induce the generation of a final diabatic doubly excited state consisting of two triplets, typically $T_1 + T_1$, which are again eigenstates of the isolated chromophores. Traditionally, the interaction Hamiltonian has been divided into its electrostatic part $\mathscr{H}_{el}$ and a Breit−Pauli spin-dependent part $\mathscr{H}_{spin}$, and these have been treated independently, $\mathscr{H} = \mathscr{H}_{el} + \mathscr{H}_{spin}$.

In the Born−Oppenheimer approximation, the electrostatic Hamiltonian $\mathscr{H}_{el}$ contains the kinetic energy and nuclear attraction of electrons, their mutual repulsion, and the constant term of nuclear repulsion. It does not mix states of different overall multiplicity and could be said to deal with the internal conversion aspect of singlet fission. This is the conversion of $S_0 + S_1$ into ^{1}(TT), described by the rate constants k_{-2} and k_2 of the kinetic model defined in eq 2. It is the primary factor affecting the rate at which singlet fission takes place as a function of molecular structure. This part of the theory of singlet fission is treated in section 2.2.

The spin Hamiltonian $\mathscr{H}_{spin}$ contains the operators of Zeeman interaction with an outside magnetic field, the spin dipole−dipole interaction, nuclear spin (hyperfine) interaction, and spin−orbit coupling. It has the ability to mix states of different multiplicity and could be said to deal with the intersystem crossing aspect of singlet fission, the conversion of ^{1}(TT) to T + T. It defines the initial conditions for the solution of equations for the diffusion of excitons in crystals that ultimately yield the rate constants k_{-1} and k_1 of the simple kinetic model described in eq 2. It involves only minute energy differences but determines the spin part of the triplet pair wave function and thus the further fate of the ^{1}(TT) state in a way that is sensitive to the strength and direction of an outside magnetic field through the Zeeman term. This dependence is the hallmark of singlet fission in molecular crystals and was the focus of much of the early work.[16−18] We summarize this theoretical treatment in section 2.3. We emphasize again that the separation of the singlet fission process into two independent steps, although convenient, is artificial and approximate.

A fundamentally more satisfactory analysis (the Suna model[18]) recognized that in a crystal k_2 and k_{-1} do not have a separate physical significance and only their ratio ε does. It avoided the use of the hypothetical state ^{1}(TT) and included a proper description of exciton diffusion in a crystal. It fitted magnetic field effects better[35] and was subsequently further refined.[36−38] This theory is unfortunately rather complicated, and as a result the simplified qualitative model described by eq 2 is still in predominant use for qualitative and semiquantitative discussions. A similarly refined treatment addressed specifically to small aggregates, polymers, oligomers, or dimers does not appear to have been published, although some initial steps have been taken for the case of dimers.[33] The discussions of these systems are thus ordinarily cast in terms of eq 2, with ad hoc assumptions related to the limited ability of the two T_1 triplet excitations to separate. This part of the theory of singlet fission is in a particularly unsatisfactory state. We will rely on the model implied by eq 2 for the organization of our summary of the state of the field.

Little is known about the detailed course of the transformations represented in eq 2 for any specific case, especially the nuclear motions involved. There are some experimental indications from work on crystalline **2** that certain unidentified vibrational motions are favorable for singlet fission[39] (see section 3.1.2). The internal conversion of $S_0 + S_1$ to ^{1}(TT) and back involves a transition between two diabatic potential energy surfaces, which could occur via a conical intersection of adiabatic surfaces, or on a single adiabatic surface if the crossing is avoided. Figure 5 shows the

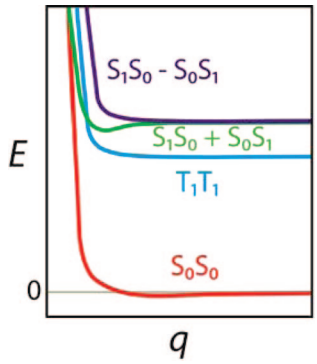

Figure 5. Schematic correlation diagram for exothermic singlet fission in a chromophore pair (see text).

correlation diagram connecting the optimal geometry of the initial and final states in exothermic singlet fission in a very schematic fashion, and the nature of the reaction coordinate q remains unknown. The number of excited singlet states that need to be considered would increase if the S_1 state is not well isolated in energy from other excited singlets. Qualitatively, one would expect favorable nuclear motions involved in the $S_0 + S_1$ to ^{1}(TT) process to occur along paths combining the conversion of S_0 and S_1 geometries to that of T_1, plus some relative motion of the two partners toward an arrangement that combines a maximization of the square of the electronic matrix element for the process with a minimization of total energy. The results of a recent pioneering explicit computation for a pair of molecules of **3** at a level that permits a description of the ^{1}(TT) state represent a promising start but are unfortunately flawed by an incorrect order of states that was produced by the method of calculation used (section 3.1.3).[40] The size of the problem imposed limitations in the scope of the calculations in that only the lowest two of the five nearly degenerate excited surfaces were treated and only one arbitrarily chosen path in the nuclear configuration space was probed. Much additional effort will be needed before general conclusions emerge.

2.2. Structural Effects

It is common to treat the rate constant k_{-2} in terms of the Arrhenius equation

$$k_{-2} = A[S_1S_0 \rightarrow {}^1(TT)] \exp(-\Delta E/k_BT) \qquad (3)$$

where k_B is the Boltzmann constant and T is the absolute temperature. The frequency factor $A[S_1S_0 \rightarrow {}^1(TT)]$, which reflects the intrinsic rate of the transformation of S_1 of one chromophore and S_0 of a neighboring chromophore into ^{1}(TT), and the activation energy ΔE, are determined from the temperature dependence of k_{-2}. The activation energy is at least equal to and could be higher than the endoergicity of the $S_1S_0 \rightarrow {}^1(TT)$ process, and can also be zero if the process is exoergic. Little or no theoretical work has been done so far on establishing whether ΔE actually exceeds the endoergicity, and it is normally assumed that they are equal. This need not be correct if some intramolecular or intermolecular distortion is needed to reach a structure for which the electronic matrix elements for singlet fission are particularly favorable.

The lifetime of the S_1 state is typically quite short, and even if no other processes intervene, fluorescence will limit it to a range between a few and a few dozen ns. Thermally activated singlet fission is therefore only significant if its endothermicity is very small, ordinarily less than ~0.2 eV.

A more general formulation that addresses the rate constant k_{-2} even when singlet fission is exothermic has been deduced from radiationless transition theory in the strong coupling limit.[41] This yielded an energy gap law expression for the rate constant k_{-2} for the production of the ^{1}(TT) state from the S_1S_0 state in a molecular crystal:[42]

$$k_{-2} = 6\pi^{1/2}|V|^2/[\hbar(2\hbar<\omega>E')^{1/2}] \exp[-(\Delta E - E')^2/4\hbar<\omega>E'] \qquad (4)$$

where V is the average electron exchange interaction matrix element among the S_0, S_1, and T_1 states of nearest-neighbor pairs of molecules in the crystal, $<\omega>$ is the average frequency of molecular vibrations, E' is the average of molecular nuclear deformation energies between S_1 and T_1 and between T_1 and S_0, and ΔE is the absolute value of the energy difference between the S_1 and ^{1}(TT) states. As stated by the author of this treatment, it suffers from definite uncertainties, such as the use of the strong coupling limit in a situation to which it may not be applicable.[41]

Singlet fission is also possible outside of vibrational thermal equilibrium, when higher vibrational levels of S_1, or higher electronic states than S_1, are temporarily populated by processes such as light absorption, charge recombination, or singlet−singlet annihilation. Such "hot" singlet fission needs to compete with internal conversion and with return to vibrational equilibrium, which normally occur at the ps time scale, and will therefore rarely be very efficient. We shall see below that there is evidence that such optically induced singlet fission can be very fast and even somewhat competitive with intramolecular vibrational energy redistribution.

To evaluate the endoergicity or exoergicity of singlet fission, the energy of the ^{1}(TT) state is ordinarily approximated by twice the energy of the T_1 state of the isolated chromophore, $2E(T_1)$, and compared with the energy of the S_1 state, $E(S_1)$. This approximation is good in molecular crystals, where the interchromophore interaction is weak, and need not be as good in covalent dimers. In section 2.2.1 we shall therefore consider the relation of the difference between $E(S_1)$ and $2E(T_1)$ to molecular structure. The factors that determine the frequency factor $A[S_1S_0 \rightarrow {}^1(TT)]$ will be taken up in section 2.2.2.

2.2.1. Energy Level Matching

If one's goal is to design a system in which the yield of independent triplets from singlet fission is maximized, as is the case in photovoltaic applications, it is clearly important to choose structures in which the $S_1S_0 \rightarrow {}^1(TT)$ process is exoergic, isoergic, or at least not significantly endoergic, and in which no processes, including the inevitably present fluorescence, compete with it significantly. As a minimum requirement for a good candidate, fission should be faster than competing intramolecular relaxation processes such as intersystem crossing and internal conversion. A chromophore with a quantum yield of fluorescence in solution that is close to unity represents a good starting point, as this indicates that all other available relaxation processes proceed much more slowly. Even in this intramolecularly most favorable case, in a dimer, aggregate, or crystal, intermolecular processes such as excimer formation or exciton dissociation into polarons may be fast enough to compete with singlet fission.

Energy level matching therefore needs to be considered in some detail. In most organic chromophores, $2E(T_1) - E(S_1)$ is strongly positive, and at room temperature, it is well above k_BT. What structural features will bring this difference to zero or make it slightly negative?

Although this may be the principal question when searching for systems whose energy level diagrams are favorable for singlet fission, it is not the only one. Once the triplets are formed, they could re-fuse and annihilate each other. If $\mathcal{H}_{spin}$ is ignored for the moment, the result of such an annihilation could be a singlet (S), a triplet (T), or a quintet (Q) state. The encounter of two T_1 states will not lead to rapid formation of the $S_1 + S_0$ states if this process is endoergic, and the formation of two S_0 states will also be slow because it will be strongly exoergic and in the inverted Marcus region. The formation of $Q_1 + S_0$ states is usually considered too endoergic and is dismissed out of hand. This need not be always justified, but the formation of a quintet state would not be necessarily detrimental because it still contains two excitations. Although the formation of $S_0 + T_1$ is also likely to be too exoergic to be of much concern, the formation of $S_0 + T_2$ could be fast if it is isoergic or slightly exoergic. For efficient formation of triplets by singlet fission, it will therefore be important to ensure that neither $2E(T_1) - E(S_1)$ nor $2E(T_1) - E(T_2)$ are distinctly positive.

Since millions of candidate structures can be imagined, finding those that meet these requirements by brute force computation will be difficult. If the purpose of the search is to find likely candidates for photovoltaic cells, the size of the search is not entirely hopeless, since the absorption coefficients in the visible region will have to be high and all likely organic chromophores will be relatively large conjugated π-electron systems. Each of these will be formally derived from a parent hydrocarbon structure by perturbations such as introduction of substituents and heteroatoms, which will usually not change the relations between the lowest singlet and triplet $\pi\pi^*$ states dramatically, unless it introduces new states such as $n\pi^*$.

For the parent π-electron hydrocarbons, the issue was addressed recently at the level of simple molecular orbital theory.[30] Commonly available parent structures that were identified as likely targets are of two types depending on the nature of their lowest singlet state S_0, either the usual closed shell or the rare biradical open shell.

Closed-Shell S_0 State. In these parent systems, the S_0 state can be approximated by a closed-shell single determinant and the S_1 and T_1 states can be often approximated by singlet and triplet HOMO to LUMO excitation from S_0, respectively (left-hand side of Figure 6; HOMO stands for the highest occupied and LUMO for the lowest unoccupied molecular orbital). In these chromophores, referred to as class I in section 2.2.2, the splitting between the S_1 and T_1 states is approximately equal to twice the exchange integral $K_{HOMO,LUMO} = K_{hl}$, whose physical significance is the repulsion of two identical overlap charge densities, defined by the product of HOMO (h) and LUMO (l). Most of this repulsion will be between charges located on the same atom. As the size of the π system increases, there will be a larger number of such one-center terms, but each will be smaller since both orbitals will tend to have smaller amplitudes on any one atom, and the magnitude of the repulsion integral K_{hl} will not change much. The critical factor for the overall size of K_{hl} will be the degree to which the HOMO and the LUMO avoid residing on the same atoms.

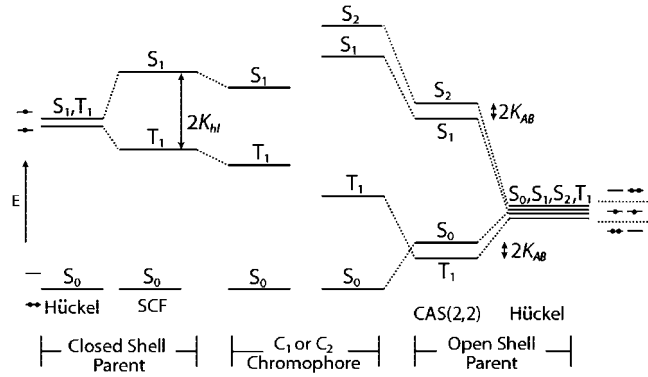

Figure 6. Schematic representation of state energy levels of a parent system at Hückel and SCF levels of approximation, with occupancies of the two frontier orbitals indicated (outside), and of the final chromophore (inside). K = exchange integral.

In certain cases, referred to as class II and class III in section 2.2.2, the lowest excited singlet state is of a different kind, but the HOMO−LUMO excited singlet is usually not much higher.

A general statement can be made at the level of semiempirical theories (Hückel[43] and Pariser−Parr−Pople[44,45]), in which the alternant pairing theorem[46,47] holds and permits the subdivision of conjugated π-electron hydrocarbons into two classes: (i) those devoid of odd-membered rings (alternant hydrocarbons,[46] so named because the atoms in the conjugated system can be separated into two groups in a way that provides each atom of one group only with neighbors from the other group) and (ii) those containing one or more odd-membered rings (nonalternant hydrocarbons, in which such a separation of atoms is impossible). The pairing theorem states that in alternant hydrocarbons molecular orbitals occur in pairs of equal but opposite energy relative to the Hückel energy zero, and two paired orbitals have the same amplitudes on any given atom, except possibly for sign, and hence overlap to the maximum possible degree. Given that the HOMO and the LUMO inevitably are paired in an electroneutral alternant system with a closed-shell S_0 state, alternant hydrocarbons with an even number of carbons in the conjugated system are ideal candidates for systems with large K_{hl} values. It is not a coincidence that all compounds in which singlet fission has been observed in the first few decades of its history were even-carbon alternant hydrocarbons or their simple derivatives.

In nonalternant hydrocarbons and in odd (charged) alternant hydrocarbons, the HOMO and the LUMO are not paired, and K_{hl} tends to be much smaller than in uncharged alternant hydrocarbons. Familiar examples are azulene and the triphenylmethyl cation or anion, from which many dyes are derived. Although the arguments provided are only strictly valid within semiempirical model theories, these models mimic reality closely enough for our purposes.

Open-Shell (Biradical) S_0 State. For a parent structure with an exactly or at least approximately degenerate pair of orbitals that are occupied by only two electrons in the ground state, there are four low-energy states that result from intrashell electron promotion, S_0, S_1, S_2, and T_1.[48−50] Choosing the most localized representation of the two degenerate orbitals, the S_0 and T_1 states usually can be approximated as carrying a single electron in each of these localized orbitals A and B. The splitting of these states is small and is approximated by twice the exchange integral K_{AB} between the two localized orbitals. In point biradicals[51] and among

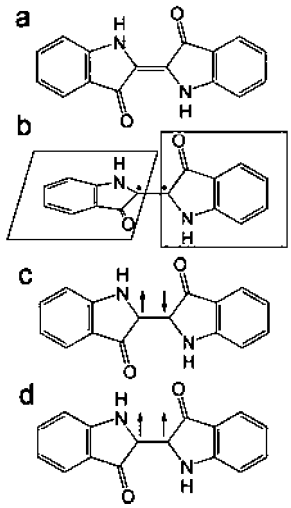

Figure 7. Ground-state electronic structures of planar (a) and twisted (b) indigo, and captodatively stabilized resonance structures of singlet (c) and triplet (d) planar indigo.

conjugated π systems, in disjoint biradicals,[50,52,53] these orbitals avoid each other very well and the S_0 and T_1 states are nearly degenerate. In axial biradicals[51] and among conjugated π systems, in joint biradicals (often called nondisjoint), the avoidance is less perfect and T_1 is significantly below S_0. Many biradicals are intermediate between these extremes. The S_1 and S_2 states tend to be considerably higher in energy. The situation is illustrated on the right-hand side of Figure 6.

To produce a stable molecule, the degeneracy of the nonbonding molecular orbitals of the biradical needs to be split and the more stable of the resulting orbitals will then be occupied twice in the S_0 state. Such a perturbation converts a biradical initially into a biradicaloid and, ultimately, when it becomes strong enough, into an ordinary closed-shell ground-state molecule. In the process, S_0 is stabilized, and the T_1, S_1, and S_2 states generally are destabilized (for certain types of perturbations, S_1 is stabilized,[51] but after this happens to a sufficient extent, it becomes the most stable singlet S_0 and the argument still holds). As a result, there is a range of perturbation strengths for which the condition $E(S_1) > 2\,E(T_1)$ is roughly satisfied. Since the T_2 state originates from intershell excitations, there is a good chance that its energy will be above that of S_1. Translated into the language of valence-bond theory, the S_0 and T_1 states of a biradical are well represented by resonance structures with two dots, and in those of a biradicaloid, such structures still carry considerable weight.

Following this line of thought, several promising parent structures were identified,[30] and one of them, 1,3-diphenylisobenzofuran (**8**), was investigated in more detail (sections 3.4 and 6.2). The conditions $E(T_2)$, $E(S_1) \geq 2E(T_1)$ were indeed found to be satisfied, and in the neat solid, efficient singlet fission was found.[32] Here, we provide another illustration by referring to the well-known dye, indigo. As shown in Figure 7, a parent biradical structure with an orthogonally twisted double bond contains two noninteracting radicals stabilized by captodative[54] substitution. Conversion to a stable biradicaloid is accomplished by planarization. In Figure 6, this motion corresponds to going from the right edge of the drawing toward the center. To illustrate the valence-bond point of view, resonance structures with two captodatively[54] stabilized radical centers are also shown in Figure 7. Note that the radical stabilizing substitution is critically important. In its absence, the stabilization of the ground state upon planarization would be too large and the $S_0 - T_1$ gap would be excessive relative to the $T_1 - S_1$ gap (this could be counteracted by incomplete planarization).

Experimentally, the condition $E(S_1) \geq 2E(T_1)$ is satisfied in indigo,[55] but no data on singlet fission in a crystal or covalent dimer are available. Because the S_1 lifetime of indigo is extremely short due to radiationless deactivation,[56] it is unlikely that singlet fission will be efficient. Nevertheless, this example suggests that a search for other planar π-electron systems for which a unique dot−dot resonance structure with two stabilized radical centers can be written is likely to yield structures that will have an energy level arrangement suitable for singlet fission.

2.2.2. Intrinsic Rate

When two or more chromophores A, B,... are brought into proximity and interact weakly, the electrostatic Hamiltonian $\mathscr{H}_{el}$ of the total system can be separated into a sum of the Hamiltonians of the individual systems $\mathscr{H}_{el}^{U}$, U = A, B,..., and an interaction term $\mathscr{H}_{el}^{int}$. In a basis consisting of products of eigenstates of the individual chromophores, such as $S_0^A S_0^B$..., the diagonal elements of $\mathscr{H}_{el}^{int}$ describe the modification of the state energies of the individual chromophores by the interaction. In weakly coupled systems, these modifications are usually negligible relative to initial state energy differences. Although the off-diagonal terms that describe the mutual mixing of the initial individual system eigenstates may be similarly small, they are not negligible relative to the initial value of zero and are sufficient to make an initially prepared state such as $S_1^A S_0^B$... develop in time. Because they are assumed to be small, the time development can be described by low-order perturbation theory. To the first order, the rate $w(I \rightarrow F)$ at which an initial electronic state I, such as $S_1^A S_0^B$..., will reach a quasicontinuum of vibrational levels in a final electronic state F, such as $^1(T_1^A T_1^B...)$, is given by the Fermi golden rule. Within the Born−Oppenheimer approximation, the rate equals

$$w(I \rightarrow F) = (2\pi/\hbar)|\langle F|\mathscr{H}_{el}|I\rangle|^2 \rho(E_I = E_F) \qquad (5)$$

where ρ is the Franck−Condon weighted density of states in F at energy E_F, which needs to be the same as the energy E_I within $2\pi\hbar/\tau$, where τ is the lifetime. If $|\langle F|\mathscr{H}_{el}|I\rangle|^2$ is small and other states are nearby in energy, it may be necessary to go to second order in perturbation theory and include the effect of such additional states on the rate $w(I \rightarrow F)$ as well. A more complete description of the time development is possible using density matrices, including both coherence and relaxation effects, but we will see below that little work has been done along these lines for singlet fission so far.

The definition of the initial and final states of the total system of two or more chromophores is easy only if the subsystems are separated by infinite distances. At finite distances, the wave functions of the subsystems overlap and ambiguities in the definition of the initial and final adiabatic states arise. We shall avoid a discussion of these matters by dealing only with weakly interacting systems, characterized by minimal overlap.

The first-order description is relatively simple if there is an infinite number of symmetry-related chromophores, as in a crystal, and this is where it was first applied to singlet

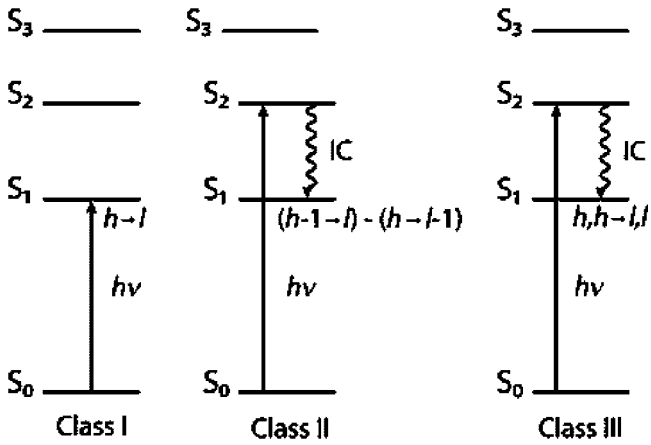

Figure 8. Jablonski diagram for singlet states of chromophores of classes I−III, with the most common mode of population of the S_1 state shown (in rare cases of chromophores of classes II and III, the $h \rightarrow l$ excited state might be S_3 or even higher).

fission.[57,58] The procedure is also simple when there are only two chromophores, A and B, and we will discuss this case in some detail. To organize the material, we shall adopt a simple model that has been used with small variations many times before for many purposes (only a few examples are listed[57−62]). It was also used in a recent study of singlet fission in which the time evolution of the $S_1^A S_0^B$ state under the effect of the one-electron part of $\mathscr{H}_{int}$ alone was followed.[33] By analogy to the cases of singlet and triplet energy transfer,[62] in which this type of term dominates, this may be an acceptable approximation.

In the model, the eigenstates of $\mathscr{H}_{el}^A$ and $\mathscr{H}_{el}^B$ are approximated by single configurations built from Hartree−Fock MOs of the chromophores A and B, respectively. The MOs on A and B are assumed to be mutually Löwdin orthogonalized, and the orthogonalization is assumed to have almost fully preserved the localization. A further simplification is introduced by limiting the MOs to h_A and l_A on A and h_B and l_B on B. In spite of these drastic assumptions, the model captures the fundamental physics of the most important two of the three main classes of π-electron chromophores, which include almost all of those that have been of interest in studies of singlet fission. We refer to these chromophore classes as classes I, II, and III (Figure 8).

Our purpose is to organize the material and provide qualitative insight into the terms that need to be considered when contemplating the origins of structural dependence of the frequency factor $A[S_1S_0 \rightarrow {}^1(TT)]$. For the purposes of an actual calculation, more rigor would be needed. In particular, it would undoubtedly be necessary to treat overlap in a manner similar to the now standard treatment of energy transfer.[62] This would involve an initial diagonalization of a subspace that contains local and charge transfer excitations and dealing with overlap explicitly. Although such a formulation appears quite straightforward, it has not yet been published for singlet fission, and we will not use it here.

Chromophores of Class I. This class comprises those π chromophores whose first excited singlet state S_1 is reasonably described as a result of an $h \rightarrow l$ (HOMO to LUMO) electron promotion from the ground state and is separated from the next higher singlet S_2 by a significant energy gap. Class I chromophores are exemplified by anthracene (**1**), tetracene (**2**), perylene (**9**), and 1,3-diphenylisobenzofuran (**8**). In compounds formally derived from a $(4N + 2)$-electron perimeter, such as these, the $S_0 \rightarrow S_1$ transition terminates in Platt[63] and Moffitt's[64] L_a state, carries considerable oscillator strength, and represents the usual point of entry into the excited singlet manifold when the ground state absorbs light. In the less common chromophores derived from a $4N$-electron perimeter, the $h \rightarrow l$ transition has low intensity and is often symmetry forbidden.[65,66] However, to our knowledge, no such chromophores have been examined for singlet fission.

Chromophores of Class II. In the less numerous chromophores of class II, the strongly allowed $h \rightarrow l$ excitation leads to the S_2 state and still represents the usual entry point into the excited singlet manifold by absorption of light. The S_1 state, which is often only slightly lower in energy and is reached from the higher singlet states by fast internal conversion, is quite well described as arising from an out-of-phase combination of $h - 1 \rightarrow l$ and $h \rightarrow l + 1$ electron promotions from the ground state, where $h - 1$ is the next MO below h and $l + 1$ is the next MO above l in energy. Its perimeter model label is L_b, and it carries low oscillator strength. Typical examples of class II chromophores are those in which the energy difference between the MOs h and $h - 1$ and that between the MOs l and $l + 1$ are small. Benzene, where the degeneracy of the h and $h - 1$ and of the l and $l + 1$ MOs is exact, making the description a little more complicated, is the best known case. Others are naphthalene, phenanthrene, and pyrene (**12**). Since the simple model adopted for our discussion does not include the MOs $h - 1$ and $l + 1$, it is incapable of describing the properties of the S_1 state of chromophores of class II. The required generalization is straightforward, but very little work has been done on singlet fission involving chromophores of this class, and we will not generalize the model here.

Chromophores of Class III. Similarly as in chromophores of class II, in chromophores of class III the strongly allowed $h \rightarrow l$ excitation provides a good description of the nature of the lowest excited state carrying a large oscillator strength from the ground state (usually the S_2 state), and again represents a typical entry point into the excited singlet manifold by absorption of light. Now, however, the S_1 state, which is usually only slightly lower in energy and can again be reached from the higher singlets by fast internal conversion, contains a large weight of a configuration in which both electrons that occupy h in the ground state have been promoted, $h,h \rightarrow l,l$. Although commonly used, the usual designation "doubly excited state" is often quite inaccurate because the description of this S_1 state may also contain large contributions from additional singly excited configurations, especially $h - 1 \rightarrow l$ and $h \rightarrow l + 1$. Our model permits a description of the doubly excited configuration, but not of these additional configurations. The results will therefore be even less accurate than those for chromophores of class I. An alternative description of the doubly excited singlet state is as two local triplet excitations intramolecularly coupled into an overall singlet (e.g., in butadiene, it corresponds to a singlet coupled pair of local triplets, one on each ethylene[9−11]).

The best known examples of chromophores of class III are polyenes and related linearly conjugated polymers, but very recently it has been proposed on the basis of ab initio calculations[40] that pentacene (**3**) is similar in that its S_1 state, which is of the $h \rightarrow l$ type, and its S_2 state, which is of the $h,h \rightarrow l,l$ type, are calculated to be almost exactly degenerate. The well studied absorption and fluorescence spectra of isolated molecules exclude the possibility that the doubly

excited state lies significantly below the singly excited state as proposed (section 3.1.3), but it is entirely possible that it lies only slightly above it. If this is correct, it is probable that even longer polyacenes such as hexacene, and similar compounds in which the T_1 state is very low in energy, may be similar. The resemblance to the ^{1}(TT) state of eq 2 is obvious, the difference being only that in the doubly excited state the two local triplets reside in different parts of a single chromophore, whereas each of the triplets of the ^{1}(TT) state resides on a different chromophore. This distinction becomes blurred in long polyenes and linear conjugated polymers, where local geometry distortions can separate different parts of what nominally is a single chromophore and allow the residence of two distinct and essentially independent local triplet excitations. Intuitively, one can expect the formation of two triplet states on two distinct chromophores to be facilitated if the initial state already contains two triplets on the same chromophore. This issue will be addressed briefly at the end of section 2.2.2.

The existence of chromophores of classes I and II was recognized very early on, but it was only in the late 1960s that it was discovered by theoreticians[67−70] that doubly excited states can be quite comparable in energy with the lowest singly excited states in short polyenes (butadiene). It was only in the 1970s that experimental evidence to this effect was secured[71] (it was obtained for longer polyenes first). At that time, the description of the doubly excited state as a singlet coupled pair of triplets was also provided.[9−11] The difference between aromatics, which tend to be of classes I or II, and polyenes, which tend to be of class III, is dictated by an interplay of topology and geometry.[68] Compact geometries favor class I behavior even in polyenes, as was found in a study of "hairpin polyenes", which also summarized the early history of all these developments.[72] In recent decades, the understanding of excited states of polyenes has grown enormously.

A Simple Model of Singlet Fission: Chromophores of Class I. Using α and β to indicate electron spin, the basis of states for a dimeric composite system is limited to the singlet ground state $S_0{}^AS_0{}^B$ ($|h_A\alpha h_A\beta h_B\alpha h_B\beta|$), low-energy locally excited singlets $S_1{}^AS_0{}^B$ ($2^{-1/2}[|h_A\alpha l_A\beta h_B\alpha h_B\beta| - |h_A\beta l_A\alpha h_B\alpha h_B\beta|]$), $S_0{}^AS_1{}^B$ ($2^{-1/2}[|h_A\alpha h_A\beta h_B\alpha l_B\beta| - |h_A\alpha h_A\beta h_B\beta l_B\alpha|]$), and $^1(T_1{}^AT_1{}^B)$ ($3^{-1/2}[|h_A\alpha l_A\alpha h_B\beta l_B\beta| + |h_A\beta l_A\beta h_B\alpha l_B\alpha| - \{|h_A\alpha l_A\beta h_B\alpha l_B\beta| + |h_A\alpha l_A\beta h_B\beta l_B\alpha| + |h_A\beta l_A\alpha h_B\alpha l_B\beta| + |h_A\beta l_A\alpha h_B\beta l_B\alpha|\}/2]$) that can be produced by excitations out of the HOMO of one or both chromophores (h_A, h_B) into their LUMOs (l_A, l_B), and the charge-transfer states $^1(C^AA^B)$ ($2^{-1/2}[|h_A\alpha l_B\beta h_B\alpha h_B\beta| - |h_A\beta l_B\alpha h_B\alpha h_B\beta|]$) and $^1(A^AC^B)$ ($2^{-1/2}[|h_A\alpha h_A\beta l_A\alpha h_B\beta| - |h_A\alpha h_A\beta l_A\beta h_B\alpha|]$), where C stands for the ground state of the radical cation and A stands for the ground state of the radical anion of one of the chromophores. Relative to the ground state, the energies of these states, including the diagonal contributions from $\mathscr{H}_{int}$, are labeled $E(S_1S_0)$, $E(S_0S_1)$, $E(^1T_1T_1)$, $E(^1CA)$, and $E(^1AC)$, respectively.

The resulting truncated Hamiltonian matrix $\mathscr{H}_{el}$ is shown in eq 6. Equations 7−15 provide explicit expressions for the off-diagonal matrix elements in terms of (i) electron repulsion integrals, for which we use the notation $\langle a(1)b(2)|e^2/r_{12}|c(1)d(2)\rangle$ or $(a(1)c(1)|e^2/r_{12}|b(2)d(2))$, and (ii) matrix elements of the Fock operator $\mathscr{F}$ of the ground state of the total system, $\mathscr{F} = \mathscr{H}_1 + \Sigma_i(\mathscr{J}_i - \mathscr{K}_i)$. Here, $\mathscr{H}_1$ is the one-electron part of $\mathscr{H}_{el}$, $\mathscr{J}$ is the Coulomb, and $\mathscr{K}$ is the exchange operator ($\mathscr{J}_i a(1) = \langle i(2)|e^2/r_{12}|i(2)\rangle a(1)$, $\mathscr{K}_i a(1) = \langle i(2)|e^2/r_{12}|i(1)\rangle a(2)$), and the sum is over the spin orbitals occupied in the ground state ($i \in h_A\alpha$, $h_A\beta$, $h_B\alpha$, $h_B\beta$). Expressions for the remaining elements follow from the Hermitian nature of $\mathscr{H}$ or from the interchange of A and B.

$\mathscr{H}_{el}=$

$$\begin{pmatrix}
E(^1CA) & \langle ^1CA|\mathscr{H}_{el}|S_1S_0\rangle & \langle ^1CA|\mathscr{H}_{el}|^1T_1T_1\rangle & \langle ^1CA|\mathscr{H}_{el}|S_0S_1\rangle & \langle ^1CA|\mathscr{H}_{el}|^1AC\rangle & \langle ^1CA|\mathscr{H}_{el}|S_0S_0\rangle \\
\langle S_1S_0|\mathscr{H}_{el}|^1CA\rangle & E(S_1S_0) & \langle S_1S_0|\mathscr{H}_{el}|^1T_1T_1\rangle & \langle S_1S_0|\mathscr{H}_{el}|S_0S_1\rangle & \langle S_1S_0|\mathscr{H}_{el}|^1AC\rangle & \langle S_1S_0|\mathscr{H}_{el}|S_0S_0\rangle \\
\langle ^1T_1T_1|\mathscr{H}_{el}|^1CA\rangle & \langle ^1T_1T_1|\mathscr{H}_{el}|S_1S_0\rangle & E(^1T_1T_1) & \langle ^1T_1T_1|\mathscr{H}_{el}|S_0S_1\rangle & \langle ^1T_1T_1|\mathscr{H}_{el}|^1AC\rangle & \langle ^1T_1T_1|\mathscr{H}_{el}|S_0S_0\rangle \\
\langle S_0S_1|\mathscr{H}_{el}|^1CA\rangle & \langle S_0S_1|\mathscr{H}_{el}|S_1S_0\rangle & \langle S_0S_1|\mathscr{H}_{el}|^1T_1T_1\rangle & E(S_0S_1) & \langle S_0S_1|\mathscr{H}_{el}|^1AC\rangle & \langle S_0S_1|\mathscr{H}_{el}|S_0S_0\rangle \\
\langle ^1AC|\mathscr{H}_{el}|^1CA\rangle & \langle ^1AC|\mathscr{H}_{el}|S_1S_0\rangle & \langle ^1AC|\mathscr{H}_{el}|^1T_1T_1\rangle & \langle ^1AC|\mathscr{H}_{el}|S_0S_1\rangle & E(^1AC) & \langle ^1AC|\mathscr{H}_{el}|S_0S_0\rangle \\
\langle S_0S_0|\mathscr{H}_{el}|^1CA\rangle & \langle S_0S_0|\mathscr{H}_{el}|S_1S_0\rangle & \langle S_0S_0|\mathscr{H}_{el}|^1T_1T_1\rangle & \langle S_0S_0|\mathscr{H}_{el}|S_0S_1\rangle & \langle S_0S_0|\mathscr{H}_{el}|^1AC\rangle & 0
\end{pmatrix}$$

$$\langle ^1CA|\mathscr{H}_{el}|S_1S_0\rangle = \langle l_A|\mathscr{F}|l_B\rangle + 2\langle h_Al_A|e^2/r_{12}|l_Bh_A\rangle - \langle h_Al_A|e^2/r_{12}|h_Al_B\rangle \quad (7)$$

$$\langle ^1CA|\mathscr{H}_{el}|^1T_1T_1\rangle = (3/2)^{1/2}[\langle l_A|\mathscr{F}|h_B\rangle + \langle l_Al_B|e^2/r_{12}|h_Bl_B\rangle - \langle l_Ah_A|e^2/r_{12}|h_Bh_A\rangle] \quad (8)$$

$$\langle ^1CA|\mathscr{H}_{el}|S_0S_1\rangle = -[\langle h_A|\mathscr{F}|h_B\rangle - 2\langle h_Bl_B|e^2/r_{12}|l_Bh_A\rangle + \langle h_Bl_B|e^2/r_{12}|h_Al_B\rangle] \quad (9)$$

$$\langle ^1CA|\mathscr{H}_{el}|^1AC\rangle = 2\langle h_Al_A|e^2/r_{12}|l_Bh_B\rangle - \langle h_Al_A|e^2/r_{12}|h_Bl_B\rangle \quad (10)$$

$$\langle ^1CA|\mathscr{H}_{el}|S_0S_0\rangle = 2^{1/2}\langle h_A|\mathscr{F}|l_B\rangle \quad (11)$$

$$\langle S_1S_0|\mathscr{H}_{el}|^1T_1T_1\rangle = (3/2)^{1/2}[\langle l_Al_B|e^2/r_{12}|h_Bl_A\rangle - \langle h_Ah_B|e^2/r_{12}|l_Bh_A\rangle] \quad (12)$$

$$\langle S_1S_0|\mathscr{H}_{el}|S_0S_1\rangle = 2\langle h_Al_B|e^2/r_{12}|l_Ah_B\rangle - \langle h_Al_B|e^2/r_{12}|h_Bl_A\rangle \quad (13)$$

$$\langle S_1S_0|\mathscr{H}_{el}|S_0S_0\rangle = 2^{1/2}\langle h_A|\mathscr{F}|l_A\rangle \quad (14)$$

$$\langle ^1T_1T_1|\mathscr{H}_{el}|S_0S_0\rangle = 3^{1/2}\langle h_Ah_B|e^2/r_{12}|l_Bl_A\rangle \quad (15)$$

If the chromophores A and B are equivalent by symmetry, $E(S_1S_0) = E(S_0S_1)$ and $E(^1CA) = E(^1AC)$, and the locally excited as well as the charge transfer states are delocalized. In the first approximation, they will occur as pairs of states $2^{-1/2}|S_1S_0 \pm S_0S_1\rangle$ separated by $2\langle S_1S_0|\mathscr{H}_{el}|S_0S_1\rangle$ (exciton or Davydov splitting, eq 13) and $2^{-1/2}|^1CA \pm {}^1AC\rangle$ separated by $2\langle ^1CA|\mathscr{H}_{el}|^1AC\rangle$ (eq 10), respectively. The pairs of locally excited and charge-transfer states interact further through matrix elements shown in cyan in $\mathscr{H}_{el}$ (eq 6), and if their energies are close, they will be mixed significantly.

Unless singlet fission is extremely fast, the singlet excited state will have time to relax and the above consideration of delocalization will usually not apply, for external and internal reasons. The former are interactions with the environment (outer sphere reorganization energy) and the latter are associated with geometrical relaxation (inner sphere reorganization energy). Both of these provide an opportunity for symmetry breaking.

In molecular crystals and aggregates, the resulting site distortion energy can be larger than the delocalization energy

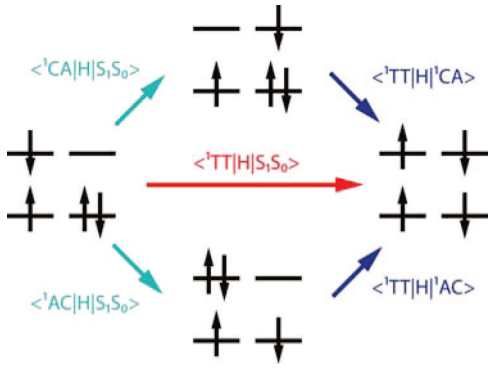

Figure 9. Singlet fission mechanisms: direct (red arrow and matrix element) and mediated (cyan arrows and matrix elements followed by blue arrows and matrix elements).

of the locally excited state, causing the excitation to localize on a single site (Frenkel exciton) or a pair of sites (excimer). Localization on a single site is common for triplet excitons, which definitely move by hopping. It is ordinarily also assumed for singlet excitons, but there is evidence that at least in some cases the size of singlet excitons exceeds a single molecule (charge-transfer excitons), and the issue is still under debate.[73−75] Formation of excimers has been proposed as a form of relaxation for singlet excitons in crystals such as pentacene[76,77] (**3**, section 3.1.3). Examples of relaxed singlet delocalization are various J and H aggregates. In covalent dimers, localization tends to be the rule, except for stacked geometries, where excimers can form and carry delocalized excitation. The solvation energy of a charge transfer state is usually larger than the delocalization energy associated with charge exchange resonance.

In the following discussion, we assume localization of the excited and charge transfer states. Modifications will be necessary if excitation is delocalized in the initial state, which is then described by $2^{-1/2}|S_1S_0 + S_0S_1\rangle$ or $2^{-1/2}|S_1S_0 - S_0S_1\rangle$, and the matrix elements of $\mathscr{H}_{el}$ change accordingly. For instance,

$$\langle 2^{-1/2}(S_1S_0 \pm S_0S_1)|\mathscr{H}_{el}|{}^1T_1T_1\rangle = (3^{1/2}/2)[\langle l_Al_B|e^2/r_{12}|h_Bl_A\rangle \pm \langle l_Al_B|e^2/r_{12}|l_Bh_A\rangle - \langle h_Ah_B|e^2/r_{12}|l_Bh_A\rangle \mp \langle h_Ah_B|e^2/r_{12}|h_Bl_A\rangle] \quad (16)$$

Singlet Fission by Direct Coupling. This is represented by the red arrow in Figure 9 and by the red matrix elements in matrix $\mathscr{H}_{el}$, eq 6. According to first-order perturbation theory (eq 5, Fermi golden rule), the intrinsic singlet fission rate $A[S_1S_0 \rightarrow {}^1(TT)]$ is proportional to the square of the matrix element $\langle S_1S_0|\mathscr{H}_{el}|{}^1T_1T_1\rangle$. In the present approximation, this matrix element is given by eq 12.[61] A similar expression is obtained for the matrix element $\langle S_0S_1|\mathscr{H}_{el}|{}^1T_1T_1\rangle$ by interchanging A and B.

Using this approach for crystalline tetracene (**2**), and assuming that the matrix element between adjacent molecules equals $10^{-4}-10^{-3}$ eV, as previously calculated for crystals of naphthalene and anthracene (**1**),[61] the first quantum mechanical studies that were specifically directed to singlet fission rate led to estimated rate constants k_{-2} equal to 10^8-10^{10} [57] and 10^9-10^{11} s^{-1}.[58] It was assumed that in a thermally equilibrated crystal the initial singlet excitation is delocalized. The results were in fair agreement with experimental data available at the time,[78] as discussed in more detail in section 3.1.2. A subsequent elaboration[42] of the conversion

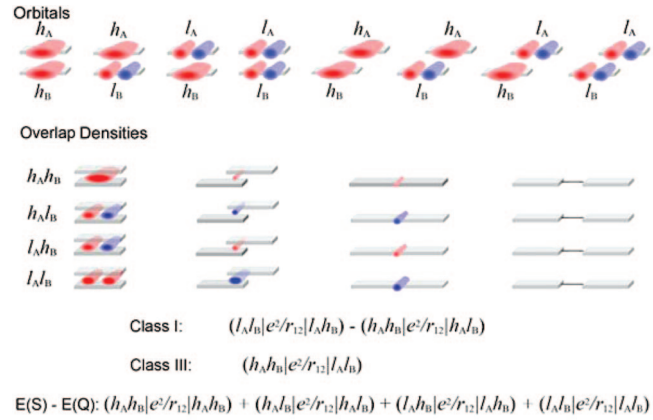

Figure 10. Chromophore dimers. Schematic representation of orbitals h_A, h_B, l_A, l_B for stacked and slip-stacked dimer geometries, and their overlap densities for stacked, slip-stacked and directly or indirectly linearly linked geometries.

of a delocalized S_1 exciton into a pair of localized triplets ^{1}(TT) used radiationless transition theory in the strong coupling limit[41] and additional simplifying assumptions to evaluate k_{-2} in **2** again as 10^9-10^{11} s^{-1}.

If the objective is to design a dimer structure for which the matrix element $\langle S_1S_0|\mathscr{H}_{el}|{}^1T_1T_1\rangle$ defined in eq 12 is large, it is useful to consider the physical interpretation of the electron repulsion integrals $\langle l_Al_B|e^2/r_{12}|h_Bl_A\rangle$ and $\langle h_Ah_B|e^2/r_{12}|l_Bh_A\rangle$ (I_1 and I_2, respectively) whose difference determines its magnitude. We could have equally well chosen to consider the matrix element $\langle S_0S_1|\mathscr{H}_{el}|{}^1T_1T_1\rangle$ and the integrals $\langle l_Bl_A|e^2/r_{12}|h_Al_B\rangle$ and $\langle h_Bh_A|e^2/r_{12}|l_Ah_B\rangle$ to reach the same conclusions.

Each integral represents the electrostatic interaction between two overlap charge densities, the first one between $el_A(1)h_B(1)$ and $el_A(2)l_B(2)$, and the second one between $eh_A(1)l_B(1)$ and $eh_A(2)h_B(2)$. Such overlap densities can only be significant in regions of space where the orbitals of the chromophores A and B overlap.

(i) Stacked Chromophores. As is seen in Figure 10, stacking the π-electron systems of the chromophores on top of each other at the usual contact distance of ~3−3.5 Å produces thin but sizable overlap densities over that part of the whole shared molecular surface where the frontier orbitals have large amplitudes, but with eh_Ah_B negative everywhere on the surface and with eh_Al_B negative on one-half of the surface and positive on the other. Therefore, if the stacking is perfect, there is as much attraction as there is repulsion in both $el_Ah_B \parallel el_Al_B$ and $eh_Al_B \parallel eh_Ah_B$, and integrals I_1 and I_2 vanish. However, if the stacked molecules are mutually shifted in the direction of the el_Ah_B and eh_Al_B dipoles, the cancellation is no longer perfect and a nonzero electron repulsion integral results. Qualitatively (Figure 10), the shift causes the integrals I_1 and I_2 to differ in sign and thus can yield a matrix element of significant size. The direction of the dipoles is the same as the direction of the eh_Al_A and eh_Bl_B dipoles, i.e., the HOMO to LUMO transition moment direction in the individual chromophores. A shift in a direction perpendicular to the transition moment does not remove the cancellation and does not lead to a nonvanishing matrix element.

Figure 11 illustrates the situation on the results of an actual model calculation[79] of the repulsion integrals I_1 and I_2 for two molecules of isobenzofuran stacked in parallel planes located 3 Å apart and slipped along the direction of the HOMO−LUMO transition moment. This type of slip-

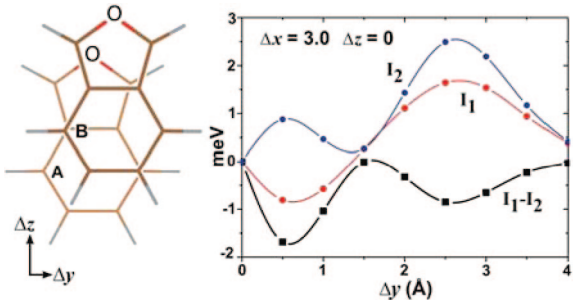

Figure 11. Model calculation for slip-stacked isobenzofuran of the electron repulsion integrals I_1 and I_2 whose difference enters the matrix element for singlet fission by direct coupling for chromophores of class I (eq 12).

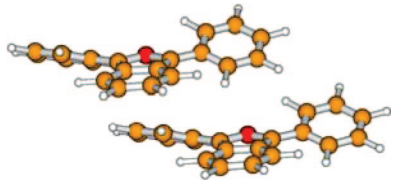

Figure 12. Pair of adjacent molecules of **8** cut from crystal structure.

stacking can be encountered in molecular crystals of some planar π systems and could be of importance for the fast singlet fission observed in those crystals in which it is isoergic or only slightly endoergic (section 3). As an example, we show in Figure 12 the geometry of a pair of adjacent molecules of **8** cut from the published[81,82] crystal structure.

The vanishing of the $el_Ah_B \parallel el_Al_B$ and $eh_Al_B \parallel eh_Ah_B$ interactions at the perfect stacking geometry could also be avoided by polarizing the h and l MOs through substituent effects, but we are not aware of any experimental studies of such systems.

(ii) Linearly Linked Chromophores. Next, we consider two chromophores that are not stacked and are instead connected through a bond or a linker such as an alkane chain or a benzene ring in a planar or twisted fashion, as the covalent dimers studied so far have been (section 6). In this case, all four overlap densities, eh_Al_B, eh_Ah_B, el_Ah_B, and el_Al_B, are essentially confined to the region of the connecting bond or linker and are not nearly as extended as they were for stacked structures. The two critical electron repulsion integrals of eq 12 will therefore be determined by the local amplitudes of the orbitals h_A, h_B, l_A, and l_B in the region of the link. If they are both small, the matrix elements $<S_1S_0|\mathscr{H}_{el}|^1T_1T_1>$ and $<S_0S_1|\mathscr{H}_{el}|^1T_1T_1>$ cannot be large.

If the amplitudes of the four MOs h_A, h_B, l_A, and l_B at the atoms where the chromophores A and B are linked are large, the matrix element could be large. In a twisted direct connection, or a connection through a nonconjugating linker such as CH_2 or an even longer structure, the orbitals on A and B avoid each other in space and overlap densities will be small. Indeed, model calculations of the kind illustrated in Figure 11 performed with the same basis set for an orthogonally twisted linearly linked covalent dimer containing the same two chromophores now connected through their positions 1 (adjacent to the oxygen atom) yielded repulsion integral values 2−3 orders of magnitude smaller. The best chance for large overlap densities and thus a potentially large matrix element $<S_1S_0|\mathscr{H}_{el}|^1T_1T_1>$ is a planar direct connection with a short distance between the strongly overlapping $2p_z$ orbitals of the directly connected atoms.

Figure 10 shows the case in which the link joining the chromophores A and B is roughly parallel to the direction of the HOMO−LUMO transition moment in each chromophore. However, the situation is the same when the link joining the chromophores A and B is perpendicular to the direction of the HOMO−LUMO transition moment in each chromophore.

If the amplitudes of the four MOs at the position of attachment are similar, the $el_Al_B \parallel el_Ah_B$ and $eh_Ah_B \parallel eh_Al_B$ interactions will also be similar and will cancel in the calculation of $<S_1S_0|\mathscr{H}_{el}|^1T_1T_1>$ from eq 12. The cancellation can be minimized by choosing chromophores and positions of attachment where either the amplitudes h_A and h_B are large and those of l_A and l_B are small, or vice versa (one but not both of the small amplitudes could even be zero). It is therefore important not to choose alternant hydrocarbons such as tetracene (**2**) or pentacene (**3**), because in these the amplitudes of h and l in any one position differ at most in sign and the cancellation is perfect. These, of course, are just the parent structures that are optimal when it comes to singlet and triplet energy level matching (section 2.2.1), and they are the ones that attracted experimental attention. Perhaps it is then not surprising that at best a very inefficient singlet fission was found (section 6.1).

Introduction of substituents or heteroatoms in strategic locations is needed to alleviate the problem, but another difficulty remains. A planar or nearly planar direct link between two π chromophores at positions where the frontier MOs have large amplitudes implies that the two chromophores are directly conjugated, and one then needs to ask whether the carefully crafted singlet and triplet energy level matching in the individual chromophores still survives in the dimer and whether the latter has not become a single chromophore, incapable of supporting two more or less independent triplet excitations that can still perform two independent electron injections in a solar cell. Possibly, some of these issues could be dealt with by the use of flexible dimeric sensitizers capable of acting initially at a conformation that makes the coupling strong and distorting thereafter into a conformation in which the coupling is weak, the two triplets are independent, and two charge injections are possible. We will reencounter this issue when we deal with the mediated mechanism of singlet fission, where direct linking appears to be an acceptable choice.

To summarize, we now believe that, in molecular dimers, singlet fission by direct coupling will be much better served by slip-stacking than by linearly linking the chromophores, and it seems entirely understandable that the dimers investigated so far (section 6.1) have not shown efficient singlet fission, although neat solids containing the same chromophores did. It is likely that a suitable choice of substituents might improve the situation, but this has not yet been examined.

Singlet Fission Mediated by a Charge Transfer State. This process is represented by the cyan and blue arrows in Figure 9 and by the cyan and blue matrix elements in matrix $\mathscr{H}_{el}$, eq 6. When the matrix element $<S_1S_0|\mathscr{H}_{el}|^1T_1T_1>$ is small, or when a singlet charge transfer state ^1CA (or ^1AC) is close in energy to the initial S_1S_0 state, first-order perturbation theory (eq 5, Fermi golden rule) may be inadequate for the calculation of the intrinsic singlet fission rate $A[S_1S_0 \rightarrow {}^1(TT)]$. In the next higher order of perturbation theory, the S_1S_0 state can couple strongly to the ^1CA or the ^1AC state through the matrix element $<^1CA|\mathscr{H}_{el}|S_1S_0>$ (eq 7) or

$\langle {}^1AC|\mathscr{H}_{el}|S_1S_0\rangle$ (eq 9), and the latter can couple strongly to the ${}^1T_1T_1$ state through the matrix element $\langle {}^1CA|\mathscr{H}_{el}|{}^1T_1T_1\rangle$ (eq 8) or $\langle {}^1AC|\mathscr{H}_{el}|{}^1T_1T_1\rangle$. The net outcome is a mediated coupling of the S_1S_0 state to the ${}^1T_1T_1$ state. Unlike the matrix element $\langle S_1S_0|\mathscr{H}_{el}|{}^1T_1T_1\rangle$, the matrix elements in question involve both the one-electron and the two-electron parts of the Hamiltonian. As noted above, in a more realistic description of the singlet fission process, the zero-order initial state should probably not be S_1S_0 but its linear combination with the charge transfer states, and then the direct and the mediated mechanism of singlet fission would be inextricably mixed.

This possibility of mediation by charge-transfer states was suggested early on for molecular crystals[58] and explored in some detail more recently in the case of covalent dimers in a study that neglected the direct coupling mechanism and considered only coupling mediated through the elements of the one-electron operator $\mathscr{F}$ in the strictly coherent limit, using the density matrix approach.[33] This may well be a reasonable approximation in many cases, but additional verification is needed. The conclusions of this study were that the rate of singlet fission is maximized when (i) the process is isoergic or exoergic, (ii) the charge-transfer configurations are low in energy, and (iii) the participating chromophores are not related by symmetry.

The structural dependence of frontier MO splitting in various covalent dimers that can be attributed to $\mathscr{F}$ was examined for three representative chromophores.[31] The results can be compared qualitatively with expectations for the efficacy of the mediated singlet fission mechanism based on the inspection of expressions 7−9 for the matrix elements $\langle {}^1CA|\mathscr{H}_{el}|S_1S_0\rangle$, $\langle {}^1AC|\mathscr{H}_{el}|S_1S_0\rangle$, and $\langle {}^1CA|\mathscr{H}_{el}|{}^1T_1T_1\rangle$. When the link is planar or only partially twisted, we assume that these elements are dominated by the one-electron terms $\langle l_A|\mathscr{F}|l_B\rangle$, $\langle h_A|\mathscr{F}|h_B\rangle$, and $\langle l_A|\mathscr{F}|h_B\rangle$, respectively, and that the electron repulsion integrals in eqs 7−9, which involve one overlap density and one orbital density, represent only minor corrections. In contrast with what is found for the case of singlet fission by direct coupling, the matrix elements might then not be disfavored by direct linking of the chromophores A and B, as opposed to their stacking. In that case, they can be approximated as products of the two MO amplitudes at the linked atoms with the resonance (hopping) integral between them, which is the largest when the link is planar and is gradually reduced to zero upon twisting to orthogonality. For $\langle l_A|F|l_B\rangle$, these are the amplitudes of l_A and l_B, for $\langle h_A|F|h_B\rangle$, the amplitudes of h_A and h_B, and for $\langle l_A|F|h_B\rangle$, the amplitudes of l_A and h_B. From this point of view alone, symmetric and planar dimerization of an alternant hydrocarbon in its most reactive position thus seems to be the best choice for favoring the mediated mechanism of singlet fission. Unfortunately, as already mentioned above, there are serious potential difficulties with such a choice, and we list these next.

Direct conjugation tends to convert the chromophores A and B into a single chromophore, reducing the excitation energy of the S_1 state the most and possibly bringing it below twice the T_1 excitation energy, thus making singlet fission in the dimer endoergic.[31] It also puts into serious doubt the ability of the dimer to support two triplet excitations and to effect two successive electron injections in a solar cell. Finally, the increased distance between the centroids of positive and negative charges encountered in linearly linked as opposed to stacked dimers is unfavorable for the energy of charge transfer states and thus for the mediated mechanism.

Also, it needs to be recognized that direct conjugation of the two chromophores severely compromises the utility of the simple model adopted here, which is based on the assumption that the interaction between them is weak, and a more detailed analysis is clearly needed.

When the energy of the charge transfer state, $E({}^1CA)$ or $E({}^1AC)$, lies high enough above those of the locally excited and double triplet states, $E(S_1S_0)$, $E(S_0S_1)$, and $E({}^1TT)$, such that even after all configuration mixing it is not responsible for the presence of a new minimum in the lowest excited singlet potential energy surface, the charge transfer state acts as a virtual state. It promotes the coherent singlet fission process but has no significant lifetime that would permit a vibrational relaxation. The energy of the charge transfer state can be manipulated to some degree through a choice of index of refraction of the environment. We now suspect that this type of mediated singlet fission mechanism may be operating, albeit not very efficiently, in the various covalent dimers of **2** that have been investigated (section 6.1).

When the coupling of the two chromophores A and B is so strong that the S_1 excitation is delocalized, the intermediate state of the coherent version of the two-step mechanism is nonpolar because the four MOs used in the model are all equally distributed over A and B. The resulting absence of charge separation should be favorable for the rate of the mediated mechanism of singlet fission, but this topic does not appear to have been investigated in detail.

We recall again the likely problems with very strongly coupled dimers (keeping singlet fission isoergic or exoergic, and assuring independent survival of the two triplet excitations, particularly with regard to free carrier generation). We consider it probable that this version of the mediated singlet fission mechanism is responsible for the observations[82] made on **32**, a nearly planar and strongly coupled covalently linked dimer of **8** (section 6.2).

The charge transfer state may also lie low enough to represent a minimum in the first singlet potential energy surface, and in that case it is observable as a real vibrationally relaxed intermediate in the incoherent transformation of the locally excited state S_1S_0 into the double triplet state ${}^1(TT)$. Its energy is now much easier to manipulate by a choice of solvent dielectric constant. Such singlet fission becomes a two-step process, in which singlet excitation is converted via a dipolar state into one of the nine sublevels of the ${}^1(TT)$ state, some of which have large or even exclusive triplet and/or quintet character. We now believe that such a process has been observed in highly polar media for **30** and **31**, weakly coupled dimers of **8** (section 6.2).[82]

When $E({}^1CA)$ is low and an excimer state, described by some combination of charge transfer and local excitation configurations, lies below $E({}^1TT)$, the initial singlet excitation will end up populating mostly such an excimer state instead of the double triplet state. This is one of the four proposed scenarios for events that follow electronic excitation in a pure crystal of pentacene (**3**).[77] As discussed in more detail in section 3.1.3, other interpretations of the observed behavior are more likely to be correct.

The second half of the two-step singlet fission process (Figure 9), a back electron transfer in an ion pair that produces a pair of triplet states, can also be viewed as a separate process in its own right, since the ion pair could be produced in other ways as well (e.g., free ion diffusion). It

represents an intersystem crossing that utilizes the spin dipole−dipole operator $\mathscr{H}_{ss}$ instead of the more common spin−orbit coupling operator $\mathscr{H}_{so}$ to produce a triplet and a quintet state.

In summary, it seems to us presently that the search for new singlet fission chromophores of class I for solar cell applications is more likely to succeed if it attempts to optimize the direct mechanism by the use of slip-stacked structures, rather than the mediated mechanism. This tentative conclusion is especially likely to be correct in cases in which the charge transfer species acts as a real intermediate, offering new channels for a loss of electronic excitation energy.

A Simple Model of Singlet Fission: Chromophores of Class III. A similar treatment is possible for chromophores whose S_1 state is not approximately described by the single excitation $h \rightarrow l$ but by the double excitation, $h,h \rightarrow l,l$. Then, the minimal list of the states of the dimer that need to be considered contains the singlet ground state $S_0{}^AS_0{}^B$ ($|h_A\alpha h_A\beta h_B\alpha h_B\beta|$) and the doubly excited singlets $S_1{}^AS_0{}^B$ ($|l_A\alpha l_A\beta h_B\alpha h_B\beta|$), $S_0{}^AS_1{}^B$ ($|h_A\alpha h_A\beta l_B\alpha l_B\beta|$), and $^1(T_1{}^AT_1{}^B)$ $(3^{-1/2}[|h_A\alpha l_A\alpha h_B\beta l_B\beta| + |h_A\beta l_A\beta h_B\alpha l_B\alpha| - \{|h_A\alpha l_A\beta h_B\alpha l_B\beta| + |h_A\alpha l_A\beta h_B\beta l_B\alpha| + |h_A\beta l_A\alpha h_B\alpha l_B\beta| + |h_A\beta l_A\alpha h_B\beta l_B\alpha|\}/2])$, as well as the excited charge-transfer states $^1(C^{*A}A^B)$ $(2^{-1/2}[|l_A\alpha l_B\beta h_B\alpha h_B\beta| - |l_A\beta l_B\alpha h_B\alpha h_B\beta|])$ and $^1(A^{*A}C^B)$ $(2^{-1/2}[|l_A\alpha l_A\beta h_A\alpha h_B\beta| - |l_A\alpha l_A\beta h_A\beta h_B\alpha|])$ plus the analogous states $^1(C^AA^{*B})$ and $^1(A^AC^{*B})$, where C* stands for the excited state of the radical cation and A* stands for the excited state of the radical anion. It may be necessary to include the singly excited states $(2^{-1/2}[|h_A\alpha l_A\beta h_B\alpha h_B\beta| - |h_A\beta l_A\alpha h_B\alpha h_B\beta|])$ and $(2^{-1/2}[|h_A\alpha h_A\beta h_B\alpha l_B\beta| - |h_A\alpha h_A\beta h_B\beta l_B\alpha|])$, and possibly the lower-energy charge transfer states, $^1(C^AA^B)$ $(2^{-1/2}[|h_A\alpha l_B\beta h_B\alpha h_B\beta| - |h_A\beta l_B\alpha h_B\alpha h_B\beta|])$ and $^1(A^AC^B)$ $(2^{-1/2}[|h_A\alpha h_A\beta l_A\alpha h_B\beta| - |h_A\alpha h_A\beta l_A\beta h_B\alpha|])$, as well, if they are close in energy. Because relatively little experimental work has been done on chromophores of this class, we do not provide the level of detail that was provided for chromophores of class I and merely note the analogous nature of the problem. The notions of direct and mediated mechanism for the production of the $^1(T_1{}^AT_1{}^B)$ state are again applicable.

It has been claimed recently[40] that an intramolecular double-triplet nature of the initial excited state $S_1{}^AS_0{}^B$ is essential for its direct conversion to the intermolecular double-triplet state $^1(T_1{}^AT_1{}^B)$, implying that chromophores of class III are required for singlet fission. Closer inspection suggests that this is an exaggeration, and indeed at the moment two of the best performers, crystalline **2** (section 3.1.2) and **8** (section 3.4), are both of class I. It is true that, for chromophores of class III, the direct coupling matrix element $\langle S_1{}^AS_0{}^B|\mathscr{H}_{el}|^1(T_1{}^AT_1{}^B)\rangle$ is not given by a difference of two integrals as was the case for chromophores of class I, $(3/2)^{1/2}[\langle l_Al_B|e^2/r_{12}|h_Bl_A\rangle - \langle h_Ah_B|e^2/r_{12}|l_Bh_A\rangle]$ (eq 12), with the numerous attendant opportunities for cancellation, but is simply equal to $-3^{1/2}\langle h_Al_A|e^2/r_{12}|h_Bl_B\rangle$. This quantity may tend to be larger, but it may also be smaller, depending on the structure of the dimer. The integral represents the electrostatic interaction of the overlap densities h_Ah_B and l_Al_B. As a result, for chromophores of class III the matrix element $\langle S_1{}^AS_0{}^B|\mathscr{H}_{el}|^1(T_1{}^AT_1{}^B)\rangle$ has a distinctly different geometrical dependence than for those of class I (cf. Figure 10). For stacked chromophores, it is maximized when the stacking is perfect, and its size is reduced when the stack slips in the direction of the $h \rightarrow l$ transition moment. As the slipping continues, it reaches zero and then reverses its sign.

A potential difficulty faced in chromophores of class III is the likely existence of a S_1-S_0 conical intersection located at a nearby geometry (e.g., in short polyenes). If it is energetically accessible, it will allow the doubly excited state S_1 to return radiationlessly to the ground state in competition with singlet fission. Such a conical intersection will be present along the reaction paths for a geometrical isomerization of a polyene and also for Woodward−Hoffmann allowed photochemical pericyclic reactions of molecules such as the polyacenes, whenever they are possible (e.g., dimerization of pentacene). Another potential difficulty with chromophores of class III is the tendency of their T_2 state to be relatively low in energy. In polyenes, for instance, T_2 tends to lie considerably below S_1. The fusion of two T_1 states to form T_2 may then represent a fast decay path. In summary, we believe that it is too early to dismiss any class of chromophores as long as they meet the basic energy criterion of isoergic or slightly exoergic singlet fission.

We have now dealt with two of the three fundamental issues faced by those interested in finding an optimal sensitizer for fast singlet fission, chromophore choice in section 2.2.1 and chromophore coupling in section 2.2.2, and have alluded several times to the difficulty that direct chromophore linking is likely to cause when confronting the third issue, easy separation of two independently behaving triplets. A more detailed consideration of this third item requires an explicit treatment of the nine sublevels of the ^{1}(TT) state, and this is inextricably tied to a discussion of magnetic field effects on singlet fission, the topic to which we turn next.

2.3. Magnetic Field Effects and Triplet Separation

An Overview

The fate of the nonstationary pure singlet ^{1}(TT) state formed in the artificially separated first step of singlet fission is determined by its projection onto the eigenstates of the full Hamiltonian that includes the spin part $\mathscr{H}_{spin}$. These nine sublevels result from the coupling of the three sublevels of each of the two triplet states. The resulting eigenstates can be, and usually are, mixtures of singlet ^{1}(TT), triplet ^{3}(TT), and quintet ^{5}(TT) eigenfunctions of the total spin operator.

A full dynamical description includes coherences among the nine wave functions and is provided by density matrix calculations, but we give below only a summary of a simplified version that applies after these coherences have been lost, patterned after a previous review article.[1] The probability that a sublevel is occupied is taken to be proportional to the square of the ^{1}(TT) amplitude it carries. Its ability to return to the S_1 state and produce fluorescence depends on the same quantity. In principle, it can also proceed to all lower energy states (such as S_0 and T_1), or slightly higher energy states, but the rates of these additional processes are disfavored by the energy gap law or by the need for thermal activation. They are usually tacitly ignored, which need not be always justified.

Since the spin wave functions of the nine sublevels are affected by the strength and direction of an outside magnetic field, so are these probabilities. As a result, the magnetic field affects the outcome of the spin fission process and influences the quantum yield of prompt fluorescence and of the formation of triplet excitons that have managed to diffuse apart and whose later fusion is responsible for the possible appearance of delayed fluorescence. Resonant application of

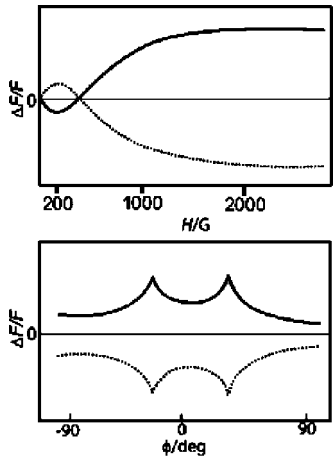

Figure 13. Schematic plot of the dependence of prompt (solid) and delayed (dotted) fluorescence intensity in **2**: with increasing magnetic field strength H (top), and in the high-field limit, with rotation in the *ab* plane with respect to the *b* axis (bottom).

outside microwave fields permits a transfer of populations among the sublevels and thus also affects fluorescence yields.

Given this account of the singlet fission process, it is not surprising that the spin level occupancies of the resulting separated triplet excitons are not in thermal equilibrium. The spin polarization has been observed by EPR spectroscopy[83] and treated theoretically.[84]

The process is more complex than the description given below suggests, because the triplet excitons lose their coherence only gradually. At early times, they can reencounter each other and return to the S_1 state by the process of triplet fusion before having lost all coherence. Thus, at least the fission and fusion processes have to be treated simultaneously in a full theoretical description.

A density matrix treatment of triplet fusion and singlet fission in a molecular crystal was first provided in a simplified form that handled exciton diffusion only approximately and became known as the Johnson−Merrifield theory.[17] It assumed that the probability of return to S_1 followed by fluorescence is proportional to the number of sublevels that have some singlet character. It accounted correctly for the general dependence of prompt and delayed fluorescence intensity on magnetic field strength. The relative fluorescence intensity is much easier to measure than the triplet quantum yield. The dependence is usually expressed as $\Delta F/F = [F(H) - F(0)]/F(0)$,[85] where $F(H)$ and $F(0)$ are the fluorescence intensity at field strengths of H and zero, respectively. As the magnetic field increases, for prompt fluorescence this quantity is initially negative, then becomes positive, and finally converges to a limit with increasing field strength, as shown schematically on top in Figure 13. For delayed fluorescence, the trends are just the opposite and a negative limiting value is ultimately reached.

The Johnson−Merrifield theory accounted well for the location of resonances that appear in the plot of $\Delta F/F$ for the prompt or delayed fluorescence against the angle θ that the direction of strong (limiting) magnetic field makes with crystal axes, as shown schematically at the bottom of Figure 13. These resonances occur for a magnetic field that is oriented just right to bring two levels with partial singlet and partial quintet character into degeneracy. When degenerate, the levels mix in a way that produces one pure singlet and one pure quintet state and thus reduces the number of sublevels with singlet character by one. This reduces the rate of singlet fission, causing an increase in prompt fluorescence and a drop in delayed fluorescence. Although the Johnson−Merrifield theory reproduces correctly the angles at which these high-field resonances in the plot of $\Delta F/F$ against θ occur, it does not render their line shapes correctly. The more elaborate Suna theory,[18] which includes a proper treatment of exciton diffusion in a crystal, succeeds in reproducing the line positions and shapes admirably and was subsequently elaborated further.[36−38]

Spin Hamiltonian

The spin Hamiltonian $\mathscr{H}_{spin}$ contains many terms, but only two are important for the description of magnetic field effects on singlet fission in molecular crystals, aggregates, or dimers that contain no heavy atoms and in which spin−orbit coupling is therefore negligible. These are the spin dipole−dipole term $\mathscr{H}_{ss}$ and the Zeeman term $g\beta\boldsymbol{H}\cdot\boldsymbol{S}$, where β is the Bohr magneton and where we have neglected the anisotropy of the g factor. The effect of the hyperfine interaction with nuclear spins is averaged to zero in crystals in which excitons are mobile and their hopping rate exceeds the Larmor frequency. If the triplet exciton is trapped, this averaging is suppressed, and the hyperfine interaction then causes a broadening of the observed resonances. A similar small effect would be expected in a covalent dimer.

The spin dipole−dipole tensor operator $\mathscr{H}_{ss}$ is diagonal in the molecular magnetic axes, x, y, z. Because the trace of a dipolar interaction vanishes, the values of its diagonal elements can be combined into only two independent molecular parameters, D and E, and the operator can be written as $H_{ss} = D(S_z^2 - S^2/3) + E(S_x^2 - S_y^2)$. Typical values for D are $\sim$0.1 cm^{-1} and for E are $\sim$0.01 cm^{-1}. We shall see below that due to the presence of permutation symmetry in homofission, the mixed-character states that can be produced by singlet fission are of only the singlet−quintet type and have no triplet character (this is not the case in heterofission, in the presence of spin relaxation, or if the partners are equal but orientationally inequivalent).

For a pair of identical triplets, the Hamiltonian $\mathscr{H}_{spin}$ is the sum of two identical single-particle Hamiltonians

$$\boldsymbol{S} = \boldsymbol{S}_1 + \boldsymbol{S}_2$$

$$\mathscr{H}_{spin} = g\beta\boldsymbol{H}\cdot\boldsymbol{S} + \mathscr{H}_{ss} = g\beta\boldsymbol{H}\cdot\boldsymbol{S} + D(S_z^2 - S^2/3) + E(S_x^2 - S_y^2) \quad (17)$$

When dealing with a crystal containing more than one inequivalent molecule in a unit cell, $\mathscr{H}_{spin}$ needs to be averaged over the molecules present, as long as the triplet excitation hops among them fast relative to the Larmor frequency, as is normally the case. The same will be true for a dimer. The averaged zero-field splitting parameters are traditionally called D^* and E^*.

The ^{1}(TT), ^{3}(TT), and ^{5}(TT) States

The Hamiltonian that describes the interaction between the molecular partners in a triplet pair consists of a major part due to $\mathscr{H}_{el}$ and a minor part due to $\mathscr{H}_{spin}$. The ^{1}(TT), ^{3}(TT), and ^{5}(TT) states are eigenstates of $\mathscr{H}_{el}$ with only three distinct space wave functions ϕ_S, ϕ_T, and ϕ_Q and energies E(S), E(T), and E(Q), but with nine distinct spin wave functions $|S\rangle$; $|T^l\rangle$, $l = 2-4$; and $|Q^l\rangle$, $l = 5-9$. When $\mathscr{H}_{spin}$ is also considered, it introduces off-diagonal elements into

the 9 × 9 Hamiltonian matrix. It also introduces small modifications to the diagonal elements, but these are normally neglected because the spin dipole−dipole interaction between electrons on different molecules is much smaller than the intramolecular zero-field splitting parameters D and E.

The size of the differences between E(S), E(T), and E(Q) is thus determined by $\mathscr{H}_{el}$. It is important for two reasons. It dictates how much effect the off-diagonal elements of $\mathscr{H}_{spin}$ will have on the eigenstates of the total Hamiltonian and therefore affects the magnetic field effects on singlet fission. It also dictates how easy it will be for outside perturbations (such as a coupling to the bath) to mix the S, T, and Q states and therefore determines how easily the two constituent triplets will lose coherence and start to behave independently, and how easily they will separate and diffuse apart.

In most molecular crystals, electronic interaction between neighboring molecules is quite weak and E(S), E(T), and E(Q) are the same within energies typical of Zeeman or spin dipole−dipole interaction effects, on the order of 1 cm^{-1}. The off-diagonal elements of $\mathscr{H}_{spin}$ can mix the nine sublevels strongly, significant magnetic field effects can be expected, and separation into an uncorrelated triplet pair is easy.

In directly linked covalent dimers, E(S), E(T), and E(Q) are far more likely to be distinctly different. An extreme example is provided by butadiene, which can be viewed as two very strongly coupled ethylene chromophores, and in which these three levels are calculated to be about 1−2 eV apart.[10,11] Even in weakly coupled covalently linked dimers, the differences can be of the order of 1 000 cm^{-1}.[86] Then, a magnetic field is not expected to have an observable effect, and separation of the double-triplet state into two independently behaving triplets becomes increasingly difficult.

The differences among E(S), E(T), and E(Q) as a function of dimer structure depend on two primary factors. One is a difference in diagonal terms, related to Hund's rule for atoms. In the simple model that led to eqs 7−15, the energy order is E(S) > E(T) > E(Q) and the largest difference in electron repulsion terms in energy expressions is given by eq 18,

$$E(S) - E(Q) = (3/2)(\langle h_A h_A|e^2/r_{12}|h_B h_B\rangle + \langle h_A h_A|e^2/r_{12}|l_B l_B\rangle + \langle l_A l_A|e^2/r_{12}|h_B h_B\rangle + \langle l_A l_A|e^2/r_{12}|l_B l_B\rangle) \quad (18)$$

which states that the difference is proportional to the sum of the self-repulsions of the overlap densities h_Ah_B, h_Al_B, l_Ah_B, and l_Al_B shown in Figure 10, and thus is amenable to an intuitive interpretation.

The other important factor is a difference in off-diagonal terms in the Hamiltonian matrices for the singlet, triplet, and quintet sublevels, which makes them mix with nearby charge transfer states to different degrees. The 6 × 6 matrix for singlet states was given in eq 6, and singlet charge transfer states have already been discussed. The 5 × 5 matrix for triplet states is similar, and the triplet charge transfer states will have similar energies as the singlets if the chromophores A and B interact weakly. However, the dimension of the quintet matrix is 1 × 1, as in the present approximation there are no quintet charge transfer states and mixing matrix elements. It is therefore likely that the interaction with charge-transfer states will lower E(S) and E(T) relative to E(Q), and this makes it hard to estimate their energy differences without a calculation. It is therefore more difficult to find simple structural guidance.

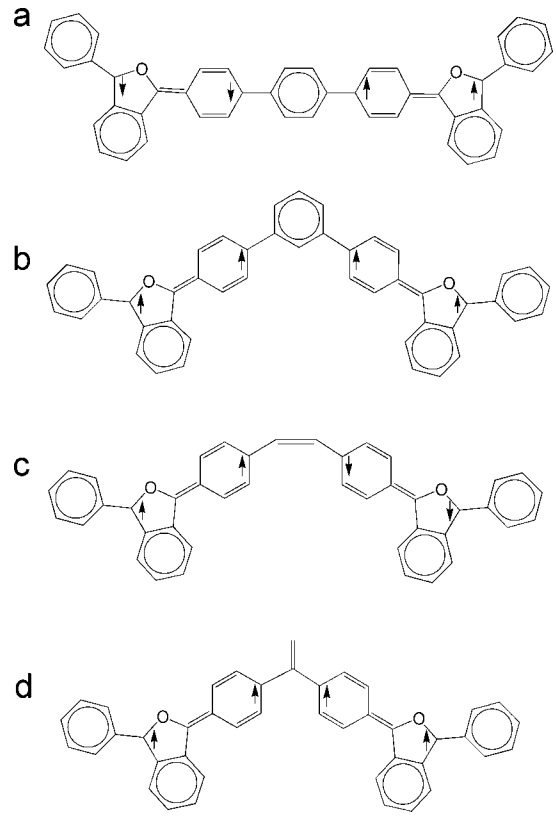

Figure 14. Antiferromagnetic (a, c) and ferromagnetic (b, d) coupling of two molecules of **8** through a linker.

In the case of relatively weakly interacting chromophores without direct conjugation and attendant charge-transfer interaction, some estimates can be obtained from qualitative arguments based on the Heisenberg Hamiltonian. In this approximation, the three levels are split equally and the order of their energies is either E(S) > E(T) > E(Q) if the coupling between the two chromophores is ferromagnetic or E(Q) > E(T) > E(S) if their coupling is antiferromagnetic. The nature of the coupling is dictated by the choice of the linker connecting the chromophores. For instance, as shown in Figure 14, when the two chromophores are attached as 1,3-substituents on benzene or 1,1-substituents on ethylene, ferromagnetic coupling results (*m*-xylylene and trimethylenemethane are ground-state triplets), whereas 1,4-substitution on benzene and 1,2-substitution on ethylene lead to antiferromagnetic coupling (*p*-xylylene and butadiene are ground-state singlets). The strength of the coupling depends on the spin densities in the triplet chromophores at the position of attachment to the linker.

In analyzing magnetic field effects on singlet fission and fusion processes in terms of the model expressed in eq 2,[1] three types of situations need to be considered separately. We address first the case of small E(S), E(T), and E(Q) differences, comparable in size to the zero-field matrix elements of $\mathscr{H}_{spin}$. Subsequently, we address the case of differences that are larger but still comparable to the Zeeman term in $\mathscr{H}_{spin}$ in the presence of a strong magnetic field. Finally, we address the case in which the differences are larger than any matrix elements of $\mathscr{H}_{spin}$ for magnetic fields achievable in the laboratory.

After diagonalization of the matrix of the full Hamiltonian $\mathscr{H}_{el} + \mathscr{H}_{spin}$, nine eigenfunctions result. The kth of these can be written as

$$\psi_k = \varphi_S C_S^k |S> + \varphi_T \sum_{l=2}^{4} C_T^{k,l} |T^l> + \varphi_Q \sum_{l=5}^{9} C_Q^{k,l} |Q^l> \quad (19)$$

where the one coefficient $C_S{}^k$, three coefficients $C_T{}^{k,l}$, and five coefficients $C_Q{}^{k,l}$ are the amplitudes of the singlet, triplet, and quintet spin states in the sublevel k, and φ_S, φ_T, and φ_Q are the earlier defined space parts of the wave functions of the singlet, triplet, and quintet sublevels, respectively. It was first proposed by Merrifield[16] that the triplet fusion rate constant increases with the number of sublevels k for which $C_S{}^k$ is different from zero.

The normalization is

$$\sum_{k=1}^{9} |C_S^k|^2 = 1, \quad \sum_{k=1}^{9} \sum_{l} |C_T^{k,l}|^2 = 3, \quad \sum_{k=1}^{9} \sum_{l} |C_Q^{k,l}|^2 = 5 \quad (20)$$

In the absence of magnetic field (indicated by zero in parentheses), it is convenient to use a basis set of spin functions constructed from the eigenfunctions of the total spin dipole−dipole operator $\mathscr{H}_{ss}$,

$$\mathscr{H}_{ss} = \mathscr{H}_{ss}(A) + \mathscr{H}_{ss}(B) = D_A(S_{Az}{}^2 - S_A{}^2/3) + E_A(S_{Ax}{}^2 - S_{Ay}{}^2) + D_B(S_{Bz}{}^2 - S_B{}^2/3) + E_B(S_{Bx}{}^2 - S_{By}{}^2) \quad (21)$$

for the two chromophores A and B, cf. eq 17. There are nine pair states, $|x_Ax_B>$, $|x_Ay_B>$, $|x_Az_B>$, $|y_Ax_B>$, etc. The singlet function is

$$|S(0)> = 3^{-1/2}(|x_Ax_B> + |y_Ay_B> + |z_Az_B>) \quad (22)$$

in a frame of axes in which the total $\mathscr{H}_{ss}$ defined in eq 21 is diagonal. In the case of heterofission, and also in the general case of homofission, the magnetic axes of A and B do not coincide and this frame has to be constructed from those of A and B by tensorial addition. The situation simplifies when the magnetic axes on A and B are the same, as is the case in polyacene crystals due to fast exciton hopping, and this is the only case that we will consider.

In a strong magnetic field H, the eigenfunctions of the Zeeman Hamiltonian $g\beta \boldsymbol{H}\cdot\boldsymbol{S}$ represent a preferable basis set, and in this basis,

$$|S(H)> = 3^{-1/2}(|0_A0_B> - |+_A-_B> - |-_A+_B>) \quad (23)$$

where $|0_A0_B>$, $|+_A-_B>$, and $|-_A+_B>$ are the spin eigenstates of A and B with spin angular momentum quantized along the direction of the magnetic field.

Small ^{1}(TT), ^{3}(TT), and ^{5}(TT) Energy Difference

This situation is typical for chromophores packed in molecular crystals and probably applies also in stacked dimers. It was examined in great detail nearly half a century ago in connection with the interpretation of magnetic field effects on triplet fusion and singlet fission in polyacene crystals and was summarized in a review chapter.[1] In the following, we provide a condensed version and refer the reader to the original for details.

Field Strength Dependence

It is apparent from eq 22 that, in the absence of magnetic field, singlet character is distributed over only three of the nine states, $|x_Ax_B>$, $|y_Ay_B>$, and $|z_Az_B>$ when A and B are symmetry equivalent (when they are not, it may be distributed over all nine states). The very weak intermolecular spin dipole−dipole interaction removes the degeneracy of terms such as $|x_Ay_B>$ and $|y_Ax_B>$, and in zero field the resulting nine pair states take the form

$$|S(0)> \text{ and } |Q(0)>, \quad |x_Ax_B>, |y_Ay_B>, \text{ and } |z_Az_B> \quad (24)$$

$$|Q(0)>, \quad 2^{-1/2}(|x_Az_B> + |z_Ax_B>), \quad 2^{-1/2}(|x_Ay_B> + |y_Ax_B>), 2^{-1/2}(|y_Az_B> + |z_Ay_B>)$$

$$|T(0)>, \quad 2^{-1/2}(|x_Az_B> - |z_Ax_B>), \quad 2^{-1/2}(|x_Ay_B> - |y_Ax_B>), 2^{-1/2}(|y_Az_B> - |z_Ay_B>)$$

It is apparent that the spin functions $|S>$ and $|Q>$ are symmetric and the functions $|T>$ are antisymmetric with respect to the exchange of A and B. For homofission and homofusion this exchange can be a symmetry operation, and in the case considered presently, it is. Then, the three triplet states cannot mix with the other six states, and the situation simplifies. Note that this is not the case if A and B are different (heterofission) or inequivalent due to orientation, solvent interactions, etc. Because the intermolecular spin dipole−dipole interaction that establishes the distinction between the symmetric and antisymmetric states is only very weak, it will not take much perturbation to break this selection rule. As long as the rule applies, ^{3}(TT) states cannot fuse to the S_1 state, but can only form an upper triplet T_n or a vibrationally hot T_1 state on A or B.[87]

If no two states with partial singlet character are degenerate, and if coherences can be neglected (diagonal density matrix), the overall rate constant γ' for singlet fission, defined in eq 1, is given by

$$\gamma' = \sum_{k=1}^{9} k_{-2}|C_S^k|^2/(1 + \varepsilon|C_S^k|^2) \quad (25)$$

where $k_{-2}|C_S{}^k|^2$ is the rate of formation of the kth substate and ε is the branching ratio, $\varepsilon = k_2/k_{-1}$, which defines the fraction of the singlet correlated triplet pairs ^{1}(TT) that return to S_1 instead of proceeding to $T_1 + T_1$. Similarly, for the overall rate constant γ_S for triplet fusion to yield the singlet S_1, we have

$$\gamma_S = (k_1/9)\sum_{k=1}^{9} \varepsilon|C_S^k|^2/(1 + \varepsilon|C_S^k|^2) \quad (26)$$

where $k_1/9$ is the rate of formation of each of the nine sublevels from thermalized triplet excitons. Similar expressions can be written for rate constants for fusion yielding a triplet or a quintet state on A or B (the quintet is usually not energetically accessible).

In the presence of the magnetic field, the Zeeman term $g\beta \boldsymbol{H}\cdot\boldsymbol{S}$ needs to be added to $\mathscr{H}_{ss}$ in eq 21. If the field is weak and $g\beta H$ is approximately equal to D, the off-diagonal elements of $\mathscr{H}_{ss}$ will then mix all nine sublevels. This will provide a larger number of these states with some singlet character, and the fission and fusion rate constants γ' and

γ_S will increase (note that their ratio is fixed by the thermodynamics of the process). As the field grows stronger and the condition $g\beta H \gg D$ is reached, the eigenstates of $\mathscr{H}_{ss}$ will acquire the form $|0_A0_B\rangle$, $|+_A-_B\rangle$, $|-_A+_B\rangle$, $|0_A+_B\rangle$, $|+_A0_B\rangle$, etc. Equation 23 shows that only the first three possess singlet character. Pairs such as $|0_A+_B\rangle$ and $|+_A0_B\rangle$ are degenerate and the weak intermolecular spin dipole−dipole interaction will mix them, ultimately yielding the following set of spin functions:

$$|S(H)\rangle \text{ and } |Q(H)\rangle, \quad |0_A0_B\rangle, 2^{-1/2}(|+_A-_B\rangle + |-_A+_B\rangle) \tag{27}$$

$$|Q(H)\rangle, \quad |+_A+_B\rangle, |-_A-_B\rangle, 2^{-1/2}(|0_A+_B\rangle + |+_A0_B\rangle), \quad 2^{-1/2}(|-_A0_B\rangle + |0_A-_B\rangle)$$

$$|T(H)\rangle, \quad 2^{-1/2}(|+_A-_B\rangle - |-_A+_B\rangle), \quad 2^{-1/2}(|0_A+_B\rangle - |+_A0_B\rangle), 2^{-1/2}(|-_A0_B\rangle - |0_A-_B\rangle)$$

Once again, as long as strict exchange symmetry between A and B applies, the three triplets will not mix with the other six sublevels. The rate constant for fusion to yield a triplet state should be field independent, and this has indeed been observed.[87]

We see that, in the high-field limit, only two sublevels have singlet character (this remains true even if A and B are different). The rate constants γ' and γ_S are expected to be smaller. On the basis of these qualitative arguments for the behavior of γ' and γ_S, the expected field dependence of prompt fluorescence from an initially excited S_1 state that can undergo fission, and of delayed fluorescence from an S_1 state populated by fusion of triplets T_1, is displayed schematically in Figure 13.

Field Orientation Dependence

In crystals, the directions of the principal axes of the zero-field splitting tensor are fixed and it is possible to perform measurements in which they form well-defined angles with the direction of the applied magnetic field $\boldsymbol{H}$. The fission and fusion rate constants depend on the angles between $\boldsymbol{H}$ and the crystallographic axes, and this leads to resonances in the intensities of prompt and delayed fluorescence. These resonances are a hallmark of singlet fission in molecular crystals.

High-field resonances are found in the limit for which the spin states are quantized with respect to the magnetic field direction. They occur at orientations at which the $|0_A0_B\rangle$ state is degenerate with the $2^{-1/2}(|+_A-_B\rangle + |-_A+_B\rangle)$ state. Then, they can mix to produce one pure singlet state, $3^{-1/2}(|0_A0_B\rangle - |+_A-_B\rangle - |-_A+_B\rangle)$, eq 23, and one pure quintet state. Since the number of singlet states is thus reduced from two to one, the rate constants γ' and γ_S are minimized, prompt fluorescence from the initially excited S_1 state is maximized, and singlet fission and therefore also delayed fluorescence due to subsequent triplet fusion are minimized (Figure 13).

The orientations at which the high-field resonances occur are those at which the two allowed $\Delta m = \pm 1$ EPR lines of the triplet exciton merge into one and are dictated by the values of the zero-field splitting tensor D and E. If cos α, cos β, and cos γ are the direction cosines of $\boldsymbol{H}$ in the magnetic axes x, y, and z, respectively, the condition for resonance is

$$D(\cos^2\gamma - 1/3) + E(\cos^2\alpha - \cos^2\beta) = 0 \tag{28}$$

Low-field resonances[17] occur at fields for which $g\beta H$ is approximately equal to the zero-field splitting parameters D and E. At these field strengths, the zero-field spin functions are generally strongly mixed and all nine have some singlet character. The off-diagonal Zeeman terms in the matrix of $\mathscr{H}_{spin}$ contain a projection of $\boldsymbol{H}$ into the magnetic axes x, y, and z, and two of them vanish when $\boldsymbol{H}$ is oriented parallel to one of the axes. At these special orientations, the state mixing will be less extensive and the number of states with singlet character will be reduced. The rate constants γ' and γ_S will be reduced, prompt fluorescence will be enhanced, and delayed fluorescence will be diminished.

Microwave-Induced Transitions between Sublevels

At resonance, microwave radiation can transfer populations between certain pairs of sublevels and thus affect fluorescence intensity. For a given frequency of radiation, the resonance condition is fulfilled at certain combinations of static magnetic field strength and orientation, and this permits an accurate determination of the zero-field splitting parameters. Measurements of fluorescence intensity on crystals of **3**[88−90] showed that the position of the resonances is correctly described by the Johnson−Merrifield theory, but the peak widths and heights are not. Moreover, the rate constant k_{-1} in eq 2 derived from these results differs by an order of magnitude from the value deduced from measurements without microwaves using the same theory. A proper description of the kinematics of exciton diffusion, such as that provided by the Suna theory,[18] will be once again needed for quantitative interpretations.

Intermediate ^{1}(TT), ^{3}(TT), and ^{5}(TT) Energy Difference

In this regime, the differences between the energies E(S), E(T), and E(Q) are much larger than the zero-field splitting parameters D and E and comparable with $g\beta H$ at fields that can be attained in the laboratory. Since $g\beta = \sim 10^{-4}$ cm^{-1} gauss^{-1}, even relatively strong fields will only span a few cm^{-1}. Little is known about this situation, which could possibly be encountered in dimers that are poorly stacked or linearly linked through a very weak coupler.

The spin states $|S\rangle$, $|T\rangle$, and $|Q\rangle$ in the magnetic axes x, y, and z are a natural zero-order choice and will be mixed by the small off-diagonal elements of $\mathscr{H}_{ss}$. In zero field, only one of the nine resulting levels will have significant singlet character. At magnetic field strengths that bring other levels into resonance with $|S\rangle$, additional sublevels will gain singlet character, and at these field strengths γ' and γ_S are expected to increase. For instance, assuming an antiferromagnetic ordering of the spin states, resonances could be expected at $g\beta H_1 = E(T) - E(S)$ for T_{-1}, $2g\beta H_2 = E(Q) - E(S)$ for Q_{-2}, and $g\beta H_3 = E(Q) - E(S)$ for Q_{-1}. This would provide information about the energy differences between the singlet, triplet, and quintet levels. Other situations that result from accidental degeneracies of the three spin states can be analyzed similarly, and the reader is referred to an earlier review[1] for additional detail.

Large ^{1}(TT), ^{3}(TT), and ^{5}(TT) Energy Difference

When the differences between the energies E(S), E(T), and E(Q) exceed a few cm^{-1}, no magnetic field effects on

singlet fission and fusion are expected. It is likely that many covalently linked dimers will fall into this category, and one will thus lose a valuable tool for proving that singlet fission is occurring. The larger the energy differences become, the stronger the two constituent triplets will be bound to each other and the harder it will be for them to act independently.

There clearly is a continuous transition from the cases of relatively weak triplet−triplet interaction that we have dealt with so far to a case of interaction so strong that one needs to think in terms of molecular singlet, triplet, and quintet states that do not easily interconvert. In cases in which singlet fission is isoergic or exoergic, $\mathscr{H}_{ss}$ could then play the role that is ordinarily reserved for the spin−orbit coupling Hamiltonian H_{soc} and convert an initially excited S_1 state into long-lived excited states of higher multiplicity. Because $\mathscr{H}_{ss}$ is a tensor of rank two, these could be not only triplets but also quintets. To our knowledge, such behavior has never been reported, but this may simply be a consequence of the fact that very few strongly coupled dimers or oligomers in which singlet fission would be isoergic have been investigated. It is also possible that excited quintet states of closed-shell ground state molecules have already been produced but not noticed.

Density Matrix Treatment

As already noted repeatedly, the neglect of coherences in the time development of the ^{1}(TT) state is a poor approximation. Although the qualitative features of the description we have provided are valid, a quantitative treatment requires the use of the density matrix formalism. This was first developed by Johnson and Merrifield[17] and subsequently greatly improved by Suna.[18] An important conclusion reached by Suna is that the rate constants k_2 and k_{-1} should not be given separate significance and that only their ratio, the branching factor $\varepsilon = k_2/k_{-1}$, has a physical meaning. A useful summary is available[1] and will not be repeated here.

Quenching of Triplets by Spin 1/2 Particles

In concluding section 2.2.2, we noted that a third factor important for the development of an optimal singlet fission sensitizer for solar cells, namely, the independent use of both triplets for charge injection, still remains to be addressed in any detail. So far in this section, we have emphasized the need to minimize the energy differences between the singlet, triplet, and quintet components of the correlated triplet pair on chromophores A and B. This requires a weak coupling between the two chromophores.

The contradiction between the need for a strong coupling in order for singlet fission to be fast and simultaneously for a weak coupling in order for the resulting triplets to be independent is only apparent, because the word "coupling" is being used to describe two different kinds of interactions. The expression for the matrix element $<S_1S_0|\mathscr{H}_{el}|T_1T_1>$ that controls the rate of singlet fission by the direct mechanism is entirely different from expression 18 that controls the diagonal contribution to the splitting of the S, T, and Q states. The interactions mediated by the charge transfer states also differ, and it might well be possible to maximize the rate of singlet fission while minimizing the splitting of the S, T, and Q states. The situation is reminiscent of the very different structural requirements for the optimization of the direct and the mediated singlet fission mechanism discussed in section 2.2.2. So far, this issue does not seem to have received attention in the literature.

However, there is another factor to be considered in the process of effecting two independent double charge separations from the triplet pair $T_A + T_B$ produced by singlet fission. This factor may play a role in molecular dimers, oligomers, and small aggregates or even crystals, as long as the triplets remain in physical proximity and do not separate entirely, say by hopping apart in a crystal. Once the first injection of an electron or a hole into an acceptor has taken place, say from chromophore A, this chromophore will carry a hole or an excess electron. Such spin 1/2 particles have been long known[91−96] to quench triplet excitons in molecular crystals at a magnetic field-dependent[97−99] rate. If the triplet on chromophore B is to produce a charge separation as well, it is important to remove the spin 1/2 particle very rapidly by charge transfer, since otherwise electrostatics will be unfavorable for the second charge separation. If this cannot be achieved fast enough, at least one should make sure that the coupling between A and B is weak and the quenching process is slow.

Triplet quenching by spin 1/2 particles is a large subject, and its magnetic field dependence is merely a side issue for our major topic, singlet fission. It will not be treated exhaustively here, and the reader is referred elsewhere for an early review.[1] However, because it may be of some relevance for the use of singlet fission in solar cells, a brief note appears appropriate.

The initial triplet and doublet can couple to a quartet and a doublet. The final state is a doublet, and the quenching therefore represents a special case of spin-allowed internal conversion. Since $\mathscr{H}_{spin}$ has the ability to mix doublets and quartets in a way that depends on magnetic field because of the presence of the Zeeman term, the overall rate of quenching that starts with a statistical occupancy of triplet and doublet sublevels is field-dependent. A detailed analysis shows that the rate decreases with increasing magnetic field.

To obtain an idea of the structural dependence of the quenching rate, one can evaluate the matrix element of the total electronic Hamiltonian $\mathscr{H}_{el}$ between the initial and final states. We first assume that the double-triplet state has injected an electron from chromophore A, which has thus become a radical cation. The initial state $D^+_{1/2}$ in the quenching process is a doublet obtained by combining the remaining $h_B \rightarrow l_B$ triplet excitation on chromophore B with an unpaired spin hole left in the h_A orbital of chromophore A. Its +1/2 spin component will be approximated as $6^{-1/2}(|h_B\alpha l_B\beta h_A\alpha| + |h_B\beta l_B\alpha h_A\alpha| - 2|h_B\alpha l_B\alpha h_A\beta|)$. The final state $G^+_{1/2}$ is the ground state of the system, and its +1/2 spin component will be approximated as $|h_B\alpha h_B\beta h_A\alpha|$. Alternatively, we can assume that the double triplet state has injected a hole and that chromophore A has become a radical anion, with an extra electron in its orbital l_A, and use similar approximations for the initial state $D^-_{1/2}$ and the final state $G^-_{1/2}$ of the quenching process. The interaction elements for the two cases are

$$<G^-_{1/2}|\mathscr{H}_{el}|D^-_{1/2}> = (3/2)^{1/2}<l_A l_B|e^2/r_{12}|h_B l_A> \quad (29)$$

$$<G^+_{1/2}|\mathscr{H}_{el}|D^+_{1/2}> = (3/2)^{1/2}<h_A h_B|e^2/r_{12}|l_B h_A> \quad (30)$$

These electron repulsion integrals are the already familiar I_1 and I_2, respectively, exactly the two whose difference was

equal to the singlet fission matrix element for the direct mechanism, eq 12. Their structural dependence was already discussed in section 2.2.2. We conclude that any attempt to speed up singlet fission via the direct mechanism by choosing a structure that maximizes these repulsion integrals is likely to speed up the quenching of the triplet excitation that remains after the first injection event, too. The only obvious remedies are either (i) to minimize $<h_A h_B|e^2/r_{12}|l_B\ h_A>$ and maximize $<l_A l_B|e^2/r_{12}|h_B l_A>$ in the case of initial electron injection and to do the opposite in the case of initial hole injection, (ii) to ensure that the triplets separate to a safe distance before any charge separation events, or (iii) to ensure an extremely fast intermolecular transfer of the hole or the extra electron generated in the initial charge separation to a safe distance from the remaining triplet excitation. Another option would be to give up on the direct mechanism of singlet fission altogether, choose a structure that makes the matrix elements in expressions 29 and 30 close to zero, and rely on the mediated mechanism.

3. Molecular Crystals

For over a decade, the phenomenon of singlet fission was only known in molecular crystals, and they still represent the best studied example. In this case, the electronic excitation behaves as a quasiparticle and is referred to as an exciton. Singlet excitons are short-lived (ns) and in some cases might be delocalized over more than one site, and this is still being argued, whereas triplet excitons are long-lived (μs) and tend to be localized on a single site. The existence of a more or less strong Davydov splitting in molecular crystals demonstrates the presence of interactions between inequivalent molecules in a unit cell and excitation delocalization at the initial energy and vertical geometry. It does not necessarily follow that the delocalization persists after site distortion by vibrational relaxation, but evidence has been slowly accumulating that at least in some cases it does.

Although we are not aware of hard evidence, it is often stated that delocalization of singlet excitation probably favors singlet fission. As we will see below, indirect evidence is provided by ultrafast absorption measurements that revealed in several cases that, in the first few ps after a pulsed excitation, singlet fission is especially fast and apparently competes with vibrational relaxation. It is very likely that, during this period, electronic excitation is delocalized more than in a vibrationally equilibrated state.

In a perfect molecular crystal, both types of excitons can, in any event, move by random hopping. The diffusion length is normally much smaller for singlet excitons (tens of nm) than for triplet excitons (tens of μm) because of the difference in their lifetimes. The ability of triplet excitons to diffuse apart reduces the chances of recombination, and it is not surprising that molecular crystals provide the best known examples of efficient singlet fission. Excitons can be trapped and localized by imperfections in the crystal. Some of these are self-induced, especially the formation of excited molecular dimers (excimers). Polycrystalline materials such as evaporated solid films with a high density of imperfections and intergrain boundaries have also been studied; in them singlet fission kinetics can differ significantly from those in a single crystal, and triplet excitons are generally shorter-lived.

We have collected in Table 1 the pertinent spectroscopic data, and in Table 2, the reported triplet quantum yields for the crystalline solids and aggregates in which singlet fission was studied.

Most of the kinetic results described below were obtained at a time when the experimentally available temporal resolution was much lower than is the case nowadays and were not a result of direct time-resolved measurements. With modern lasers, rates of the various processes can be measured directly and do not need to be deduced from fits to approximate models. In the process, the full complexity of the transformations implied by eq 2, possibly including coherences between the nine sublevels, may perhaps be revealed. An early harbinger can be seen in the observation of magnetic field-dependent quantum beats in the fluores-

Table 1. Singlet $E(S_1)$ and Triplet $E(T_1)$ Excitation Energies and Singlet Fission Activation Energies E_a in Solids (eV)

compd.	ref	$E(S_1)$	$E(T_1)$	E_a
1	12		1.83	
2	14	2.40		0.16
2	39		1.25	
2	78			0.24
2	85			0.175
2	102		1.24	
2	103	2.32	1.25	0.18
2	104		1.255	0.175
2	105			0.16
3	106	1.83		
3	107		0.81	
phenazine-**6**	108	2.06	1.10	0.14
fluorene-**6**	108	2.05	1.22	0.40
biphenyl-**6**	109	2.18	1.21	0.24
biphenyl-**7**	109	1.94	1.08	0.21
8	30	2.7	1.4	0−0.1
21	110	1.8	0.85	
22a	111		0.95−1.0	<0.1
22b	111		0.9−0.95	<0.1
22c	112	1.9	1.1	0.3
22d	113		1.07	
24	112, 114, 115	2.6	1.6	0.6
25	112, 116, 117	2.45	1.55	0.65

Table 2. Triplet Quantum Yields Φ_T from Singlet Fission in Solids, Aggregates, and Dimers[a]

compd.	ref	Φ_T (%)
1	118	6
1	119	6
1 doped with **2**	119	8
2	120	200[b]
8	32	200
10	121	30
13[c]	122	∼5
13[d]	123	2
14[e]	123	1.5
15[f]	21	32
15[f]	122	5−10
15[f]	123	30
15[f]	124	35
21	110	90−200[g]
22b	22	∼0.1
22c	125	0.4
27, **28**[h]	126, 127	∼3
30, **31**, **32**[h]	82, 86	1−9

[a] We estimate the accuracy at ±(20−30)% of the quantum yield given. [b] A very crude estimate from the rate constants of disappearance of the initially excited S_1 state in a polycrystalline film and the fluorescence lifetime in solution; the triplet was not detected. [c] Within the bacterium *Rhodobacter sphaeroides*. [d] Within the bacterium *rps. sphaeroides* 2.4.1. [e] Within the bacterium *rps. sphaeroides* GC1. [f] Within the bacterium *r. rubrum*, which contains mainly **15**. [g] The lower limit was obtained from a direct measurement (triplet formed), and the upper limit was obtained from an indirect measurement (ground-state bleach). [h] Dimers in solution.

cence decay of **2**.[100,101] It needs to be noted as well that the singlet fission rate constants obtained by direct transient absorption measurement refer to the rate at which triplet absorption appears, whereas those obtained earlier indirectly by fitting to kinetic models usually refer to the rate at which the initially formed triplet pair ^{1}(TT) dissociates. The latter rate could be substantially slower, and this may account for some of the disagreements.

3.1. Polyacenes

It was emphasized in section 2.2.1 that in alternant hydrocarbons the $S_1 - T_1$ energy gap is particularly likely to be large and does not decrease rapidly with increasing size of the hydrocarbon. Then, it is only a matter of identifying those with a sufficiently small $S_1 - S_0$ gap if one wishes the condition $E(S_1) \geq 2\,E(T_1)$ to be satisfied. This requires the π-electron system to have some minimal size. Annelation of benzene rings beyond naphthalene can lead to different topologies (linear in polyacenes, angular in polyphenes, and peri in pyrene, the rylenes, and elsewhere). It has been long known that the first excitation energies drop the fastest in the polyacene series (a relatively recent comprehensive summary of the spectra and photophysical properties of polyacenes up to hexacene is available[128]). Indeed, although anthracene (**1**) is still colorless, tetracene (**2**) and longer acenes are colored. In **2** the condition $E(S_1) \geq 2\,E(T_1)$ is nearly fulfilled, in pentacene (**3**) it is fulfilled, and one expects it to be fulfilled in the longer acenes as well.

A qualitative rationalization of the rapid reduction in excitation energy in the polyacene series is provided by the recognition that both singlet and triplet valence-bond structures with the maximum number of aromatic sextets are of biradical nature and contribute increasingly to the ground-state wave function as the length of the chromophore grows. As alternant biradicaloids, the longer acenes thus are simultaneously members of both classes identified as favorable in section 2.2.1. Indeed, as argued there for biradicaloids, they also meet the condition $E(T_2) \geq 2\,E(T_1)$.

The nature of the S_1 state in these chromophores changes with their size. The shortest two, benzene and naphthalene, are of class II (as defined in section 2.2.2, with S_1 of L_b nature in the perimeter model description), whereas **1**−**3** are of class I (S_1 is of L_a nature). A recent computational paper has claimed[40] that in **3** a doubly excited state, which can be thought of as a singlet-paired combination of two triplet excitations localized in two halves of the molecule, lies below the L_a state and plays a critical role in singlet fission. We do not believe that this proposed state ordering is correct, as spectra and photophysical parameters leave no doubt that the optically allowed L_a state is the lowest singlet, and this is discussed in more detail in section 3.1.3. However, the computational results are likely to be correct in predicting that the doubly excited state lies at a fairly low energy. Its relative energy might be lower still in even longer polyacenes, and it is conceivable that these chromophores will be of class III, with the doubly excited state as S_1. However, published spectra[128] show no indication that this is true in hexacene.

The primary difficulty with potential practical applications of the longer polyacenes is their chemical and photochemical instability, but perhaps this could be overcome in suitable derivatives. Very little work has been done with polyacenes longer than **3**, and to our knowledge none of it dealt with singlet fission.

3.1.1. Anthracene

Anthracene (**1**) is the shortest member of the polyacene family for which singlet fission in the crystalline state has been observed. Since $E(S_1) = 3.13$ eV[129] and $2E(T_1) = 3.66$,[130] the singlet fission process is endoergic by 0.53 eV, which greatly exceeds kT at room temperature and is the largest endothermicity for any polyacene known to exhibit singlet fission. Excited near its absorption edge, crystalline **1** has a fluorescence quantum yield of 0.95,[131] and singlet fission is not competitive at practical temperatures. However, it is possible to overcome the energy barrier by optical excitation at higher energies.[12,102,118,119,132−135] The nature of the high-energy fissionable state from which singlet fission in **1** occurs has received much attention and depends on both excitation energy and intensity, as described below.

The first suggestion that singlet fission to two triplets takes place was made in 1965 for a crystal of **1**,[12] based on observation of delayed fluorescence resulting from triplet−triplet annihilation. The triplet state was populated (i) directly by exciting hot bands with low-intensity 1.79 eV laser excitation (temperature dependence suggested the existence of an additional thermal activation energy of 0.043 eV before the triplet state is actually reached), (ii) by intersystem crossing upon two-photon absorption of high-intensity 1.79 eV laser light, and (iii) by singlet fission using excitation of hot bands with 3.57 eV light to a vibrationally hot singlet state (temperature dependence suggested the existence of an additional thermal activation energy of 0.087 eV before the singlet fission threshold is actually reached). The energy for singlet fission was thus found to be twice the energy for the directly excited triplet, which was in agreement with previously reported[130] T_1 energy of 1.83 eV. Conclusions regarding the number of photons needed for the excitation were made based on the power dependence of delayed fluorescence intensity.

Later studies focused on the observation of magnetic field effects on prompt and delayed fluorescence of **1** as evidence of singlet fission (section 2.3).[37,102,118,119,132−135] Under magnetic resonance conditions, the prompt fluorescence gains intensity as excitation energy increases.[134,136] Fine structure in the action spectrum of $\Delta F/F$ (defined as $[F(H) - F(0)]/F(0)$, cf. section 2.3) was initially attributed[136] to a progression in symmetric C−H vibration modes as suggested previously for tetracene (**2**),[137] but this interpretation was not supported by a later study of the action spectrum of perdeuterated **1**.[138]

Preponderant evidence suggests that fission in **1** occurs from vibrationally hot states, but a charge transfer state has also been considered as a possible intermediate.[139,140] Fission from the lowest charge transfer state would have an activation energy of ∼0.2 eV.[140] Fission can certainly be initiated by generation of a charge transfer state, as demonstrated by magnetic field effects on electroluminescence.[139,140] The effects of changes in magnetic field orientation observed in delayed electroluminescence were the same but ∼30 times weaker than those observed for optically excited prompt fluorescence.[139] This was assigned to fission of the charge transfer state, and it was estimated that ∼5% of charge transfer excitons undergo fission. However, in a study of optically excited **1**, an initial belief that a charge transfer state was likely the fissionable state[134] was later abandoned in favor of vibrationally hot lower electronic states, based on excitation energy dependence of prompt fluorescence in both **1** and **2** at 77 K.[102] At this temperature, fission from

the first charge transfer state should not be thermally allowed for **1**, $E(^1CT) = 3.4$ eV, but would be for **2**, $E(^1CT) = 2.9$ eV. Yet the low-temperature results for the former are very similar to those obtained at room temperature, and the increases in $\Delta F/F$ for **1** and **2** are of the same order of magnitude. For **1**, the threshold energy for the initial rise of $\Delta F/F$ is 3.66 eV, and for **2**, it is 2.48 eV, values close to twice the respective triplet excitation energies.[102] This interpretation has gained general acceptance.[12,118,119]

In single crystals of **1** excited at 4.89 eV, the triplet quantum yield due to singlet fission was 6%, a value compatible with fast vibrational relaxation.[119] Fitting the dependence of prompt fluorescence intensity on magnetic field angle to the Johnson−Merrifield model yielded $k_{-1} = 3 \times 10^9\ s^{-1}$ for the dissociation of the correlated triplet pair. Upon excitation of a crystal of **1** doped with **2** at 3.20 eV, which is below $2E(T_1)$, homofission of **1** does not occur, but this energy is sufficient for **1** + **2** heterofission.[119] In one report,[118] no evidence of singlet fission from a directly excited hot singlet was found even though the 4.03 eV excitation energy was above twice the triplet energy. The reason for this discrepancy is unclear.

A vibrationally hot singlet state of **1** may also be reached by the fusion of two excited singlets, as evidenced by a decrease in fluorescence quantum yield and a nonexponential fluorescence decay at sufficiently high excitation densities. Under intense 4.03 eV excitation[118] the characteristic magnetic field dependence of fluorescence intensity is observed only under conditions where singlet−singlet fusion is dominant, indicating that a highly excited singlet is the species that undergoes fission. Highly excited singlets have also been produced in the paths of high-energy protons used to irradiate a crystal of **1**.[141] Fission from these singlets was observed using fine-structure modulation of radioluminescence.

Although the Johnson−Merrifield theory explains many of the observed magnetic field effects in an anthracene single crystal,[118,134] deviations are found below ~75 K, where the magnetic field effects on fission and fusion are no longer inverses of each other.[132] The suggested rationalization is that one of the two triplet excitons becomes trapped and the traps may be deeper in the case of fusion than in fission.

When very high excitation energies are used, triplet pairs may be formed in crystalline **1** through charged intermediates.[133,135,142] The ionization threshold is 5.75 eV, and the probability of ionization or autoionization increases sharply between ~5 and 10 eV. Magnetic field effects on prompt fluorescence[133] and a time-resolved magnetic modulated fluorescence technique that separates the prompt and the delayed component[135] have been used to observe the formation of triplet pairs. The delayed fluorescence component and the negative effect of magnetic field increase with increasing excitation energy. Autoionization is believed to form triplet pairs from highly excited singlets (S**), with electron hole pairs (*eh*) as intermediates:

$$S_0 + h\nu \rightarrow (S^{**}) \rightarrow {}^1(eh)^*$$

$${}^1(eh)^* + S_0 \rightarrow {}^1[{}^3(eh), T]$$

$${}^1[{}^3(eh), T] \rightarrow {}^1(TT)$$

3.1.2. Tetracene

With regard to singlet fission, tetracene (**2**) has been the prototypical and by far the most thoroughly investigated molecular crystal. The notion that singlet fission represents a decay channel for singlet excitons in **2** was first proposed in 1968[13] in response to earlier observations[152] of temperature dependence of fluorescence in crystalline **1**, and a fission rate of $4 \times 10^{10}-10^{12}\ s^{-1}$ was estimated. Much subsequent work has supported the notion that both the fission of the singlet exciton into two triplet excitons and the reverse process of fusion of two triplet excitons into one singlet exciton are fast in solid **2** at room temperature. As a result of their interplay, the photophysical behavior of crystalline **2** is complicated and excitation density dependent.

Table 3. Rate Constants for Singlet Fission in Solids[a]

compd.	ref	fission rate const.[a] (s^{-1})
2	13	$4 \times 10^{10}-10^{12}$ (estimate)
2	35	2.2×10^9
2	37	6.7×10^9
2	39	2×10^9
2	78	6.4×10^8 [b]
2	85	2.2×10^9
2	90	2×10^8
2	101	5.8×10^9
2	104	$\sim 10^{11}$
2	105	3×10^9, 4.3×10^9 [d]
2	120	1.1×10^{11}
2	143	5.7×10^9
2	144	5.1×10^9 [b]
2	145	2.2×10^9 [c]
2	146	2.1×10^9
2	147	$\sim 2 \times 10^{10}$
2	148	8.1×10^9
3	149	$> 2 \times 10^{13}$
3	150	1.3×10^{13}
3	151	$> 5 \times 10^{12}$
8	32	4×10^{10}, 5×10^{11}
21	110	$> 2.5 \times 10^{11}$
27	126, 127	2.8×10^6
28	126, 127	4.0×10^6

[a] For **2**, we consider values near $10^{10}\ s^{-1}$ most likely to be correct. [b] Value calculated from the published data using a concentration of 3.37×10^{21} molecules of **2** per cm^{-3} of solid.[155] [c] Value at 300 K calculated from published infinite temperature value. [d] Fit to data published in ref 14.

The bulk of the work on singlet fission in neat **2** is now several decades old, and in spite of all the effort invested, the quantum yield of the resulting triplets has apparently never been directly measured. Early available indirect evidence, primarily based on measurements of prompt and delayed fluorescence, suggested that the yield must be high at room temperature, surely above 100% and possibly close to 200%. The most recent estimate[120] of 200% is based on a directly measured rate of S_1 decay, assumed to be due exclusively to singlet fission (lifetime of 9.2 ps) and the further assumption that all competing processes provide the same sum of decay rate constants as they do for an isolated molecule of **2** in solution (fluorescence lifetime of 4.2 ns). It is clearly an upper limit, because there is a larger number of competing decay channels in the neat solid than there is in the isolated molecule in solution. The recent measurements by ultrafast spectroscopic methods[120,147,153,154] support the overall picture developed in the early days but indicate that the photophysics of crystalline **2** is more complicated than was initially believed. As noted above, within the approximate Johnson−Merrifield description,[17] the singlet fission rate constants obtained more recently from ultrafast absorption measurements refer to the formation of the $^1(TT)$ pair, whereas most of the indirect previous determinations based on model fitting referred to its dissociation.

Table 4. Diffusion Coefficients in the *ab* Plane (D_{ab}) and in the *c* Direction (D_c) and In-Plane (Ψ_{in}) and Out-of-Plane (Ψ_{out}) Hopping Rates

compd.	ref	D_{ab}/cm^2 s^{-1}	D_c/cm^2 s^{-1}	Ψ_{in}/s^{-1}	Ψ_{out}/s^{-1}
2	85[b]	4×10^{-3}	10^{-6}	6×10^{12}	6×10^{7}
2	85[b]	4×10^{-4}	2×10^{-6}	7×10^{11}	10^{8}
2	85[b]	6×10^{-5}	10^{-7}	10^{11}	10^{7}
2	101	5.3×10^{-5}		1.31×10^{10}	6×10^{6}
2	143[a]	4.8×10^{-2}			
2	146	2×10^{-3}			
2	161[c]	4×10^{-3}			
2	162		3.3×10^{-3}		

[a] Value for D_{ab} was extrapolated to infinite temperature. [b] Several sets of parameters were tried. [c] This value was calculated for the *b* direction and may be viewed as a lower limit for D_{ab}. We suspect that it is the most reliable of the results reported.

In perusing the old literature on singlet fission in **2**, the reader needs to be aware of two potential pitfalls. The first is minor, in that different authors favor different units for first-order rate constants. Some use s^{-1} whereas others use $cm^3\ s^{-1}$, and the two are related by the density of molecules of **2** in its crystal, $3.37 \times 10^{21}\ cm^{-3}$.[155] We have converted all results to s^{-1}. The second complication is more serious, in that most of the published rate constants have been derived using the approximate Johnson−Merrifield theory[17] and their absolute values need to be taken with a large grain of salt (section 2.1). Strictly speaking, the rate constants k_{-1} and k_2 defined in eq 2 do not have separate significance and only their ratio $\varepsilon = k_2/k_{-1}$ is meaningful. The inadequacy of the Johnson−Merrifield model for a quantitative description is perhaps best illustrated by noting[90] that it permits a fit of the dependence of fluorescence intensity of **2** on the orientation of a static magnetic field both in the presence and in the absence of microwave radiation, but the resulting rate constants k_{-1} differ by an order of magnitude. Even fitting to the more accurate Suna model[18] requires assumptions that lead to considerable uncertainties. The widely varying published values of singlet fission rate constants (Table 3) clearly represent no more than order-of-magnitude estimates. The most recent directly measured S_1 lifetimes favor the higher values among the previously reported rates.

The spread in the values of the diffusion coefficients of triplet exciton determined for **2** by various methods is huge (Table 4). Even though the numerical values of parameters derived from fitting to approximate models are of limited utility, it seemed worthwhile to summarize the results because there is no reason to question the underlying experimental data.

Thermally Activated Singlet Fission. An activation barrier to fission is expected, since the process is slightly endoergic. The best determination of the endoergicity probably is the observation of the 0−0 transition of $S_0 \rightarrow T_1$ excitation at 1.25 eV and that of $S_1 \rightarrow S_0$ emission at 2.32 eV, yielding 0.18 eV for the activation energy.[103] Other determinations of the $2E(T_1) - E(S_1)$ energy that appear reliable range from 0.15 to 0.24 eV[14,78,85,103,104,152,162] (additional old values of activation energy for fluorescence quenching are 0.02[156] and 0.10[157] eV). Above 160 K, this energy barrier can be overcome thermally fast enough for fission to compete successfully with fluorescence, and at room temperature, fission is believed to be the fate of nearly all singlet excitons. This accounts for the low room-temperature fluorescence quantum yield of crystalline **2** (0.002)[158] compared with **1** (0.95).[131] A much higher value of room-temperature fluorescence quantum yield (0.15) was reported more recently by one set of authors,[153] possibly because they were investigating another crystal form, but the results may be unreliable since one of the authors was subsequently shown to have falsified a large amount of other experimental data.[159]

Fluorescence. The fluorescence of single crystals of **2** has been investigated by many authors. With ps pulsed laser excitation, a fluorescence rise time of 12 ps and decay time of 145 ps were found.[143] From the fluorescence decay time, the fission rate constant was calculated to be $5.7 \times 10^9\ s^{-1}$ at 300 K and $1.7 \times 10^{13}\ s^{-1}$ at infinite temperature. From the latter, the hopping rate in the *ab* plane is $10^{13}\ s^{-1}$, and the diffusion coefficient for the *ab* plane (D_{ab}, "in-plane") is $4.8 \times 10^{-2}\ cm^2\ s^{-1}$, ~100 times larger than for the *c* direction (D_c, "out-of-plane"). The diffusion of triplet excitons is known to be highly anisotropic, and D_{ab} has been variously reported to be 100−4000 times larger than D_c.[35,85,143] These rates are important for the description of singlet fission by the Suna model.[18]

Using less intense synchrotron radiation, biexponential decay was observed.[160] The fast component was fitted to a lifetime of 0.2 ns and is consistent with other measurements.[143−145] The slow component had a lifetime of 1.7 ns and was later[37] attributed to a slow decay of triplet exciton pairs. The authors[160] argued convincingly that a previously reported even slower component of fluorescence with a 10−14 ns lifetime observed at 77 K[144] and 100−300 K[145] was an artifact due to nonlinear effects caused by high laser excitation intensity (the original attribution was to emission from a second level separated by 0.05 eV,[145] perhaps due to a different crystalline form at grain boundaries, or a monomer-like and a dimer-like form within the crystal). The fast fluorescence decay obtained with synchrotron radiation[160] was later fitted[37] to the Suna diffusion model,[18] taking into account the possibility of fusion of triplet exciton pairs into a singlet exciton. The fit yielded an in-plane hopping rate (Ψ_{in}) of $2 \times 10^{11}\ s^{-1}$, an out-of-plane hopping rate (Ψ_{out}) of $2.8 \times 10^9\ s^{-1}$, and a fission rate constant of $6.7 \times 10^9\ s^{-1}$.

A later study of fluorescence decay in **2** using a series of excitation densities separated the effects due to singlet exciton annihilation.[146] The singlet exciton lifetime was 300 ps at 293 K. No slow component was observable in single crystals of **2** (<1% of the total). Modeling yielded a fission rate constant of $2.1 \times 10^9\ s^{-1}$ and a two-dimensional diffusion rate constant of $2 \times 10^{-3}\ cm^2\ s^{-1}$. In polycrystalline films a component with a 1−2 ns lifetime was observed and was attributed to the presence of traps. Traps were also suggested as a possible source of the long-lived component observed by earlier authors.

The most recent measurement[120] of time-resolved photoluminescence was performed on polycrystalline films and single crystals at fluences that were below the threshold for exciton−exciton annihilation. In films, 90% of fluorescence decayed with a time constant of 80 ps and the remainder decayed with a time constant of 55 ns, attributed to delayed fluorescence resulting from triplet recombination. The longer decay time varied with film quality and thickness. In a single crystal, this time was estimated at 5−10 μs. The variation was rationalized as due to the migration of triplet excitons to grain boundaries or other defects followed by quenching.

Diffusion coefficients were determined[161] using a transmission grating to create excitons that were unevenly spatially distributed and measuring delayed fluorescence due to triplet fission. Kinetic treatment of the data yielded a room-

Table 5. Level Crossing Resonances in 2 for Rotation of a Magnetic Field Direction[a] and Zero-Field Splitting Parameters *D*, *E*, *D, and *E**[b]**

ref	res. angle/ deg	D/cm^{-1}	E/cm^{-1}	D^*/cm^{-1}	E^*/cm^{-1}	*E/D*
14	23.5, −30					−0.077
15	18, −34					−0.095
35	22, −30					
83[c]		0.0520	−0.0052	−0.0062	0.0248	−0.1
90[d]	22.7, −30.6	0.0515	−0.00455	−0.00703	0.0241	−0.088
163				−0.00703	0.0241	

[a] Rotation about the *b* axis, angle measured relative to the *ab* plane. [b] *D* and *E* are molecular properties, while *D** and *E** are exciton properties (averaged by rapid exciton hopping over the two independent lattice sites). [c] From EPR. [d] We consider these to be the most reliable values. The reported error margins were ±0.0005 for *D* and ±0.00005 for *E*.

temperature diffusion coefficient for the *b* direction that was stated to be 4×10^{-3} cm^2 s^{-1}. The ratio of diffusion coefficients in the *ab* plane of **2** relative to **1** was found to be equal to ∼30. The diffusion length of singlet excitons in the *c* direction was determined for **2** by oxidizing the surface molecules or coating the crystal surface with capri blue.[162] Both of these treatments provide surface fluorescence quenchers, and observation of fluorescence at various excitation depths then provides information about the diffusion length. The diffusion length increased as temperature was reduced. Since the diffusion coefficient was temperature independent, this was attributed to an increase in the singlet lifetime at lower temperatures, where singlet fission rate was reduced. The calculated value of D_c of 3.3×10^{-3} cm^2 s^{-1} was about 4 times higher than that of **1**, as would be expected from the increased Davydov splitting. The activation energy for singlet fission determined in this experiment was 0.175 eV.

Magnetic Field Effects (cf. section 2.3). In single crystals of **2**, level crossing resonances occur with a static magnetic field orientation reported[90] at ∼23 and ∼−31° from the *b* axis in the *ab* plane, yielding a ratio of zero-field splitting parameters $E/D = -0.09$ (Table 5). The most detailed investigations[85] recorded prompt fluorescence in the strong field limit (5 kG), varying the direction of the magnetic field in the *a′b*, *bc′*, and *ac′* planes, as well as two planes simultaneously. At higher light intensities, the magnetic field effect was smaller. The results showed that the excitons were free as opposed to trapped and were used to check the validity of the Johnson−Merrifield[17] and Suna[18] theories for fission and fusion. Both theories account well for the position of resonance in the orientation dependence of fluorescence intensity, but only the more complicated Suna theory accounts for line shapes. From the Johnson and Merrifield model, the time constant for the dissociation of the triplet pair was calculated to be 2.2×10^9 s^{-1}. Several sets of adjustable parameters used in fitting to the Suna model were discussed. For this model, time constants for the dissociation of the triplet pair ranged from 3×10^9 to 2×10^{10} s^{-1}. The diffusion constant in the *ab* plane is likely to be larger and at least as anisotropic as that of **1** (anisotropies in excess of 300). In **2**, an initial increase of the magnetic field strength *H* to 200 G reduces the relative intensity of prompt fluorescence *F*(*H*) to a minimum of ∼95% of the zero field value *F*(0). A further augmentation of *H* increases *F*(*H*) to a saturation value variously reported as 127% at fields above 3 kG[15] or 128−137% at 2 kG.[14] The saturation value remains constant over excitation energies of 2.6−4.6 eV.[14] The magnetic field effect decreases with temperature until ultimately below 160 K it is no longer observable, and a singlet fission activation energy of 0.16 eV has been deduced.[14]

As explained in section 2.3, an especially accurate determination of the zero-field splitting parameters *D* and *E* is possible by optically detected magnetic resonance (ODMR), which combines the use of a static magnetic field with a microwave field. Two earlier studies[88,89] were superseded by a subsequent most complete study,[90] which employed static magnetic fields (2.35−4.35 kG) in the *a′b* plane of a single crystal of **2** and synchronously detected the reduction of intensity of fluorescence excited with 488 nm laser light upon application of 6 W of square modulated 9.38 GHz radiation. Two principal resonance lines and an uninterpreted weak central line were observed at each field orientation as a function of static magnetic field strength. The principal lines coalesced at level crossing resonances, and an analysis yielded the results shown in Table 5. The Johnson−Merrifield theory accounted for the positions but not for the heights and widths of the resonances and yielded a 3 ns lifetime for the triplet pair state ^{1}(TT) and a rate constant for triplet separation $k_{-1} = 2 \times 10^8$ s^{-1}. This rate constant is an order of magnitude smaller than that derived from static measurements by some of the same authors ($k_{-1} = 2.2 \times 10^9$ s^{-1}),[35,85] further demonstrating the shortcomings of the Johnson−Merrifield[17] kinetic model.

An observation of both prompt and delayed fluorescence provides a simultaneous view of the concurrent processes of singlet exciton fission and triplet exciton fusion.[78] For the study of fission, 2.84 eV excitation was used and prompt fluorescence was monitored, and for the study of fusion, triplets were excited directly with 1.24−1.77 eV light and delayed fluorescence was monitored. The observed magnetic field effects were opposite for the two types of measurement. The deduced singlet lifetime was 1.45 ns, and the activation energy was 0.24 eV. At 273 K, the fission rate constant was 6.4×10^8 s^{-1}.

Photoconductivity in crystalline **2** is caused by the detrapping of carriers either by singlet or triplet excitons. It is thus not surprising that it is affected by magnetic field. The situation is complicated because the field affects both the rate of singlet fission and the rate of the triplet−doublet interaction that leads to detrapping.[98] At 3.1 eV excitation energy, singlet excitons are produced and undergo fission. Photoconductivity is enhanced in the magnetic field and shows the same dependence on field orientation as fluorescence. Level crossing resonances are observed and fit the *E/D* value[14] listed in Table 5. At these resonances, the singlet fission rate is decreased and the concentration of singlet excitons is increased. Singlet excitons detrap holes efficiently and cause the conductivity to increase. At 2.19 eV excitation energy, triplet excitons are being produced in **2** by intersystem crossing. In this case, level crossing resonances are again observed but the effect on hole conductivity is negative. The proposed interpretation is that the interaction between the triplets and the carriers (holes) is reduced in the magnetic field, thereby reducing hole detrapping.

The interaction between triplets and charge carriers also impacts the observed behavior of electroluminescence in a magnetic field.[164] Electroluminescence from **2** displays a similar dependence on field orientation as does photoluminescence of **2** excited at 3.39 eV, suggesting that fission occurs from charge transfer states. At the red edge of the electroluminescence spectrum, a delayed component due to

triplet−triplet annihilation has a greater relative contribution. Delayed electroluminescence is affected by the triplet−charge carrier interaction rate, which has the same dependence on magnetic field direction as the triplet−triplet interaction, but is enhanced at both high and low field strengths. As the proportion of delayed electroluminescence increases, the low-field decrease in the total electroluminescence is reduced until it is no longer observable.

The role of singlet excitons in detrapping and the role of the triplet-hole interaction strength were subsequently studied by photoconductivity detected magnetic resonance (PDMR) and optically detected magnetic resonance (ODMR).[163] In the PDMR experiment, holes were injected into **2** and it was simultaneously excited into the singlet band. Characteristic peaks in photoconductivity were observed as the magnetic field modulated the strength of triplet−doublet interaction. The effect of magnetic field on the total photocurrent was expressed as the sum of the effect on detrapping photocurrent and on fluorescence. To examine the relative contributions of detrapping by triplets and singlets to the total photocurrent response, PDMR and ODMR were used to determine changes in triplet−doublet and triplet−triplet interaction rates, respectively. The conclusion was that the detrapping of carriers by triplets causes a larger effect than detrapping by singlets. Suna's kinematic model[18] was used to fit the observed photocurrent, and the deduced fine structure zero-field splitting parameters D^* and E^* were in reasonable agreement with values obtained from electron paramagnetic resonance measurements[83] (Table 5).

Excitation with α Particles. Bombardment of crystals of **2** with α particles creates a situation that differs from the more common optical excitation, in that both singlet and triplet excitons are initially produced within the particle tracks.[165] Superexcited states are created by a ∼10 eV Å^{-1} energy deposition and ∼30% of them decay to singlet excitons directly, whereas the remaining ∼70% form electron−hole pairs, which then recombine to form both singlet and triplet excitons. At the resulting high excitation density (∼10^{19} excitons cm^{-3}), random recombination of electrons and holes dominates over geminate recombination, creating a 3:1 ratio of triplets to singlets. The directly formed singlets contribute to prompt scintillation, whereas singlets formed from the fusion of two triplets contribute to delayed scintillation. Because singlets and triplets are both formed, a fission-type magnetic field dependence of scintillation intensity is observed at room temperature, but it is weaker than that observed upon optical excitation of pure singlets (∼3% vs ∼35%) because of the simultaneous presence of fission and fusion effects. At 148 K, a fusion-type magnetic field dependence of scintillation intensity is observed. The authors concluded that, at low temperature, delayed scintillation is responsible for ∼50% of the total, as opposed to only ∼10% at room temperature. At 150 K, **1** and **2** have similar values of scintillation efficiency as well as a similar magnetic field effect. Extended irradiation of a crystal of **2** causes the formation of permanent quenchers, which provide an important decay path for singlet excitons. A fusion-like dependence of scintillation is then observed at room temperature.

Optically Activated Singlet Fission−Continuous Excitation. At low temperatures, thermally activated singlet fission in **2** is suppressed. The energy barrier can still be overcome optically,[39,102,137] and the results show that singlet fission is competitive with intramolecular vibrational energy relaxation. Upon excitation at 77 K, the threshold energy for the magnetic field effect on prompt fluorescence of **2** is 2.48 eV, or approximately twice the T_1 excitation energy.[102] The temperature dependence of the change in fluorescence efficiency with increasing excitation energy, as well as a 10 times smaller fission-induced decrease in fluorescence intensity than expected, led to a dismissal of the initially entertained assumption that the same vibrationally excited first singlet state of **2** is reached by optical and by thermal excitation.[104] At temperatures too low for significant thermally induced fission in **2**, a drop in the yield of photoinduced fluorescence is anticipated when the excitation energy reaches or exceeds $E(2T_1)$. Indeed, at 183 K, fluorescence intensity decreased sharply at 2.51 eV, and this was attributed to the onset of singlet fission.[104] The decrease in fluorescence intensity was temperature dependent and varied from ∼10% below 200 K to less than the experimental error at room temperature. The activation energy was determined to be 0.175 eV, and the fission rate constant was estimated as 10^{11} s^{-1}. The authors concluded that the intermediate state was not the same for thermally and optically induced fission and that favorable changes in molecular orientation in the case of thermally induced fission may cause the increased efficiency relative to optically induced fission. Somewhat surprisingly, it appears that intramolecular vibrational energy redistribution is not fast enough to randomize the optically introduced vibrational energy on a 10 ps time scale.

Subsequent measurement of prompt fluorescence[39] confirmed the onset of singlet fission at 2.5 eV, but these authors deduced a much smaller fission rate constant of 2×10^9 s^{-1}, even more difficult to reconcile with the conclusion that it is competitive with intramolecular vibrational energy redistribution. Additional increases in the magnetic field effect at 2.9 and 3.2 eV were noted, with a relatively flat region in between, and it was concluded that some vibrational modes probably are more significant for the fission process than others.

The stepwise increase in the magnetic field effect on prompt fluorescence has been attributed[137] to harmonics of a totally symmetric C−H stretch of **2** at 0.37 eV. Using the coupling constants g_1 and g_2 appropriate for each of the two possible crystal sites in **2**, the expected intensities were I(2.48 eV):I(2.85 eV):I(3.22 eV) = 1:(1 + g_1^2 + g_2^2):(1 + g_1^2 + g_2^2 + 1/2g_1^4 + 1/2g_2^4). Assuming $g_1^2 + g_2^2$ is on the order of 1, the intensity ratios are 1:2:2.5, in good agreement with the observed structure of the action spectrum. However, this interpretation is questionable in light of the negative result obtained subsequently[138] when **1** and perdeuterated **1**-d_{10} were compared.

Equations for the on-resonance and off-resonance magnetic field induced fluorescence enhancement were also presented.[137] In this case, the vibrationally hot singlet of **2** undergoes fission to produce a vibrationally hot correlated triplet pair. The fluorescence enhancement was shown to depend on the branching ratio between re-fusion to the singlet and vibrational relaxation of the triplet pair, and also on the ratio of the rates of vibrational relaxation and fission. On-resonance conditions produce the largest fluorescence enhancement for a given branching ratio. The enhancement becomes zero as the branching ratio approaches zero or infinity.

Optically Activated Singlet Fission−Pulsed Excitation. This type of measurement provides additional information. Pulsed laser excitation with sub-ns resolution permitted the

observation of quantum beats in the fluorescence decay of single crystals of **2**,[100,101] and they were attributed to the effect of spin evolution on geminate re-fusion of triplet pairs produced by singlet fission. The quantum beats were studied as a function of magnetic field orientation. In one study of triplet−triplet interactions in **2**, they were found to be negligible for the conditions used.[100] In a second study, a two-dimensional random walk model was used to fit the fluorescence decay.[101] The resulting rate constants were as follows: singlet fission, 5.8×10^9 s^{-1}; in-plane hopping, 1.31×10^{10} s^{-1}; and out-of-plane hopping, 6×10^6 s^{-1}. The in-plane diffusion constant was 5.3×10^{-5} cm^2 s^{-1}. The authors considered their smaller value of the hopping rate constant to be an improvement over that obtained earlier[37] from a biexponential fit over a shorter time period.

The results of an initial room-temperature examination of photoinduced excited state absorptions by single crystals of **2** after 100 fs pulse excitation were independent of the excitation energy in the range examined, 2.6−3.6 eV, for times longer than 1 ps.[153] They were interpreted in terms of a sub-ps formation of a vibrationally relaxed S_1 exciton characterized by absorption bands at 1.0 and 1.8 eV. Its ∼1 ps decay time matched the decay of stimulated emission. A fraction of the S_1 excitons had a lifetime of 156 ps at room temperature and 310 ps at 77 K. Their decay was accompanied by the formation of an intermediate with a broad absorption band at 1.5−2.1 eV and a temperature-independent 180 ns lifetime determined by frequency modulation spectroscopy. This absorption band preserved its initial polarization as would be expected for the triplet. The authors indeed considered the assignment of the long-lived state to a triplet exciton but were uncomfortable with the observed lifetime and, especially, low energy of the observed absorption peaks (in solution, the triplet absorption of **2** is characterized by strong bands at 2.6−2.9 eV[166,167] and there is no detectable absorption at lower energies). They tentatively assigned it to trapped (presumably singlet) excitons instead and suggested that singlet fission is not nearly as prevalent in crystalline **2** as had been generally believed. We believe that the evidence for extensive singlet fission is overwhelming, but share the concern of these authors regarding the assignment of the observed absorption band to the triplet of **2**, in spite of the long lifetime. We would expect the triplet absorption to be much closer to its spectral location in solution, and wonder if it is perhaps not being observed in the solid because of a poor alignment of its transition moment with the electric field of the monitoring beam. Because it was subsequently found that one of the authors falsified results in numerous publications,[159] not only the interpretations but also the results could be best viewed with some skepticism.

However, more recently, the observations have gained additional credence in a reinvestigation of photoinduced $T_1 \rightarrow T_n$ and $S_1 \rightarrow S_n$ absorptions by single crystals of **2** after fs pulse excitation.[147] The 3.0 eV excitation energy used lies well above the ∼2.4 eV absorption threshold. The 1.5−2.1 eV absorption band of a long-lived transient, peaking at ∼1.7 eV, was again observed. Without commenting on the reservations expressed in the earlier publication, the later authors assigned it to absorption by the T_1 state based on its lifetime, much longer than 1 ns. We share the doubts expressed by the initial investigators.[153]

The conversion from S_1 to the species absorbing at 1.5−2.1 eV takes place on two different time scales.[147] A temperature-independent fast process occurs in ∼0.3 ps, and a thermally activated slower component, which disappeared at low temperatures and had an activation energy of 0.07 eV, occurs on a time scale of ∼50 ps. The activation energy is less than half of that nowadays considered correct for singlet fission in **2** (see above), casting further doubt on the assignment of the observed species to the triplet exciton. The fast component was attributed to singlet fission from an optically excited singlet state ($S_n \rightarrow 2\ T_1$), where it seems to us S_n could also be a vibrationally hot S_1 state. The time scale of the slow component coincided with the decay of the photoinduced $S_1 \rightarrow S_n$ absorption and it was attributed to thermally activated fission ($S_1 \rightarrow 2\ T_1$) from the relaxed S_1 state coexisting in quasiequilibrium with the T_1 state. At room temperature, the slow and the fast components were each responsible for about half of T_1 formation.

A somewhat more satisfactory set of interpretations has been suggested very recently[120] in a study that compared room-temperature fs transient absorption of thin films of **2** deposited on SiO_2 and solution of **2** in toluene with their time-resolved photoluminescence to provide a more consistent picture of excited state dynamics. The properties of the thin films were distinctly different from those observed with single crystals, both by these[120] and mostly by previous[147,153] authors. The difference was tentatively attributed to inherently different morphologies. In contrast to the previous work, in this latest study attention was paid to the potentially important effects of molecular orientation in the solids.

The transient absorption spectrum of **2** in solution excited at 3.02 eV after 300 fs included S_0 ground-state bleach and stimulated emission as well as absorption from S_1. The features associated with S_1 could be fitted with a decay constant of 4.2 ns.[120] The spectrum obtained after a 20 ns delay agreed with the previously known T_1 absorption, which has a maximum at 2.67 eV and negligible intensity at energies below ∼2.5 eV.

Upon excitation of a thin film of **2** at 3.10 eV, 90% of the resulting fluorescence decayed with an 80 ps time constant. The remainder decayed with a time constant of 55 ns and was attributed to delayed fluorescence resulting from triplet−triplet fusion. A kinetic model of the fluorescence decay was consistent with singlet fission being the primary relaxation pathway.

In the first few ps, the transient absorption of the thin film was dominated by a negative peak at 2.33 eV, which decayed with a 9.2 ps time constant and was attributed to stimulated emission from an initially excited superradiant singlet state S_1 delocalized over several molecules. An absorption at 1.91 eV attributed to a $S_1 \rightarrow S_n$ transition decayed with the same time constant. Assuming that the 9.2 ps decay time (fission rate constant 1.1×10^{11} s^{-1}) is solely due to singlet fission and comparing it with the 4.2 ns decay time of the isolated molecule of **2** in solution, where fission is absent, yielded a crude estimate of the triplet yield as ∼200%. This estimate requires a further assumption that there are no important decay channels in the solid in addition to those present in the isolated molecule, which is somewhat questionable. The decay of the bleach at long delays and the decay of delayed fluorescence both have a lifetime of 33 ns, consistent with a high triplet yield. It was suggested that the longer 80 ps decay time observed in photoluminescence measurements may be due to fluorescence from a superradiant defect state that is not seen in absorption and not to the initially populated S_1

state. The presence of a defect state was consistent with a calculated increase in localization based on line shapes.

Surprisingly, the long-lived transient absorption at 1.5−2.1 eV, which dominates the transient spectra of crystals of **2**, was not observed in the thin films. No explanation of the difference has been offered, although it may hold the key to the correct assignment of this presently disputed feature, which the authors considered unlikely to be due to absorption by T_1, as do we. Triplet−triplet absorption is easily observed in solution at 2.67 eV, and was not observed in the thin film. The authors put forward two possible explanations for its absence. The first is that the $S_0 \rightarrow S_1$ transition is exciton coupled (superradiant) in the solid, but the $T_1 \rightarrow T_n$ and $S_1 \rightarrow S_n$ transitions are not. The resulting enhancement of the bleach then covers up the triplet−triplet absorption. The second explanation is based on a preferred orientation of the molecules of **2** in their polycrystalline sample, generally believed to deposit with the *ab* crystal plane parallel to the substrate surface. If the molecular orientation is the same as in a single crystal, the long axis is at an angle of 21° to the surface normal, and for monitoring at normal incidence, the intensity of the long-axis polarized $T_1 \rightarrow T_n$ transitions is reduced by a factor of 8 relative to the short-axis polarized $S_0 \rightarrow S_1$ transition. The authors suggest that an even smaller angle with the surface normal may be more realistic due to interaction with the surface. For an angle of 10° to the surface normal, the relative intensity of $T_1 \rightarrow T_n$ transitions would be reduced by a factor of 60. This second interpretation, which seems preferable to us, could be easily tested by measurements at oblique incidence, which ought to permit a direct observation of the triplet state. Such measurements would also provide a verification of the assumption that the 9.2 ps decay of S_1 is due to triplet formation by singlet fission. In summary, we believe that several aspects of the interpretation of the results of ultrafast transient spectroscopy on solid **2** remain uncertain and that the matter deserves additional attention.

Effects of Light Intensity. The fluorescence quantum yield in crystalline **2** is a function of the exciting light intensity.[14,144,168] The results of different authors do not always agree because the observed intensity dependence may itself be a function of the absorption depth for a particular excitation energy. In one case,[145] no fluorescence intensity variation was observed over an intensity range of 3×10^{14} to 1×10^{18} photons cm^{-2} s^{-1}, and this was attributed to a greater absorption depth for the excitation energy used and therefore a lower density of triplets. At room temperature, but not at 77 K, the fluorescence quantum yield has two distinct values.[14] In the region of $10^{15}-10^{17}$ quanta cm^{-2}, it is 1.4 times higher than at intensities below 10^{15} quanta cm^{-2}.[14] The same authors[144] reported no effect below 210 K and, above this temperature, an increase in the quantum yield with increasing excitation intensity. In the low-intensity regime ($<5\times 10^{14}$ quanta cm^{-2} s^{-1}), the quantum yield was constant. In contrast to another report,[14] in the high-intensity regime ($>2 \times 10^{16}$ quanta cm^{-2} s^{-1}), the quantum yield was found to increase with increasing intensity. This effect was attributed to high triplet densities created in the high-intensity regime, with their fusion leading to an increased fluorescence yield.[144] It was calculated that 1 of 12 collisions leads to annihilation and 36% of annihilations generate an excited singlet. A similar report of increased fluorescence quantum efficiency with increasing excitation intensity in single crystals of **2** appeared independently, and a good fit to the experimental intensity dependence at 300 and 243 K was found using the product of branching ratio and triplet quantum yield (equal to 1.276 at 300 K and to 1.09 at 243 K).[168] Photoionization of triplet excitons created by singlet fission creates a transient photocurrent in tetracene crystals irradiated at 1.79 eV.[169] Within the intensity range of 5×10^{24} to 4×10^{25} photons cm^{-2} s^{-1}, the charge carrier density varies as I^3, which requires the triplet density to vary as I^2.

Fluorescence enhancement by the magnetic field is the greatest at low light intensity, where triplet fusion is not active. On the basis of fluorescence yields at 300 and 77 K, the fission rate constant at 300 K was calculated to be 5.1×10^9 s^{-1}.[144]

Pressure Effects. Singlet fission in **2** is affected by increased pressure, which modifies[170] the energy gap between $E(S_1)$ and $2E(T_1)$. Moreover, at high pressures phase transitions between crystalline forms occur. Van der Waals bonded molecular crystals have a relatively high compressibility, and a red shift in absorption with increased pressure is typical. The magnitude of the shift of a transition is related to its oscillator strength, and the $S_0 \rightarrow S_1$ excitation energy drops faster than the $S_0 \rightarrow T_1$ energy. Because in **2** $2E(T_1)$ lies above $E(S_1)$, this augments the activation energy for singlet fission. Because of a decreased rate of singlet fission, the fluorescence quantum yield increases with increasing pressure and is 2.55 times larger at 4.1×10^{-2} MPa than at atmospheric pressure. Pressure modulation of fluorescence was used to calculate the activation energy for singlet fission as a function of pressure, and it was found that this energy varied linearly, with a slope of 7.8×10^{-5} eV/MPa.[170] The energy of T_1 was found to decrease by 1.9×10^{-5} eV/MPa. This value was improved in a subsequent study[105] of the low-pressure phase, which found the pressure dependence of the energy gap to be 6.2×10^{-5} eV/MPa, with the singlet energy decreasing by 1.6×10^{-4} eV/MPa and the triplet energy decreasing by 5×10^{-5} eV/MPa. The larger value for the triplet energy decrease relative to the original finding was attributed to the fact that the previous study[170] produced an average value of the energy gap over the low- and high-pressure crystal phases. Both the first- and second-order rate constants and the branching ratio decrease with increasing pressure.

Phase transitions between crystalline forms cause discontinuities in fluorescence intensity as a function of both temperature (120−300 K) and pressure (up to 600 MPa) in a single crystal of **2** and indicate the existence of two low-temperature and one high-pressure phase transition.[105] The thermal activation energy for fission is 0.16 eV at 1 atm and grows with increasing pressure. From a fit of the temperature dependence of the magnetic field induced fluorescence enhancement, the fission rate constant was calculated to be 3×10^9 s^{-1}, and a fit of literature data[14] yielded a value of 4.3×10^9 s^{-1}. However, others[170] failed to find the discontinuous fluorescence enhancement at 300 MPa, and this issue remains to be settled.

Confined Spaces. The behavior of singlet fission and refusion in confined spaces[148] may be relevant to its application in solar cells, as the dimensions of TiO_2 structures within the Grätzel cell are on the nanoscale.[171] To achieve confinement, crystals of **2** were doped with various concentrations of 2,3-benzocarbazole, which acts as a triplet exciton reflector.[148] The dopant thus restricted the motion of the triplets but did not completely trap them. The doped systems of **2** were considered to be two-dimensional because diffusion

of triplets tends to be within the *ab* plane. This was supported by a computer model that showed a good fit to experimental data for one out-of-plane hop for every 1000 in-plane hops. Because the cages were incomplete or "leaky", the authors used the computer model to confirm that diffusion of the excitons was restricted at the concentrations studied. In their experiments, fission was used to produce a concentration of triplets that is locally very high and this is maintained due to the confinement. The high local concentration of triplets reduces the efficiency of the fission channel and therefore increases the singlet lifetime. Geminate recombination was enhanced by nearly 50%, and this enhancement exceeded the decrease in fusion caused by the diminished number of tetracene sites.

At increasing excitation intensities there was an enhancement in prompt fluorescence efficiency in both pure and doped **2**. The energy at which enhanced fluorescence efficiency sets in increased with increasing 2,3-benzocarbazole concentration. This occurs because in caged systems the local concentration of triplet excitons is already high, and even greater intensities are needed to further enhance geminate recombination. At 298 K, the fluorescence decay rate decreased from 10×10^9 s^{-1} at 0 mol % to 2.8×10^9 s^{-1} at 50 mol % 2,3-benzocarbazole. The inverse fluorescence lifetime for 50 mol % 2,3-benzocarbazole is close to the decay rate of 2.8×10^9 s^{-1} that was found for **2** at 77 K. At this temperature fission is suppressed, and it was therefore concluded that fission no longer takes place at 50 mol % 2,3-benzocarbazole. A computer model was used to correct for the replacement effect (the replacement of **2** with 2,3-benzocarbazole decreases the probability that any one molecule of **2** will have a second molecule of **2** nearby, as required for singlet fission). The corrected fission rate was found to be 8.1×10^9 s^{-1} for pure **2**, decreasing to 4.1×10^9 s^{-1} at 29% 2,3-benzocarbazole. A later study of magnetic field effects in the same system[172] concluded that the branching ratio, k_2/k_{-1}, increased linearly with increasing percentage of 2,3-benzocarbazole for a given crystal phase, reflecting the enhancement in geminate recombination for spatially confined triplet pairs.

The system of 2,3-benzocarbazole doped **2** has also been used to maintain locally high concentrations of triplet excitons to study geminate versus nongeminate recombination.[173] Using both steady-state and pulsed excitation, delayed fluorescence decay rates were compared for doped **2** (geminate recombination) and naphthalene (nongeminate recombination). In the case of geminate recombination, steady-state and pulsed experiments both create a Poisson distribution of excitons and therefore have identical fluorescence decay rates. This was observed in doped **2**. In the case of nongeminate recombination, the decay rates from the two types of excitations differ, and this was observed in naphthalene.

Branching Ratio. The branching ratio ε, defined as k_2/k_{-1} in eq 2, is the ratio of the probability with which the correlated triplet pair proceeds to a singlet exciton and the probability with which it proceeds to two triplet excitons. Even in the more advanced Suna model,[18] in which the individual rate constants are not defined, it is a measure of the ratio of singlets to triplets produced from the correlated triplet pair. One curiosity that has been found in singlet fission in **2** is a branching ratio on the order of 0.6, a value which is larger that would be expected based solely on spin statistics. The value for ε of 0.67 would mean that an equal number of triplets and singlets are being produced from the ^{1}(TT) pair, as opposed to a 3:1 ratio ($\varepsilon = 0.4$) that would be expected based on spin statistics. It has been suggested that the large value of ε is due to a small Franck−Condon factor for the transition from the ^{1}(TT) state to the T_1 state and the energetic closeness of ^{1}(TT) to S_1.[148,168] Branching ratios are magnetic field[85] and pressure[105] dependent. The branching ratio calculated[85] from the Suna model is 0.56−0.61, and the value calculated from the Johnson and Merrifield model is 0.68. In an exciton caging study, the branching ratio was found to increase linearly with increasing dopant level.[172] A later study of the temperature and intensity dependence of fluorescence efficiency allowed the quantity $\varepsilon g^*/2$ to be determined,[168] where g^* is the triplet quantum yield. At 300 K, it was found that the value of ε was 0.64, assuming a value of 2 for g^*. The temperature dependence of $\varepsilon g^*/2$ was also studied. It was found that the value is relatively constant from 300 to 380 K but is nearly 20% smaller at 220 K. The temperature dependence was attributed to a change in g^* with a constant value of ε. On the basis of the temperature dependence of $\varepsilon g^*/2$, it was found that the rate of singlet decay by nonfission processes was 1.3×10^8 s^{-1}. This value is not consistent with singlet trapping as an explanation for nonexponential fluorescence decay.

3.1.3. Pentacene

Pentacene (**3**) is well known for its importance in organic electronics.[174,175] It is the shortest linear polyacene for which singlet fission is exoergic in the crystal. On the basis of the values $E(S_1) = 1.83$ eV from an absorption measurement on a polycrystalline film[106,176] and $2E(T_1) = 1.62$ eV,[107] later modified to 1.72[177] eV, from the activation energy of heterofission with **3** as a guest in host crystals of **2**, and 1.7 eV from direct measurement on a film,[178] the exoergicity of singlet fission in solid **3** is 0.1−0.2 eV.

In the early years, homofission in **3** received much less attention than in **1** and **2**, but more recently it has been studied extensively by pump−probe spectroscopy, both in thin films[76,77,147,149,150,151,179,180] and a crystal.[147,179] In spite of this effort, it is not well understood. Most results obtained for solid **3** in different laboratories are similar but some differ considerably, and they appear to be sensitive to the detailed nature of the sample, possibly because insufficient attention has been paid to the effects of molecular orientation in the solid on observations made with polarized light. The analysis of the data and the identification of the various transient species encountered is made difficult by the multitude of transient species formed and by the severe overlap of their spectral features with each other and also with the ground-state bleach. The overlap makes it difficult to perform a global analysis that would more clearly separate and define the spectrum of each species. The analysis of the observations is in a rather chaotic state,[40,76,77,147,149,150,179,181] as there are several competing mutually incompatible proposals. We shall describe them in detail and comment on each. Some can be excluded based on what is known about the isolated chromophore, but none is fully satisfactory.

It will be helpful to describe the simple and quite well understood molecular properties of **3** first before starting a discussion of the complicated properties of the solid. Photophysical studies of **3** typically start with an excitation of the fairly intense short-axis polarized first transition into the L_a state in the visible region (HOMO−LUMO, or $^1B_{2u}$ with x as the long axis and y as the short axis), and higher

excited states are not of much relevance in the present context. In the low-resolution absorption spectrum of the S_0 state of the isolated molecule of **3**, the L_a band is located at 2.1−2.7 eV and its vibrational structure consists of four peaks separated by ∼1500 cm^{-1}.

Although really accurate calculations for a molecule of the size of **3** are difficult, many more or less approximate calculations have been published and reproduce the main spectral features of the isolated molecule within 0.2−0.3 eV. Recent examples are single-reference TD-DFT[30,181] and CC2[182] and multireference CAS-MP2[40] calculations. Multireference calculations were used to obtain useful results for doubly excited states.

Properties of Gas Phase and Rare-Gas Matrix Isolated 3. In isolated molecules cooled in a supersonic jet, the L_a band origin occurs at $E(S_1) = 2.31$ eV.[183−185] Fluorescence originates in the same state and is a fairly close mirror image of the absorption. Low-temperature matrix-isolation absorption and emission spectra[186,187] are similar to the jet-cooled spectra, but somewhat red-shifted. In a neon (krypton) matrix,[188] the shift of the 0−0 transition is ∼0.025 (∼0.125) eV relative to the gas phase. There are no indications of a presence of additional electronic transitions nearby. These results leave no doubt that in an isolated molecule of **3** the optically allowed L_a state is the lowest excited singlet and that the probably present recently calculated doubly excited singlet state must lie above L_a, not below as proposed.[40]

Flash photolysis of the vapor[189] yields a transient whose absorption spectrum lasts for tens of μs and which was assigned to the T_1 state. It contains four intense peaks starting at 2.68 eV, separated by ∼0.17 eV. If the T_1 state also absorbs at lower energies, it does so only very weakly.

For a hydrocarbon, the gas-phase ionization potential of **3** is unusually low, 6.61 eV,[190] and electron affinity is unusually high, 1.35 eV.[191] Gas-phase spectra of the radical cation and the radical anion do not appear to have been reported, but rare-gas matrix absorption spectra are known and resemble each other closely,[188] as expected from the alternant pairing theorem.[192] In both cases, the lowest-energy absorption peaks occur near 1.3−1.4 eV and are due to two nearly degenerate transitions. The radical cation has a $^2B_{3g}$ ground state, and the two transitions are to states of symmetries $^2B_{1u}$ (*y*-polarized) and ^2A_u (stronger, *x*-polarized). In a Ne matrix, they lie at 1.26 and 1.31 eV, respectively. They are red-shifted by ∼0.01 and ∼0.025 eV, respectively, in a Kr matrix. The radical anion has a $^2B_{1u}$ ground state, and the two transitions are to states of symmetries $^2B_{3g}$ (*y*-polarized) and $^2B_{2g}$ (stronger, *x*-polarized). In a Ne matrix, they occur at 1.37 and 1.41 eV, respectively. They are again red-shifted, by ∼0.01 and ∼0.025 eV, respectively, in a Kr matrix.

Properties of 3 in Solutions. Solution absorption spectra closely resemble the gas-phase and rare-gas matrix spectra but are broadened and considerably red-shifted. In benzene, the red shift from the gas phase amounts to ∼0.2 eV and $E(S_1)$ equals 2.15[193] (2.13[194]) eV. In cyclohexane, the value reported as an average of the energies of the first peaks in absorption and in fluorescence is 2.10 eV.[128] The Stokes shift between these peaks is very small, e.g., in 2-methyltetrahydrofuran at 77 K, only 2 nm even without correction for self-absorption (in this solvent, $E(S_1)$ is 2.13[194]).

From phosphorescence in frozen cyclohexane, $E(T_1)$ is 0.95 eV.[128] Early flash photolysis measurements in hexane[166,195] revealed a transient with three absorption peaks separated by ∼1400 cm^{-1} and with the first peak at 2.51 eV in a spectrum that lasted for tens of μs. More recent work in benzene produced an essentially identical spectrum with the fourth peak now visible as an indistinct shoulder, and the first peak shifted to 2.46 eV.[193] The red shift of this fairly strong transition is thus again about 0.2 eV between gas phase and benzene solution. A search for weak absorption at energies as low as 1.1 eV did not reveal any, down to a sensitivity limit of 50 M^{-1} cm^{-1} (numerous calculations suggest that there is a very weakly allowed transition in the low-energy region, variously predicted for instance at 1.24[40] or 1.41[182] eV). Several bands are present at higher energies, with the most intense one at 4.04 eV. A comprehensive determination of photophysical parameters in cyclohexane[128] yielded the quantum yields of fluorescence, intersystem crossing, and internal conversion as 8, 76, and 16%, and a fluorescence lifetime as 7.0 ns, which corresponds to an intersystem crossing rate constant of $\sim 1.1 \times 10^{-8}$ s^{-1}.

All the authors agree on the assignment of the ∼2.5 eV transient to T_1 based on its long lifetime. The transient spectrum measured in benzene upon sensitization with triplet **1** (54 μs single exponential lifetime) is identical with the spectrum obtained upon direct excitation,[194] proving the identity of this transient as triplet with certainty. There is no doubt that the T_1 state is of HOMO−LUMO nature and that its symmetry is B_{2u}. All computations since the pioneering semiempirical effort in 1956[47] have agreed that the intense transition at 2.4−2.7 eV is to a B_{1g} state and is polarized along the long axis (*x*). In solution, the triplet reacts with ground-state **3** to yield a transient that absorbs in the UV and has a lifetime in the ms range. This was assigned to a thermally unstable photochemical dimer.[193]

Properties of Solid 3. The situation is complicated because **3** is known to crystallize in at least four polymorphs characterized by different layer periodicity.[196] The four have been grown as thin films and one also as a single crystal, whose structure has been determined.[196,197] The structure of one form, obtained by vapor deposition of a fiber-structured very thin film on a suitable substrate, is known as well[198] and is complicated in that the molecular arrangement within the unit cell depends on the substrate used. Unfortunately, in most optical studies of films, little attention was paid to the structural characterization of the film used.

Nevertheless, all authors find similar general features of single-crystal and polycrystalline film absorption. The first absorption band shows fairly broad peaks reminiscent of those found in isolated molecules, but the first peak exhibits a 0.14 eV Davydov splitting[199,200] into a pair of peaks at 1.83[106,201] and 1.97[201] eV, polarized parallel and perpendicular to the crystal *b* axis, respectively.[201] The others occur at 2.12 and 2.3 eV[149,202] and have been assigned to intermolecular charge-transfer transitions.[106] The red shift of the average of the Davydov pair relative to the gas phase is 0.4 eV, twice the shift observed upon going from the gas phase to benzene solution.

It was reported a long time ago that that solid **3** does not fluoresce detectably,[158] and there is general agreement on the subject. The $E(T_1)$ energy is 0.86[177] eV from the activation energy of heterofission with **3** as a guest in host crystals of **2** and 0.85 eV from direct measurement on a film.[178] If the red shift from the gas phase to the solid were to be again the same for the strong absorption band of the T_1 state as it is for the L_a transition from the S_0 state (0.4 eV), as is the case in benzene solution (0.2 eV), the average

for the Davydov pair of peaks in the triplet spectrum would be found at 2.28 eV. Depending on the magnitude of the Davydov splitting, the first peak in the triplet spectrum would then appear at this or a somewhat lower energy. Because the strong absorption from the T_1 state is long-axis polarized, whereas the visible absorption from the S_0 state is short-axis polarized, no simple relation between the two Davydov splittings can be expected. As we shall see below, the actual energy at which the T_1 state absorbs is a matter of contention.

The size of the red shift of S_0 absorption of **3** between the gas phase and the solid is enormous and may be used to support the proposal that singlet excitation is not present in the solid as a simple Frenkel exciton localized on a single site but is actually delocalized.[73−75]

In the solid, the radical cation of **3** has been found by charge modulation spectroscopy on field-effect diode structures[203] to have a weak flat absorption at 1.24−1.65 eV that fits well the expectations from work on matrix isolated molecules described above, but also to have a strong absorption at 0.6−0.9 eV, in a region not examined by the authors of the matrix work and not predicted by their calculations.[188] If this transition indeed belongs to the radical cation of **3**, it is due to intermolecular effects. A transient peak in solid **3** at 1.9 eV has also been attributed to the radical cation,[147] but this assignment is almost certainly incorrect since neither the charge modulation spectrum nor the matrix-isolated cation absorption spectrum contains any significant peaks in this region.

This brings us to the controversial subject of ultrafast transient absorption studies on **3**. We start by noting that independent evidence in favor of excitation multiplication in solid films of **3** is available from the observation of a 145% quantum efficiency observed with a photodetector composed of 30 alternating layers of **3** (2 nm thick) and C_{60} (1 nm thick).[180] The photocurrent is believed to originate in charge transfer to C_{60} from triplet excitons produced by singlet fission. The charge transfer is feasible in spite of the relatively low triplet energy since the ionization potential of solid **3** is only 5.0 V[204] and the electron affinity of solid C_{60} is 4.5 eV.[205] At a voltage bias of −3.5 eV, the external quantum efficiency spectrum of the photodetector was fitted using an internal quantum efficiency for **3** of 128%. At excitation wavelengths where **3** predominantly absorbed, there was a decrease in photocurrent of up to 2.7% upon the application of a magnetic field. The magnetic field effect along with the quantum efficiency in excess of 100% strongly suggest that triplet excitons produced by singlet fission are the source of the photocurrent enhancement. Excited at 1.91 eV, **3**/C_{60} multiple heterojunctions have a photocurrent response that decays with a 0.8 μs time constant,[206] considered consistent with a system in which triplet excitons are the main source of photocurrent. Decay by charge transfer accounts for the relatively short triplet lifetime.

Very recently, charge separation in a **3**/C_{60} bilayer was examined by fs time-resolved transient absorption spectroscopy, and additional evidence for the generation of an internal electric field by dissociation of triplets at the interface was obtained.[151] A transient absorption at 1.77 eV that arises in 2−10 ns was attributed to electroabsorption (distortion of the first peak in the ground-state bleach by the effect of strong internal electric field). Its growth is too slow to be attributable to interfacial singlet exciton charge dissociation, because singlet excitons are estimated to live <200 fs based on the absence of stimulated emission. This relatively slow growth is, however, compatible with interfacial triplet exciton charge separation. The ground-state bleach is long-lived on the ns time scale, and this is also compatible with efficient formation of long-lived triplet excitons by fast singlet fission. The authors attribute a similarly long-lived photoinduced absorption at 1.44 eV to triplet exciton absorption, but as noted below, this assignment is unlikely to be correct.

We shall next describe the observations reported from transient spectroscopy measurements and their proposed interpretations more fully. The experimental details regarding the excitation source and sample preparation appear to be important and we list them first. Ultrafast transient measurements were performed (i) on a thin film, vapor deposited on glass, excited with 200 nJ 60 fs pulses at 2 eV,[150] (ii) on a thin film, vapor deposited on an amorphous polyalkene plastic (~1 μ crystalline grains ~30 monolayers thick, with the long molecular axis nearly perpendicular to the surface[198]), excited with 30 fs pulses at 1.85 eV,[76,77] (iii) on single crystals and on a ~150 nm thick film, vapor deposited on MgO (in one case doped with ~0.03% C_{60}), excited with sub-50 fs pulses at 3.0 eV (10−200 μJ/cm^2),[147,179] (iv) on glass and on silver nanohole sheets, excited with ~35 fs pulses at 2.3 eV (200 μJ/cm^2),[149] (v) on thin films deposited on an unspecified substrate and excited with 90 fs pulses at 2.53 eV (80 μJ/cm^2), and (vi) on both thin films and **3**/C_{60} bilayers (150 and 10 nm, respectively) on an unspecified substrate excited with 600 ps pulses at 2.33 eV (120 μJ/cm^2).[151]

The S_1 State. The first features that appear simultaneously with the fs exciting pulse in all samples of neat **3** are a ground-state bleach that reflects peak positions in the absorption spectrum of the S_0 state (1.86, 1.96, 2.12, and ~2.3 eV), a rapidly decaying broad absorption below 1.7 eV with a peak at 1.61 eV, and possibly stimulated emission with an ultrashort decay time of 70 fs,[76,77] indicated by a fast decay at the red edge of the ground-state bleach (which has, however, also been attributed instead to a repopulation of the ground state by triplet−triplet annihilation[149]).

The fast decay of the 1.61 eV absorption peak is well documented. It has been reported to lose 75% of its intensity in 175 fs[150] and to decay with a 70 fs time constant.[76,77] This transient is assigned as S_1.[76,77,149,150] It was not observed in one of the ultrafast studies[147] (the same material was republished later[179]) in which no data points were taken between ~1.4 and ~1.7 eV.

Species A. The fast decay of S_1 in a film of **3** is associated with an equally fast (80 fs rise time) formation of a very long-lived species that we shall refer to as A. Its properties are agreed upon by all authors who investigated thin films of **3**[76,77,149−151] except one group whose spectra show the peaks very indistinctly.[147,179] In thin films of **3** deposited on glass and Ag nanohole film substrates,[149] a lower bound for the rate constant for the formation of A was estimated as 2×10^{13} s^{-1}. It shows some decay within the first 30 ps but not much more out to 4 ns, but there is some variation in the decay times reported by different authors.

The absorption peaks of A lie at 1.88, 1.97, and 2.16 eV, and are at least partly short-axis polarized, based on a comparison of their relative intensities in film spectra taken at normal and 65° incidence angle with the relative intensities of the long-axis polarized absorption peak of species B discussed below at the same two angles of incidence.[76,77] In these films, the long axis of the molecules of **3** is oriented at 6° from the surface normal.[198] Species A was not observed

in transient absorption measurements performed under identical conditions on a single crystal of **3**, and the authors attributed its absence to different morphology.[147,179] However, since they did not specify the monitoring laser beam polarization direction relative to crystal or molecular axes, one cannot exclude the possibility that A was formed but its transition moment was out of alignment with the electric field of the monitoring laser beam.

The dynamics of the decay of A can be altered by the presence of underlying structures. For **3** on glass,[149] there is an initial fast (~175 fs) component of absorption decay, which is not observed for **3** on Ag nanohole films. This is thought to be due to changes in the rate of vibrational cooling or in the relative energies of the S_1 and T_1 states due to interaction with surface plasmons.

In ultrafast transient absorption studies of films of **3**,[147,179,151] the spectral signature of A is less clear. Upon cooling to 5 K,[151] the spectra change considerably, and the peak of A becomes more prominent relative to ground-state bleach. It is not obvious whether the results represent an observation of an additional transient species (D) with a sharp peak at 1.9 eV that also lives for many ns and whose formation is enhanced when the film is doped with C_{60}.

Species B. This transient has only been detected in a thin film of **3** observed at 65° incidence, as a weak absorption band at 2.30 eV.[76,77] Its rise time of ~1 ps and a lifetime of a few hundred ps are clearly distinct from those of A and demand the assignment of B as a different species. The 2.3 eV band is not seen at normal incidence under otherwise identical conditions and is therefore evidently polarized along the long axis of **3**.

Species C. This transient, with a broad absorption peak at 1.4 eV, a temperature-independent 700 fs rise time, and a lifetime of many ns, was observed in a study[147,179] of a single crystal and in thin films of **3**,[147,179,151] where its rise time is shorter than the 200 fs time resolution of the measurement.[151] In a thin film, the intensity of this absorption peak relative to the ground-state bleach was much weaker than in the single crystal and was reduced further when the film was doped with C_{60}.[147,179] The authors attribute the difference between results for a single crystal and a film to different morphology. Another possible explanation is that the 1.4 eV transition in C is mostly long-axis polarized and therefore hard to observe in their thin films at normal incidence (the ground-state absorption is short-axis polarized).

Proposed Interpretations. Four different hypotheses have been presented to account for the fast decay of the initially excited S_1 state to the species A observed in solid **3**, and the authors often differ in the interpretation of the nature of the transients B and C as well. The proposed fates of S_1 are (i) fission to free triplet excitons, which have been assigned by some authors[150] (and later accepted by certain others[149,207]) as species A, in other publications as species C,[147,179,151] and in one paper as species B[77] (which we consider the most likely), (ii) formation of an excimer[76,77] (this also is one of the two possibilities considered likely in ref 151), (iii) fission to a strongly bound triplet exciton pair, an intermolecular doubly excited state ^{1}(TT)[181] (this is the other possibility considered likely in ref 151), and (iv) internal conversion to a intramolecular doubly excited state (which we believe can be safely excluded), followed by conversion to a pair of free triplet excitons.[40] We find none of these four hypotheses entirely satisfactory but are unable to propose a convincing detailed alternative. We have considered the possibility that A might be a quintet state of **3**, formed by energy transfer from a quintet state of the intermolecular triplet pair ^{5}(TT), but a few simple density functional theory (DFT) calculations convinced us that such a locally excited quintet is probably too high in energy and that its absorption spectrum is unlikely to fit A.

(i) An assignment of A as the T_1 state of crystalline **3** was made based on its long lifetime and the vague similarity of its absorption spectrum to that of the triplet of **3** in solution.[150] It was felt that the large red shift of the bands of A relative to the solution spectrum of the triplet of **3** would be acceptable. This assignment of A as the triplet exciton of **3** was later convincingly criticized.[76,77] It was pointed out that the red shift of the absorption peaks of A, which start at 1.88 eV, relative to the solution spectrum of the triplet of **3**, which starts at 2.46 eV,[193] actually is unreasonably large. Moreover, the observed intensity of the bands of A is comparable to that of the ground-state bleach, whereas in solution, the absorption intensity is an order of magnitude higher for T_1 than for S_0. Here, it could be argued that the S_1 state is delocalized and exciton-coupled (superradiant) and the ground-state bleach intensity is thus enhanced, similarly as has been recently proposed for solid **2**.[120] However, most importantly, the first intense absorption band of monomeric **3** is long-axis polarized, whereas the absorption of A is short-axis polarized. Others concurred with the criticism,[181] and it now seems inevitable to us that the assignment of A as triplet exciton must be rejected. The proposed attribution of A to the radical cation of **3**[147] can be rejected as well, based[151] on the analysis given above.

Still assuming that singlet fission to triplet excitons is the dominant fate of the initially excited singlet state, we need to next consider the proposal that it actually is species C that is the free triplet exciton.[147,151,179] This species was observed in a single crystal of **3**, and only much more weakly in a solid film,[147,179] where the peaks of A also were observed only weakly if at all, and species B was not observed. The long decay time of C, its sub-ps rise time, and the temperature independence of its formation, expected for exothermic singlet fission, were taken to be sufficient evidence for the assignment.

Because the location of the absorption peak of C (1.4 eV) differs so dramatically from that of triplet **3** in the gas phase (2.68 eV[189]) or in solution (2.46 eV[193]), it is hard to imagine that the assignment of C to a triplet exciton could be correct. It is true that calculations predict a long-axis polarized T_1 to T_2 transition in this energy range (e.g., 1.24[40] and 1.41[182] eV), but its calculated intensity is[182] 300 times lower than that of the transition at 2.68 eV. Indeed, all efforts to observe such a transition in the isolated molecule have failed, and it has been established that in benzene solution the absorption coefficient of triplet **3** in this region is $<50\ M^{-1}\ cm^{-1}$.[193] If C were triplet **3**, equally polarized absorbance in the region of 2 eV and above would have to be far off scale, and it is not.

A different assignment of the nature of C is therefore needed but has not been made. Because its intensity is weak in a film yet strong in a single crystal, it probably is at least partly long-axis polarized. Both the radical cation and radical anion have absorption peaks of both polarizations at 1.3−1.4 eV,[188] and in our opinion they are possible candidates. Given the low ionization potential and high electron affinity of **3**, it seems conceivable that C is a charge-transfer exciton (intermolecular charge-transfer state) formed by dissociation

of the hole and the electron in an initial (probably somewhat delocalized) S_1 state to neighboring molecules of **3**. This assignment was considered before for species A and was found improbable.[76,77]

If C is a charge-transfer exciton, the reduction of the intensity of the peak associated with C upon doping with C_{60}[147,179] would be due to the removal of the radical anion of **3** by charge transfer to C_{60}. It would be interesting to see whether C has the intense absorption peak at 0.6−0.9 eV that is believed[203] to be characteristic of the radical cation of **3** in the neat solid but not in the isolated radical cation. If thermal activation permitted a return of the charge-transfer exciton to the S_1 state and its subsequent fission, C could serve as a long-lived reservoir of triplet excitons, accounting for the apparent contradiction between the dominant role that they seem to play in photocurrent generation in **3**/C_{60} bilayers[180,151] and the low (2%) triplet exciton yield[77] (species B).

(ii) In an effort to find an alternative assignment of the structure of A, it has been suggested that it is an excimer, stabilized by ∼0.3 eV relative to the S_1 state, that is only capable of singlet fission upon thermal activation.[76,77] The stabilization energy value was supported by a TDDFT calculation, and agreed with an Arrhenius fit of the small triplet population assigned as species B.[77] The identification of the triplet as B was based on the anticipated energy and long-axis polarization of the relatively weak band at 2.36 eV, observed only in the 65° and not the normal incidence angle measurement. From the intensity of the 2.36 eV band, these authors deduced that the triplet yield is only ∼2%. In our opinion, the assignment of transient B as the triplet exciton is correct.

The correctness of the tentative assignment of species A as an excimer is another matter. It has been criticized rather convincingly in a study that reported extensive quantum mechanical and molecular mechanical (QM/MM) calculations on pentacene crystal and found no easy way for the excimer to form.[181] The authors also pointed out that an excimer stabilization energy of 0.3 eV would be highly unusual in a herringbone-type crystal structure and that it greatly exceeds the excimer stabilization energy in α-**9**, where the monomers are stacked parallel in a far more favorable arrangement. The arguments seem convincing to us and we believe that the assignment of A as an excimer is highly improbable, although perhaps not completely ruled out.

(iii) Another assignment of A that has been proposed is the ^{1}(TT) state, in which two triplet excitations reside on the two molecules located in the unit cell in an energetically favored arrangement that inhibits their diffusion apart. The Davydov-like splitting due to the interaction of their transition moments for absorption from the T_1 state was estimated from experimental data to be 0.82 eV, bringing the triplet excitation energy of the short-axis polarized lower Davydov-like component from the benzene solution triplet excitation energy of 2.46 eV[193] to within 0.17 eV of the 1.88 eV value observed for the first peak of A. If one included the 0.2 eV general solvent shift upon going from benzene solution to the solid mentioned above, the agreement would be perfect. The long-axis polarized upper Davydov-like component is expected to lie high enough that it would escape detection.

There are at least two difficulties with this interesting proposal. Most important, it is hard to believe that the two geminate triplets in the pair fail to diffuse apart over a period of many ns, given that, in the absence of significant geometrical perturbation of the ground-state crystal structure, their interaction energy cannot be very different from what it is in other molecular crystals such as **2**, i.e., of the order of cm^{-1}. The issue of the binding energy of the geminate triplet pair is essential but was not addressed by the authors. Second, the assignment depends critically on the small deviation from a parallel alignment of the long axes of the two molecules in the unit cell. If they were exactly parallel, the lower Davydov-like component would have no intensity at all, and all of the absorption by the ^{1}(TT) state would be by the upper component and polarized normal to the film surface. The relatively strong absorption of A is polarized parallel to the film surface, and it is not easy to believe that it all comes from a very minor perturbation of a symmetry-forbidden transition.

Both objections might conceivably be overcome if the proposed formation of a "^{1}(TT) triplet pair state" were replaced with a reversible conversion to a chemically weakly bound dimer associated with a significant geometry change. One such structural possibility would be a singlet biradical containing two molecules of **3** connected with a long single bond. Such a biradical could revert to a singlet-coupled pair of triplet excitons upon thermal activation, serving as another possible reservoir for triplets and thus helping to account for the surprisingly low observed triplet exciton (B) yield.

(iv) Intramolecular doubly excited state. A very original proposal concerning the initial fate of S_1 has been made recently.[40] Multireference perturbation theory (CAS MP2 with (12,12) active space) calculations of excitation energies of isolated monomeric **3** predicted that the lowest excited singlet S_1 is a doubly excited state with an energy 0.18 (vertical) or 0.27 eV (adiabatic) below the allowed L_a state normally considered to be the S_1 state of **3**, but 0.11 eV higher than twice the triplet excitation energy in monomeric **3**. The situation would then be similar to the one well established for long polyenes.[71] The computed doubly excited state is best described as reached from the ground state by a mixture of double excitations from the HOMO and HOMO-1 to the LUMO and LUMO+1 orbitals and can be viewed as a singlet-coupled pair of triplet excitations located in two distinct regions of the molecule. The authors identified a C_s symmetric conical intersection 0.18 eV below the L_a state that connects the two states and proposed that the transition from the initially reached L_a state to the lower doubly excited state occurs on a sub-ps time scale. Although one could attempt to do so, they did not actually assign this intramolecularly doubly excited state as species A, but more cautiously proposed that "it acts as the intermediate connecting the optically excited state S_1" (which is their label for the L_a state, calculated to be the second excited singlet) "to two triplets ($2 \times T_1$)",[40] i.e., that the intramolecular doubly excited state immediately proceeds to form two triplets T_1 (Figure 1 in ref 40).

Once the pair of triplet excitons is formed, the authors assign it as the species that we call C and compare its 1.4 eV transition energy to their computed first triplet excitation energy of 1.24 eV. They disregard the problem of a nearly vanishing intensity expected for the transition from T_1 to this upper triplet state from both experiment and theory and the other considerations mentioned above that made us reject the proposed identification of C with the triplet exciton.

The accuracy of the method used for the monomer may be estimated at about the anticipated ±0.25 eV from a

comparison of the computed (2.08 eV) and gas-phase (2.31[183−185] eV) L_a transition energies. The accuracy is better for the adiabatic $S_0 - T_1$ energy difference calculated in the gas phase (0.85 eV), which compares very well with the value measured in a crystal (0.86[177] or 0.85[178] eV), which is probably more accurate than the value obtained in frozen cyclohexane (0.95 eV[128]).

Unfortunately for this proposal, the numerous observations made over the decades on isolated molecules of **3** in the gas phase, in matrices, and in solutions (summarized above) leave no doubt that the lowest state of isolated **3** is of the allowed L_a (singly HOMO → LUMO excited) nature, as traditionally believed, and not a doubly excited state as in long polyenes. Specifically, the fluorescence of monomeric **3** clearly originates in its L_a state, even at temperatures as low as 1.8 K. The proposal that the doubly excited state of isolated **3** is populated from the L_a state on a sub-ps scale without a barrier through a conical intersection cannot be correct because one would then expect most of the emission to come from this doubly excited state by the vibronic mechanism, resulting in a significant Stokes shift similarly as in long polyenes.[71] The observed shift is however close to zero even at very low temperatures, and the absorption and emission shapes are approximate mirror images of each other. Thus, even if one made the unlikely assumption that the doubly excited state is so forbidden and so incapable of vibronic coupling that it does not lead to any absorption and emission at all and merely serves as a reservoir for replenishing the population of the higher-energy allowed and emitting L_a state, even at 1.8 K, the two states would have to be essentially degenerate.

Clearly, the estimated ±0.25 eV accuracy of the method of calculation is not sufficient to deal with the very small energy differences involved. There is little doubt that the computed doubly excited state actually exists, and it is useful that its presence has been pointed out. Nevertheless, although it may have an energy only a little above that of the L_a state, it does not lie below the L_a state, and mechanism (iv) needs to be dismissed. The computed intramolecular conical intersection between the two states is spurious, and it is not clear what if any role the intramolecularly doubly excited state plays in singlet fission.

In addition to examining the states of an isolated molecule of **3**, the authors calculated in a smaller (8,8) active space approximation the potential energy surfaces of the excimer state and the ^{1}(TT) state along an assumed reaction coordinate represented by the distance of the two molecules of **3** in their S_0 geometries, from an excimer-like value of 3.5 to 8 Å. They only computed and showed two of the anticipated five closely spaced excited state curves of the molecular pair (in addition to the singlet-coupled triplet pair, they correspond to either single or double excitation on one or the other member of the pair, possibly partly or fully delocalized). The avoided crossings that one might expect to occur along the path chosen (or conical intersections likely present along appropriate geometrical paths) are therefore not apparent.

In summary, it seems to us that descriptions of the fate of S_1 provided under (i) and (iv), and the associated structures proposed for A, cannot be correct, and that possibility (ii) is unlikely. A suitably modified version of option (iii) seems to have the best chance of correctly describing the fate of S_1 and the structure of A. It appears to us very probable that species B is the triplet exciton and at least possible that species C could be a radical cation−radical anion pair (charge-transfer exciton). Additional investigation is clearly needed before the photophysics of solid **3** is understood.

3.1.4. Mixed Crystals

Heterofission is the conversion of a singlet excitation on one chromophore to two triplet excitations on two different chromophores. In the case of molecular crystals, heterofission is studied by doping a host compound with molecules of a guest compound. A guest with a lower triplet energy than that of the host can allow singlet fission to proceed exoergically even when it is endoergic in the neat guest and/or host. When heterofission occurs in a crystal with a low concentration of such a guest, the triplet of the host molecule is free to move whereas the triplet on the guest molecule spends its entire lifetime at the same site. The zero-field splitting parameters D and E of the guest are therefore not averaged over the possible lattice sites, and the signature of heterofission in a crystal with two sites in a unit cell is that two sets of level crossing resonances occur as the magnetic field is reoriented.[119]

Two early studies were made of heterofission of doped polyacenes, (i) **2** doped with **3**, in which singlet fission occurs from the excited guest molecules,[107] and (ii) **1** doped with **2**, in which singlet fission occurs after excitation of the host molecule.[119] In the **3**-in-**2** system,[107] **2** is excited directly and then transfers energy to **3**, producing its S_1 excited singlet. Green fluorescence from **2** and red fluorescence from **3** were observed separately. Heterofission was attributed to the singlet of **3** because the red fluorescence signal showed a double set of level-crossing resonances whereas the green fluorescence showed only a single set due to the homofission of **2**. Heterofission is expected to be endoergic by 0.23 eV [$E(S_1,\mathbf{3}) = 1.83$ eV,[106] $E(T_1,\mathbf{3}) = 0.81$ eV,[107] and $E(T_1,\mathbf{2}) = 1.25$ eV[103]]. From the temperature dependence of the red fluorescence intensity, an activation energy of 0.08 eV was determined initially. It was later refined upon observing the temperature dependence of the two sets of level crossing resonances independently.[177] The fact that they differ indicates that the two possible substitutional sites for the pentacene guest have different activation energies, 0.13 and 0.06 eV. The magnetic field enhancement of fluorescence from guest molecules of **3** decreases as the exciting light flux increases from 10^{15} to $>10^{17}$ photons/(cm^2 s).[208] This behavior is characteristic of the increase in fusion at higher light intensities, demonstrating that heterofusion occurs along with heterofission in this system.

The **2**-in-**1** system[119] differs from the previous case in that singlet fission occurs from the host **1**, making the process exoergic by 0.05 eV [$E(S_1,\mathbf{1}) = 3.13$ eV,[129] $E(T_1,\mathbf{1}) = 1.83$ eV,[130] and $E(T_1,\mathbf{2}) = 1.25$ eV[103]]. When the excitation energy was below $2E(T_1,\mathbf{1})$ but above $E(T_1,\mathbf{1}) + E(T_1,\mathbf{2})$, only heterofission of the singlet of **1** occurred. Two sets of level crossing resonances were observed in the magnetic field dependence of the prompt fluorescence. An excitation energy higher than $2E(T_1,\mathbf{1})$ was also used, and heterofission and homofission of **1** both occurred. In this case the magnetic field dependence of the prompt fluorescence was the product of the spectra for the heterofission and homofission of **1**. The singlet fission triplet quantum yields were reported to be 6% for homofission of undoped **1** and 8% for heterofission.

3.2. Oligophenyls

p-Terphenyl (**4**) and *p*-sexiphenyl (**5**) crystals have been studied. In the former, correlated electron−hole pairs are formed by autoionization upon excitation with 130 ps 5−40 eV light pulses[135] (a similar study was later performed on a liquid aromatic polyether[209]). Magnetic field modulation of fluorescence indicated that electron−hole pairs were formed in the triplet state, in a manner inconsistent with the scheme given in section 3.1.1. Whereas the mediated fission that was observed for **1** thus is not an active process in **4**, it was not excluded that singlet fission may take place in the traditional manner at energies below the threshold energy for autoionization.

In **5**, singlet fission has been observed only at high excitation densities[210] using fs pump−probe measurements. At low densities of light with energy estimated to be below $2E(T_1)$, long-lived triplets are formed in <200 ps. These triplets were attributed to polaron formation by excited singlets followed by nongeminate recombination of polarons to produce a mixture of singlets and triplets. At high pump excitation densities (2×10^{20} cm^{-3}), an additional population of triplets was observed with a formation time of 10 ps and decay time constant of 75 ps, and these were thought to be due to the fusion of excited singlets into a higher excited singlet state, followed by singlet fission. The short time constant was thought to be due to fast geminate recombination.

3.3. Tetracyano-*p*-quinodimethane

Tetracyano-*p*-quinodimethane (TCNQ, **6**) is often used in charge transfer crystals as an electron acceptor. Singlet fission has been observed in several of these charge transfer complexes.[108,109,211] A temperature-dependent magnetic field effect on fluorescence that varies with field strength and orientation has been observed in the complexes of phenazine and fluorene with **6**.[108] On the basis of an Arrhenius analysis of fluorescence intensity, fission was determined to be thermally activated with an activation energy of 0.14 eV in the former case and 0.40 eV in the latter. Using a value of $E(S_1)$ of 2.06 eV for phenazine-**6** and 2.05 eV for fluorene-**6**, $E(T_1)$ was calculated to be 1.10 and 1.22 eV, respectively. Results consistent with thermally activated singlet fission were obtained for phenazine-**6** using time-resolved electron paramagnetic resonance (EPR)[211] and for biphenyl-**6** and biphenyl−tetrafluorotetracyano-*p*-quinodimethane ($TCNQF_4$) (**7**) using zero-field optically detected magnetic resonance (ZF-ODMR).[109]

At 290 K, the absorptive or emissive character of the initial optical electron polarization in the EPR experiment on phenazine-**6**[211] could only be attributed to triplets generated by singlet fission. At lower temperatures the initial optical electron polarization decreased, and it changed from enhanced absorption to emission at 200−250 K. Below 50 K, the signal is consistent with triplet generation exclusively by intersystem crossing.

In the complexes of biphenyl with both **6** and **7**,[109] the intensity of the three triplet transitions in ZF-ODMR decreased with temperature, and they disappeared at 200 K. Room-temperature ZF-ODMR signals were consistent with a singlet fission rather than intersystem crossing origin of the triplet spin populations. Fluorescence spectra yielded $E(S_1)$ values of 2.18 and 1.94 eV for biphenyl-**6** and biphenyl-**7**, respectively. The activation energies determined from the temperature dependence of ZF-ODMR were 0.24 eV for biphenyl-**6** and 0.21 eV for biphenyl-**7**, giving $E(T_1)$ values of 1.21 and 1.08 eV, respectively. Lower S_1 and T_1 energies for biphenyl-**7** relative to biphenyl-**6** are expected since **7** has a higher electron affinity than **6**.

3.4. 1,3-Diphenylisobenzofuran

1,3-Diphenylisobenzofuran (**8**) has been selected for singlet fission studies as a result of theoretical considerations and subsequent calculations that were performed for a series of biradicaloid species and identified this heterocycle as a chromophore in which singlet fission should be nearly isoergic.[30] In solution, the state energies are $E(S_1) = 2.8$ eV and $E(T_1) = 1.5$ eV, and in the crystalline solid, they are $E(S_1) = 2.7$ eV and $E(T_1) = 1.4$ eV.[82] The compound has two conformers (C_s and C_2 symmetry) with nearly identical spectroscopic properties, except for the distribution of intensities in the vibrational structure of the first absorption band. In solution, the quantum yield of fluorescence is close to unity and no triplet formation has been detected, suggesting that the rates of spin−orbit coupling induced intersystem crossing and other nonradiative decay processes are negligible.

At least two different kinds of polycrystalline solid films can be grown by sublimation.[32] In films grown on sapphire, X-ray diffraction and optical measurements show that the phenyl−phenyl line of the molecules lies parallel to the surface (the symmetry axis passing through the oxygen atom is oriented perpendicular to the surface). The triplet yield determined directly from triplet absorption and ground-state bleach is above 100% at all temperatures between ambient and 12 K. About half of the triplet absorption, which is due primarily to T_1-T_6 and T_1-T_8 transitions, appears within 2 ps after excitation ($k = \sim 5 \times 10^{11}$ s^{-1}), and the other half arises with a time constant of ~25 ps ($k' = \sim 4 \times 10^{10}$ s^{-1}). The T_1-T_7 transition contributes to the triplet absorption in solution obtained by flash photolysis in the presence of a sensitizer but does not contribute in the solid film since it is polarized along the symmetry axis, and the two triplet−triplet absorption spectra therefore have different shapes in this spectral region.

The ~25 ps time constant is the same as the time constants for the decay of the S_1 absorption and for the additional decrease of S_0-S_n absorption (increase of ground-state bleach) after the initial excitation pulse, leaving no doubt that the triplet arises by singlet fission. The triplet lives for at least a ns. The maximum yield is reached at about 77 K and is 200 ± 30%, as determined independently from (i) a comparison of the ground-state bleach immediately after excitation and 200 ps later and (ii) a comparison of the ground-state bleach and triplet absorption intensities, assuming that the ratio of their absorption coefficients is the same in solution and in the solid (a correction for the anisotropy of the solid, based on a comparison of results obtained at normal and oblique incidence, was performed). The assumption regarding the ratio of absorption coefficients is supported by the near identity of solution and film spectra in the region of the purely polarized S_0-S_1 transition, both absorption and fluorescence.

In films grown on other substrates, which have a similar but not identical crystal structure as judged by their X-ray powder patterns, the triplet yield is an order of magnitude smaller. At present (Table 2), the triplet yield observed on the films of **8** grown on sapphire represents by far the highest singlet fission yield directly observed in a neat organic solid layer, although less direct evidence suggests that the room-temperature triplet yield in solid **2**[14,120,148] must be similarly

high, as is the yield recently indirectly determined from ground-state bleach for a carotenoid aggregate by ps time-resolved resonance Raman spectroscopy[110] (section 4.1).

These results make **8** the first successful compound purposely designed to exhibit efficient singlet fission, using the design principles outlined in section 2, although it is admittedly only accidental that the crystal structure of the C_2 conformer of **8** contains slip-stacked pairs of molecules in an arrangement that appears to be nearly optimal for the direct mechanism of singlet fission based on the arguments made there (Figure 12). It is not presently certain that the same crystal structure is present in the film sublimed on sapphire.

Triplet formation was also observed in polycrystalline solids of three dimers of **8** (**30**, **31**, and **32**),[82] presumably again due to singlet fission, because in cyclohexane solution these compounds exhibit no detectable triplet formation. These materials have not yet been examined in detail.

3.5. Miscellaneous

*Perylene (**9**)*

The study of singlet fission in **9** is made particularly interesting by the fact that this hydrocarbon is available in two crystalline forms, α-**9** and β-**9**, the former of which forms excimers. Optically induced fission is a suitable probe for excimer formation because it provides information about whether the excimer forms on a faster time scale than vibrational relaxation and fission.[212,213] If it does, the excimer-forming α form should exhibit a higher threshold energy for singlet fission due to the additional energy needed to break the excimer. This has been found to be the case.[138,212,213] Using the magnetic field effect on prompt fluorescence as a function of excitation energy for an indicator, the threshold energy for α-**9** is 3.51 eV, blue-shifted by 0.5 eV from the β-**9** threshold of 3.01 eV,[212] and one can conclude that in the α form excimer formation is faster than singlet fission. A theoretical estimate puts the rate of excimer formation at 10^{13} s^{-1}.[212] On the basis of the blue shift of the threshold energy in α-**9**, the binding energy for two triplets on neighboring molecules is 0.04 eV.

Singlet fission has been observed in single crystals of **9** (unspecified form, α or β) excited with vacuum UV radiation at energies higher than twice the triplet energy, as evidenced by magnetic field effects on the prompt fluorescence intensity.[80] The fluorescence enhancement increased with increasing magnetic field strength before eventually saturating and was anisotropic with respect to magnetic field orientation.

*Tris-(8-hydroxyquinoline)aluminum (Alq3, **10**)*

This material is of interest for use in organic light-emitting diodes (OLEDs), where it is often desirable to keep triplet formation as low as possible to produce light by fluorescence rather that phosphorescence. Because high current densities are commonly used, it is of interest to study triplet formation and decay under these conditions. At high excitation intensities, transient absorption signals in thin films of **10**[121] show that excited singlets fuse to form higher excited singlets. Because of the prevalence of annihilation as a relaxation process for singlets under these conditions, the singlet population is proportional to $I_{ex}^{1/2}$. Triplets formed by singlet fission were also observed at high excitation intensities. Triplets formed by intersystem crossing have a density proportional to $I_{ex}^{1/2}$, whereas those formed by singlet fission have a density proportional to I_{ex}. Thin films were excited with various intensities of 3.49 eV light. At $I_{ex} < 2 \times 10^{21}$ photons cm^{-2} s^{-1}, intersystem crossing accounted for all triplet generation. At $I_{ex} > 2 \times 10^{22}$ photons cm^{-2} s^{-1}, the density of triplets is proportional to the excitation intensity. By subtracting the triplet density expected from intersystem crossing, the triplet quantum yield from singlet fission was determined to be 30%.

*Benzophenone (**11**)*

Singlet fission has been observed in single crystals of **11** under two different excitation intensities using ps time-resolved absorption spectroscopy.[214] At lower excitation intensities, the triplet rise time equals the decay time of excited singlet absorption, indicating that intersystem crossing is solely responsible for triplet formation. At four times higher excitation intensities, the total triplet rise time was faster than would be expected from intersystem crossing alone. A two-photon absorption to a highly excited singlet, followed by singlet fission, was consistent with the observed triplet formation. A good fit of the triplet rise time under high excitation intensity was obtained assuming that 40% of triplets are formed by fission.

*Rubrene (**12**)*

In a recent study of exciton diffusion in rubrene single crystals using photoconductivity measurements, long-lived excitons assigned as triplets were observed. Singlet fission was suggested as a possible source of these triplets, but no attempts to obtain direct evidence for singlet fission were made.[235]

4. Aggregates

As crystal size diminishes, the relative importance of surface molecules increases, and by the time nanocrystal size is reached, order tends to decrease. Very small nanocrystals are difficult to differentiate from molecular aggregates. The exact structure of such species is frequently known only approximately or not at all. The limiting cases are noncovalent dimers.

With one exception, no singlet fission work seems to have been done on nanocrystals and aggregates. This is unfortunate, because one can easily imagine that they could be used as sensitizers on semiconductor nanoparticles in photovoltaic cells. The striking exception is the carotenoids, which occur naturally in the photosynthetic apparatus in the form of aggregates and have been almost exclusively investigated for singlet fission in aggregates only.

4.1. Carotenoids

Carotenoids contain a series of linearly conjugated double bonds and can be viewed as oligomers on the way from ethylene and 1,3-butadiene to the simplest conjugated polymer, polyacetylene. As mentioned in section 2.2.2 and summarized in more detail in the introduction to section 5, in the usual all-anti configuration of such structures the lowest excited singlet electronic state S_1 is the doubly excited $2A_g^-$ state that can be viewed as a singlet-coupled combination of triplet excitations localized in two different parts of the chromophore. The strongly allowed $1B_u^+$ HOMO−LUMO state that represents the usual optical entry into the excited

state manifold is significantly higher in energy. Thus, carotenoids are representative of class III chromophores in the sense introduced in section 2.2.2. The excitation energy of the T_1 state is approximately half of that of the S_1 state, making singlet fission isoergic or even somewhat exoergic and thus favorable.

Singlet fission in carotenoids was initially proposed[21] following the observation of magnetic field effects on the fluorescence of carotenoids that occur naturally in bacterial whole cells and antenna complexes, similar to the effects characteristic for singlet fission in molecular crystals. The progression of excited states reached upon carotenoid excitation has been elucidated by ultrafast spectroscopic measurements.

Fission is thought to occur from the S_1 ($2A_g^-$) state.[215] It is still debated whether this state is populated from the $1B_u^-$ state,[215,216] which lies between the $1B_u^+$ and $2A_g^-$ states[122,124,215,216] and has been identified using resonance Raman excitation,[215] or from the $1B_u^+$ state.[122,124] The vibrational progressions of the carotenoids spheroidene (**13**, 10 conjugated double bonds) and lycopene (11 conjugated double bonds) also indicate the presence of a $1B_u^-$ state between the states $1B_u^+$ and $2A_g^-$. A study of hexane solutions of neurosporene (**14**, 9 conjugated double bonds) by time-resolved absorption spectroscopy found that, after excitation into the $1B_u^+$ state, internal conversion to the $1B_u^-$ state occurred within 80−300 fs.[215] Conversion from the $1B_u^-$ to the $2A_g^-$ state occurred on a time scale of 300 fs. The transient absorption spectrum of hexane solutions of spirilloxanthin (**15**, 13 conjugated double bonds) contains three components with lifetimes of 100 fs, 1.4 ps, and 6 ps.[124] The 100 fs component was assigned to the $1B_u^+$ state, which was thought to decay simultaneously to the $2A_g^-$ state and a state tentatively identified as $1B_u^-$. The $2A_g^-$ state was assigned the 1.4 ps lifetime, and the $1B_u^-$ state was assigned the 6 ps lifetime. Triplet formation was not observed in this case nor was it observed in the hexane solution of **14**.[215] The simultaneous decay of the $1B_u^+$ state to both $2A_g^-$ and $1B_u^-$ states was also observed for **13** as part of an isolated *Rhodobacter sphaeroides* antenna complex.[217] This progression differs from that proposed by other authors,[215] in which the $2A_g^-$ state is populated from the intermediate $1B_u^-$ state.

Perhaps the easiest case of singlet fission in a carotenoid aggregate to understand is described in a very recent ps time-resolved resonance Raman study of several hundred nm long and 20−30 nm wide rod-shaped aggregates of all-*trans*-3R,3′R-zeaxanthin (**21**, 11 conjugated double bonds) produced by adding water to a tetrahydrofuran (THF) solution.[110] The excitation energy of the S_1 state of monomeric **21** is 1.8 eV, and that of the T_1 state is 0.87 ± 0.1 eV. The triplet yield is 0.2%. The characteristic Raman spectrum of the S_1 state of the monomer is not observed at all when the aggregate is excited, and the S_1 decay is complete in less than 4 ps, within the duration of the exciting pulse. Instead, for both monitoring pulse wavelengths employed, the Raman spectrum of the T_1 state is observed already at zero delay and reaches a maximum within 4 ps. The bleach of the ground state is maximized on a similar time-scale. There is no indication that radical ions are formed. The clean ps-scale S_1 to T_1 conversion has been attributed to singlet fission.

The T_1 signal and the ground-state bleach decay in a multiexponential fashion, with time constants of 5−7 ps (40%), 600−700 ps (30−40%), and in excess of 3 ns (20−30%). The rapid decay is attributed to the exothermic annihilation of $T_1 + T_1$ to $S_0 + T_2$. The fastest component is believed to be caused by geminal recombination. For different initial excitation pulse energies, both monomeric **21** and its aggregate show a linear depletion up to 20% excitation ratio examined, but the slope of the dependence of the depletion on pulse energy is twice steeper in the aggregate than in the monomer sample. The depletion of two chromophores per absorbed photon would be expected if the singlet fission yield were 200%. If annihilation occurred after fission, the vibrationally hot S_0 state produced would not cancel any of the ground-state bleach as long as its peaks are shifted relative to the cold S_0 state. An alternative interpretation of the slope difference in terms of coherence effects in strongly interacting chromophores was considered unlikely because all indications are that the exciton coupling in the aggregate is weak.

This indirect determination of a ∼200% singlet fission yield can be compared with an independent direct determination based on a comparison of the T_1 signal and ground-state bleach intensities at 4 ps pump−probe delay, which yields 90%. This value is the lower limit, since any annihilation that takes place within 4 ps will reduce the T_1 signal.

Understanding fission in carotenoid aggregates contained in whole bacteria is complicated by the presence of several different components, including an antenna complex containing bacteriochlorophyll and one or more types of carotenoid, and a photosynthetic reaction center. By oxidizing the reaction center, which can be done chemically or by using saturating excitation intensities, energy transfer from the antenna chromophores to the reaction center can be blocked, allowing the photophysics of the antenna complex to be studied. This is desirable because carotenoids in the antenna complex have been identified as essential to the singlet fission process, either in homofission or as one of the partners in heterofission. Singlet fission is observed upon carotenoid excitation but not bacteriochlorophyll excitation,[123,218−220] and the occurrence of fission in the antenna complex has been confirmed by the study of reaction center-free bacterial mutants of *rhodopseudomonas capsulata*.[220] The mutant Y142 contains **13** and spheroidenone (**16**, 9 conjugated double bonds), and the mutant BY1424 contains **14**, hydroxyneurosporene (**17**, 9 conjugated double bonds), and methoxyneurosporene (**18**, 9 conjugated double bonds). Upon carotenoid excitation, Y142 exhibited a 0.6% increase, and BY1424 exhibited a 2.1% increase in fluorescence in a 3 kG magnetic field. Magnetic field-dependent triplet yields are observed in oxidized cells of both *Rhodospirillum rubrum (r. rubrum)* and *rhodopseudomonas sphaeroides* (*rps. sphaeroides*) and in their isolated antenna complexes upon excitation of the antenna carotenoid, but not in the corresponding carotenoid-free mutants (*r. rubrum* FR1 VI, *rps. sphaeroides* R26).[123]

Carotenoid excitation dynamics in antennae or whole cells are similar to those in hexane solutions; however, an additional long-lived triplet state is observed.[215] In **14** as part of the *Rhodobacter sphaeroides* antenna complex,[215] a long-lived component arises 0.5−3 ps after excitation. This component was assigned to the combined triplet states of **14** and bacteriochlorophyll and thought to be due to heterofission from the $2A_g^-$ state of **14**. Femtosecond transient absorption spectroscopy of membrane fragments of *r. rubrum,* which contains mainly **15**, has pointed to a $1B_u^-$ state as an intermediate between $1B_u^+$ and $2A_g^-$ in **15**.[124] The lifetimes of the $1B_u^+$, $2A_g^-$, and $1B_u^-$ states were

60 fs, 1.45 ps, and 5.3 ps, respectively, with an additional long-lived component that was assigned to the triplet of **15**. The fast formation (within 5.3 ps) of the triplet state suggested singlet fission as the source, and a yield of 35% at room temperature was estimated. Triplet formation has also been observed in *Chromatium vinosum*[221] and attributed to the carotenoids, **15** and rhodopin (**19**, 11 conjugated double bonds), that it contains. When studied by transient absorption and ps time-resolved resonance Raman spectroscopy with 8 ps pulses, the initially excited carotenoid 1^1B_u state was found to decay into the 2^1A_g state in <1 ps. The 2^1A_g state accounted for the fastest observed decay component with a constant of 6 ps. Additional components with decay constants of 80 ps and 200 ns were also seen. Triplet formation was observed in the ps time-resolved resonance Raman spectrum with a rise time of about 6 ps, which is correlated with the decay of the 2^1A_g state, leading to the conclusion that triplets are formed by fission of the 2^1A_g state. The 80 ps decay component of the transient absorption was attributed to fast triplet decay due to fusion, and the 200 ns component was attributed to the slower decay of triplets formed by intersystem crossing. Aggregates of bacteriochlorophyll and β-carotene (**20**, 11 conjugated double bonds) with similar spectral properties to naturally occurring chlorosomes can be formed by self-assembly.[222] An excited state absorption of the aggregates which forms on a time scale of ~15 ps and has a lifetime of 2.3 μs is attributed to absorption of triplets created by homofission of **20**.

It remains in debate whether heterofission or homofission is the process that takes place in the bacteriochlorophyll antenna complex. Both are expected to proceed without an activation energy. In a study by fs transient absorption spectroscopy of *r. rubrum* membrane fragments,[124] no bacteriochlorophyll triplet states were observed, indicating that homofission and not heterofission was the active process. A study of triplet formation in *r. rubrum* suggests that homofission takes place in the carotenoid.[219] Carotenoids were excited in whole cells of oxidized *r. rubrum* using 35 ps pulses of 532 nm light. Bleaching of the carotenoid ground state and triplet−triplet absorption were observed in the absorption difference spectra. The fast formation of triplets (within 100 ps) and high yields compared with **15** in solution made triplet formation consistent with singlet fission rather than intersystem crossing. Because no bacteriochlorophyll triplets produced after excitation of the antenna carotenoid were detected, homofission of two carotenoids was identified as the likely source of carotenoid triplets.

Magnetic field effects on triplet formation were studied using absorption difference spectroscopy upon excitation of the carotenoid (530 nm) in *r. rubrum*.[21] Triplet formation was attributed to singlet fission in the antenna complex, but it could not be determined whether homofission or heterofission was occurring. The triplet quantum yield upon carotenoid excitation was 32% and decreased by 45% in a 0.6 T magnetic field. In studies of *r. rubrum* and *rhodopseudomonas sphaeroides* (*rps. sphaeroides*) oxidized cells and isolated antenna complexes, fission was monitored both indirectly by bacteriochlorophyll emission[218] or by absorption difference spectroscopy[123] upon excitation of the antenna carotenoid. The triplet quantum yield is magnetic field dependent. It is 30% for *r. rubrum* S1 (contains **15**), ~2% in *rps. sphaeroides* 2.4.1 (contains **13**), and 1.5% in *rps. sphaeroides* GC1 (contains **14**). The excitation spectrum of the magnetic field-dependent bacteriochlorophyll emission was similar to the absorption spectrum of the carotenoid, suggesting that the carotenoid is the fissionable species. It was not unequivocally determined for *r.rubrum* S1 whether homofission or heterofission involving one carotenoid and one bacteriochlorophyll was the active process. In both *rps. sphaeroides* GC1 and 2.4.1 homofission was thought to be more likely.

Finally, in hexane solutions **15** does not undergo singlet fission, but in *r. rubrum* antennae, where individual molecules of **15** are believed to be separated by 20 Å, it does.[124] If the separation is indeed this large, the participation of two molecules of **15** in the singlet fission event is very unlikely. To explain the observations, it has been proposed that in this case the fission is intramolecular. The protein environment has been postulated to encourage a distortion of the carotenoid backbone that effectively breaks it up into two chromophores, permitting a conversion of the $2^1A_g^-$ state into two triplets localized in two different parts of the molecule.[124] This proposal is supported by a study of triplet quantum yields in **13** and **15** incorporated into a carotenoid-free antenna complex of *Rhodobacter sphaeroides*.[122] Resonance Raman measurements indicated that, whereas **15** is in a twisted conformation when part of *r. rubrum,* it becomes closer to planar in *Rhodobacter sphaeroides.* The carotenoid **13** is also planar as part of the *Rhodobacter sphaeroides* antenna complex. It showed a triplet yield of ~5% when incorporated into the carotenoid-free antenna complex of *Rhodobacter sphaeroides* as it does as a naturally occurring part of the bacteria. In contrast, **15** showed a marked decrease in triplet yield when it was within *Rhodobacter sphaeroides* compared with *r. rubrum* (from 30% to 5−10%). The decrease in triplet quantum yield for a more planar configuration of **15** supports the hypothesis that both triplets might be localized on different parts of the same carotenoid molecule.

Biologically, carotenoids serve the dual purpose of light harvesting and accepting triplets formed in bacteriochlorophyll by intersystem crossing, thereby preventing harm to the organism.[124] The production of triplets by singlet fission does not appear to provide any biologic advantage as they do not contribute to light harvesting,[124] and it is unclear why nature chose to develop photosynthetic apparatus in this manner. It is possible that advantages in terms of triplet acceptance from bacteriochlorophyll outweigh disadvantages in terms of light harvesting.[124]

5. Conjugated Polymers

In section 2.2.2 we have already provided a brief historical introduction to the excited states of short linearly conjugated polyenes (in particular, butadiene) and mentioned that in these chromophores the two lowest excited states, S_1 and S_2, are nearly degenerate. One of them is predominantly singly excited and the other can be described approximately as doubly excited and can be viewed as a singlet-coupled combination of two local triplet excitations in two halves of the chromophore. As the number of double bonds in the linearly conjugated π-electron system increases, the energy of the doubly excited state diminishes faster than that of the singly excited state, and it becomes increasingly obvious that the longer polyenes belong to chromophores that we have referred to as class III, with S_1 not of the HOMO−LUMO type, but clearly of doubly excited nature. As far as we can tell, carotenoids, discussed in section 4, and linear conjugated

polymers, discussed in the present section, are the only known cases of this situation.

Electronic states of polyenes are usually classified more formally according to the C_{2h} symmetry group, although only the all-anti ("all-*s*-trans") conformers of the all-trans polyenes actually possess this symmetry. In this notation, the S_1 state of the shorter polyenes is $2A_g$ and their S_2 state is $1B_u$. Further classification is possible using an approximate pairing symmetry operation that exists within the framework of the semiempirical Pariser−Parr−Pople (PPP) model.[44,45] This allows an assignment of electronic states into "plus" and "minus" categories[47] and provides a selection rule according to which only transitions between states of opposite character are one-photon allowed. A closed-shell ground state is of "minus" symmetry. Although the pairing symmetry is not truly exact, it holds well enough that in practice only transitions from the ground state to states of the "plus" type can have substantial intensity in an ordinary absorption spectrum of an alternant hydrocarbon such as a polyene. In common notation, the ground state is $1^1A_g^-$ and the S_1 state, which can be viewed as singlet-coupled combination of two locally excited triplet states,[9−11,223] is $2^1A_g^-$. The first optically allowed state is $1^1B_u^+$ and in the shorter polyenes it is S_2, but in the longer ones forbidden transitions to other states intervene between transitions to the $2^1A_g^-$ and $1^1B_u^+$ states. For a sufficiently long polyene, it only takes a lattice distortion for the optically forbidden $2\ ^1A_g$ state (S_1, TT) to dissociate to form two localized triplets.[223]

5.1. Polydiacetylenes

Polydiacetylenes can be viewed as polyacetylenes dehydrogenated by removal of both hydrogen atoms on every other single bond. Thus, newly introduced additional π bonds are formed by orbitals that are perpendicular to the conjugated π system of the polyacetylene and do not interact with its conjugated π system, but they make every other single bond of the parent polyacetylene shorter and thus modify the usual bond length alternation. In parent **22**, the remaining substituents are hydrogen atoms, but in actually studied systems they are alkyls or substituted alkyls, as shown in formulas **22a**−**e**.

These polymers are available in a sol form in solution (presumably as coiled chains) and a gel form formed by adding a poor solvent to the solution (presumably aggregated straight chains with few or no interchain interactions). The polymers **22c**, **d**, and **e** occur in the "red form" and the "blue form". The blue form has fewer defects and a greater extent of conjugation than the red form.[224] The structure is determined by the method of polymerization. The red form is formed in solution and can be cast into films, whereas the blue form is produced by polymerization in KBr pellets or using a mechanically aligned monomer.[113] Isolated linear polymer chains can be generated at low concentrations (∼0.01% by weight) by polymerization within crystals of the diacetylene monomer.[111] They are isolated, linearly aligned, and have lengths of ∼2.6 μm, making them good approximations to one-dimensional conjugated systems.[111]

In polydiacetylenes, triplets are believed to be formed by fission of the S_1 state.[225] Singlet fission triplet yields for **22** are typically low: for **22b**, on the order of 0.1%,[22] and for **22c**, 0.4%.[125] Variations in singlet and triplet energies occur with conformational defects introduced by twists in the polymer backbone. A rise in the quantum efficiency of photogenerated triplet excitons in **22c** is observed over several tenths of an eV increase in excitation energy.[112] This has been modeled in terms of inhomogenous broadening due to varying conjugation lengths within the polymer and the release of vibrational energy in the formation of triplet excitons. From the model, $E(T_1)$ was calculated to be 1.1 eV and $E(S_1)$ was calculated to be 1.9 eV.

The intensity dependence of triplet formation has been used to estimate the threshold energy for singlet fission. In energy ranges where the intensity dependence is quadratic, triplet formation by fission has been proposed to occur by an initial two-photon absorption process,[22,111] which allows the energy requirements to be met even when the photon energy is below 2 $E(T_1)$. Triplet formation in isolated chains of **22a** and **22b** exhibits this type of intensity dependence.[111] In **22b** triplet formation has a quadratic dependence on intensity at 1.82 eV and the exponent steadily decreases to a value of 1.5 at energies greater than ∼2 eV. The corresponding triplet yield increases by 2 orders of magnitude between 1.82 and 2 eV. The variation of the power law exponent with excitation energy is due to simultaneous quadratic and linear processes with similar yields. A fit for **22b** indicated that at 2 eV ∼50% of singlet fission is due to a one-photon process. In **22a**, there is a similar trend in the intensity dependence and an order of magnitude increase in triplet yield between 1.82 and 1.9 eV. On the basis of the threshold for a linear intensity dependence, $E(T_1)$ is between 0.9 and 0.95 eV in **22b** and 0.95 to 1.0 eV in **22a**. In both of these cases, the activation energy for singlet fission is <0.1 eV.

The energy threshold for fission in isolated chains of **22b** is lower than what is observed in its sol and gel forms.[22] The intensity dependence of triplet yield in **22b** measured by transient absorption spectroscopy is quadratic at excitation energies of 2.48 eV (sol phase) and 2.32 eV (gel phase) and linear at an excitation energy of 3.49 eV in both phases.[22] A similar dependence of triplet yield on pump intensity at various excitation energies is found for thin films of **22c**.[125] In this case, the triplet yield is linear over a range of pump intensities at excitation energies above 2.15 eV and quadratic at excitation energies between 1.95 and 2.15 eV. On the basis of these observations, 2.15 eV is the threshold energy for singlet fission, with $E(T_1) = 1.07$ eV. However, at energies where the intensity dependence is quadratic, the proposed[22] simple two-photon process has been questioned, as there are no corresponding changes in two-photon absorption in the region. The proposed alternative[125] is a low-energy (0.1−0.2 eV) structural change induced by the first absorption and followed by a second absorption step that fulfills the energy requirements for singlet fission.

In the case of diffusive excitons in one-dimensional systems, decay due to fusion will be proportional to t^{-1} at times much shorter than the inverse of the hopping rate and to $t^{-1/2}$ at longer times.[226] Alternatively, a lack of bimolecular decay indicates that triplets become trapped along the polymer chain. In **22b** the triplet decay in the sol phase was exponential, whereas the gel phase decayed with t^{-1}, and only in the gel phase did the triplet lifetime show a magnetic field dependence.[22] The sol phase was thought to support increased localization of the triplet excitons, accounting for the lack of both bimolecular decay and magnetic field dependence. Nonexponential triplet decays on a time scale of 10 ps were observed for isolated chains of both **22a** and **22b**.[111] The short lifetime of triplets in this case, compared to the 30 μs[125] for films of **22c**, was attributed to decay by

a refusion of the correlated triplet pair, with a calculated fusion probability of 70%. The lower limit of the diffusion coefficient was calculated to be 10^{-4} cm^2 s^{-1} with a corresponding one-dimensional fusion rate constant of 5 cm s^{-1}. No evidence of self-trapping was observed for **22a** and **22b**. For films of **22c**,[125] the three-dimensional fusion rate constant was estimated to be $<7 \times 10^{-15}$ cm^3 s^{-1}. This is a small value that implies that the triplets are self-trapped and immobile.

In the isolated chains of both the red form and the blue form of **22d**, triplet formation has been observed by measuring ms photoinduced absorption spectra.[113] The triplet lifetime at 77 K was 150 μs in the red phase and 210 μs in the blue phase. These lifetimes were independent of pumping power, indicating that the decay was unimolecular. The triplet lifetimes found at 20 K were very similar to those at 77 K, indicating that triplet excitons are deeply trapped. Measurements of fs on isolated red phase **22d** demonstrated a triplet state with a rise time within the 200 fs resolution of the experiment.[113] Singlet fission occurred when the pump energy was at the absorption edge and the upper limit of $E(T_1)$ was estimated at 1.07 eV. Further fs pump−probe measurements on the red phase of **22d** revealed that triplet decay had the form of a stretched exponential [$\exp(-t/\tau)^{\alpha}$, $\tau = 13.6$ ps, $\alpha = 1/3$] plus a plateau.[227] The decay is consistent with one-dimensional diffusion in the presence of traps, which were estimated at one per every 50 sites and thought to be twists in the polymer chain. The plateau was thought to be caused by deeply trapped triplets, which are excluded from recombination.

Observation of the formation dynamics of the triplet excitons on the red form of **22e** in benzene solution using transient transmission difference spectroscopy with 7 fs pulses revealed that the initially excited ^1B_u state is converted to the 2^1A_g state with a time constant of 30 fs.[225] The 2^1A_g state then separates into two triplet excitons with a time constant of 70 fs. A triplet exciton of **22e** was calculated to extend over 2.5 polymer units; thus, triplets must be >5 units apart to be considered separated.

5.2. Poly(diethyl dipropargylmalonate)

Poly(diethyl dipropargylmalonate) (**23**) can be prepared with conjugation lengths that typically exceed 100 double bonds and is therefore used to approximate an infinite chain polymer. When THF solutions of **23** were excited in the range of 1.8−2.5 eV, overlapping the peak absorption, transient signals decayed to zero after 5 ps.[228] When excited at 3.2 eV with a 200 fs pulse, an additional long-lived excited state absorption at 1.85 eV appeared within the excitation time. This excited state absorption has been assigned to triplets created by fission of the $2^1A_g^-$ state.

5.3. Poly(*p*-phenylene)

Poly(*p*-phenylenes) are electroluminescent polymers that can be used in solar cells, as photoconductors and laser materials.[229] The triplet yield action spectrum of methyl-substituted ladder-type poly(*p*-phenylene) (**24**) films has been measured using a photomodulation technique.[114,115,230] A step due to intersystem crossing can be seen near the S_1 energy of 2.6 eV. At higher energies, a rise in the triplet photogeneration takes place with an onset of 3.2 eV and continues for several tenths of an eV before reaching a plateau at 3.7 eV. This triplet photogeneration is attributed to fission of hot excitons. The triplet energy $E(T_1) = 1.6$ eV. The gradual rise in the triplet photogeneration action spectrum has been modeled, taking into consideration two factors: inhomogeneous broadening due to variations in conjugation length and the release of vibrational energy.[112]

5.4. Poly(*p*-phenylene vinylene)

These polymers have been of interest in organic solar cells.[231] The triplet yield action spectrum of poly(*p*-phenylene vinylene) (**25**) thin films has been measured[112,116,117] by the same photomodulation technique as described above for **24**,[112,114,115] with qualitatively similar results. For poly(*p*-phenylene vinylene), the onset of triplets produced by singlet fission in the action spectrum occurs at 3.1 eV, with a gradual increase to a plateau at 4.4 eV. The corresponding triplet energy $E(T_1)$ is 1.55 eV, whereas the energy of the singlet $E(S_1)$ is 2.45 eV. The authors attribute the gradual rise in triplet yield with excitation energy to the same causes as described above for **24**, namely, inhomogeneous broadening and generation of strongly coupled vibrations. The intensity dependence of the triplet yield is linear at low pump intensities, becoming proportional to $I^{1/2}$ at higher pump intensities.[117] The latter is indicative of bimolecular decay of the triplets. The spatial extent of the triplet exciton wave function is 3.2 Å, based on photoinduced absorption detected magnetic resonance measurements.[116]

5.5. Polythiophene

Regiorandom (RRa-) and regioregular (RR-) poly(3-hexylthiophene) (**26**) are of interest for use in organic solar cells and optoelectronics.[232,233] RR-**26** forms 2D lamellar structures with strong interactions between polymer chains and with delocalized singlet excitons. In contrast, RRa-**26** films are amorphous and singlet excitons are localized. Exciton formation has been studied in both RRa-**26** and RR-**26** using transient absorption spectroscopy.[234] In RRa-**26**, $2E(T_1)$ was slightly above the excitation energy used and triplet excitons were formed on the ps time scale by fission of a highly excited singlet produced by singlet−singlet fusion. In RR-**26**, $2E(T_1)$ was approximately equal to the excitation energy used. No triplet formation was observed in this case, presumably because the interchain interactions in RR-**26** favor the formation of polaron pairs over the singlet fission process.

6. Dimers

Covalently linked dimers are interesting systems for the study of singlet fission as they contain the minimum number of chromophores necessary for the process to occur. They offer an opportunity to study singlet fission on isolated molecules in solution and to examine the effect of various modes of interchromophore coupling. At the same time, they do not permit the two triplet excitations to diffuse apart, and they allow a study of their interaction as a function of time.

Singlet fission in covalently linked dimers has been demonstrated for two types of parent monomeric chromophores, **2** and **8**. Both monomers undergo efficient singlet fission in their crystalline form, albeit in the former case only at temperatures above ~165 K[82] (see section 3.1.2). However, it is not immediately obvious that singlet fission will be efficient in the covalent dimers as well.

(i) As discussed in section 2.2.2, depending on the dimer structure the intermonomer electronic coupling responsible for fission could be quite different in the dimer and in the crystal.

(ii) Even if singlet fission is exoergic in the crystalline monomer, creation of a dimer could lower the energy of S_1 to a greater extent than that of T_1, making singlet fission endoergic in the dimer. The role of interchromophore coupling was examined computationally using DFT for variously coupled dimers of three parent chromophores, **2**, **8**, and 3-dicyanovinylidene-6-(2′-imidazolidinylene)-1,4-cyclohexadiene (**33**).[31] The electron transfer integral t was calculated to measure interchromophore coupling for the HOMO (t_h) and LUMO (t_l) and the energy difference ΔE^0 was used as a measure of the thermodynamic driving force. The approximate expression that was derived, $\Delta E^0 = 2[E(T_1) - E(S_0)] - [E(S_1) - E(S_0) - |t_h| - |t_l|]$, indicates that stronger coupling causes a larger decrease in the thermodynamic driving force for singlet fission, and singlet fission was calculated to be endoergic for strongly coupled dimers of **2** and **8**.

(iii) Whereas in the crystal the triplet excitons created by singlet fission can diffuse apart and live for a long time, this cannot happen in an isolated dimer. The two triplet excitations are forced to coexist in the same molecule and there is an increased danger that this doubly excited state will rapidly decay to a singly excited state. From the point of view of possible applications in solar cells, this would be disastrous.

6.1. Polyacenes

We saw in section 3.1 that, among crystalline polyacenes, **2** is a most promising candidate for an efficient chromophore for singlet fission, because the process is only slightly endothermic and other channels are not competitive (**3** may be even better, but at the moment its properties with regard to singlet fission are unclear). Not surprisingly, **2** attracted attention as a possibly suitable building block for the construction of a dimer. Evidence for singlet fission was looked for in three covalently linked dimers of **2**, 1,4-bis(5-tetracenyl)benzene (**27**), 4,4′-bis(5-tetracenyl)-1,1′biphenylene (**28**), and 1,3-bis(5-tetracenyl)benzene (**29**).[126,127] At optimal ground state geometries of **27**−**29**, the benzene linker is calculated to be considerably twisted out of the tetracene planes,[127] and weak interchromophore coupling would be expected. Indeed, steady-state fluorescence spectra of the dimers are only slightly red-shifted and broadened relative to the spectrum of monomeric **2**. Referring back to section 2.2.2, we see that these dimers are of the linearly linked as opposed to stacked type. The linker is relatively large and effectively reduces the overlap of orbitals located on different chromophores. In contrast to the situation in a crystal of **2**, one might therefore expect the direct mechanism of singlet fission to be suppressed and the mediated mechanism to prevail, if singlet fission occurs at all.

In degassed solutions of **27** and **28**, the fluorescence decay is biexponential. The amplitude of the long-lived (>100 ns) component decreases with decreasing temperature in the range of 175−325 K, and in oxygenated solutions, this long-lived fluorescence is absent. Both of these observations suggest that triplet excitations are present in both halves of the dimer and that they are produced by thermally activated singlet fission. The nature of the long-lived dark state capable of reverting to S_1 on one of the chromophores in terms of the nine sublevels is not known. It could be carrying two uncorrelated triplet excitations, but it could also be best described as containing populations of excited singlet, triplet, and quintet double triplet states of the covalent dimer, or as containing populations of the nine eigenstates of the total Hamiltonian $\mathscr{H}_{el} + \mathscr{H}_{spin}$ (section 2.3).

Fission yields were ∼3% for both dimers **27** and **28**. The fission rate constants were 2.8×10^6 and 4.0×10^6 s^{-1}, respectively, several orders of magnitude below those of crystalline **2** (Table 3). The activation energies were similar to those in crystalline **2**, 0.10 eV in **27** and 0.04 eV in **28**, but the Arrhenius prefactors for fission were only 1.5×10^8 and 1.7×10^7 s^{-1}, respectively. The very low efficiency thus appears to be due to insufficient electronic coupling.

No evidence of singlet fission was observed in the *m*-coupled dimer **29**, in which the overlap of MOs located on different chromophores **2** would be expected to be particularly small. The absence of activity in **29** and the low fission rates in the dimers **27** and **28** are thus entirely compatible with the arguments made in section 2.2.2 for the overlap densities involved in the direct singlet fission mechanism in linearly linked dimers. It is possible that only the mediated mechanism effectively contributes to the slow singlet fission observed. Solvent effects have not been examined, and it would be interesting to return to the subject and see whether in a polar solvent a two-step singlet fission process proceeding via a charge-transfer state and similar to that described in section 6.2 for **30** and **31** could be observed for these dimers of **2** as well.

According to DFT calculations,[127] in the ground state the linker benzene ring is at an angle of ∼90° to the planes of the chromophores **2**. The rotational barrier is on the order of kT at room temperature, and relaxed S_1 and T_1 state energies reproduce the trend in activation energies, with that of **29** equal to twice that of **27**. The calculated T_1 energies for each of the three dimers are very similar, whereas the S_1 energies vary more.

The relative importance of through-bond and through-space interactions to the interchromophore coupling was examined.[127] The latter was approximated by the point dipole interaction between transition moments of the two chromophores **2** and was 85, 25, and 90 cm^{-1} for **27**, **28**, and **29**, respectively. These energy differences are considerably smaller than the splitting of the S_1 energies found by TDDFT for **27** and **29**, whose phenylene linker contains only a single benzene ring (240 and 380 cm^{-1}, respectively). No splitting in the S_1 energy was predicted by TDDFT for **28**, whose linker contains a chain of two benzene rings. It was therefore concluded that through-bond interactions were dominant over through-space interactions, but of course one could question the approximation that was used for the through-space part.

These dimers were among those subsequently examined theoretically,[31] and it was suggested that the yield of fission in this case was low because the interchromophore coupling was too weak for the mediated mechanism to work well (in this study the direct mechanism was neglected altogether).

6.2. *o*-Quinodimethanes

The chromophore **8** has been designed as particularly hopeful for isoergic singlet fission[30] and indeed shows an ∼200% triplet yield in a neat solid (section 3.4). Its covalent dimers **30**−**32** were examined in the hope of finding efficient singlet fission.[82,86] Once again, the hope was disappointed and only triplet yields of 9% or less were observed. Nevertheless, interesting observations resulted, especially the

first direct evidence for a two-step version of the mediated singlet fission mechanism (section 2.2.2).

Methane bis[4′,4″-(1,3-diphenylisobenzofuran)] (**30**), bis[4′,4″-(1-(2′,6′-dimethylphenyl))-3-phenylisobenzofuran] (**31**), and bis(*p*,*p*′-1,3-diphenylisobenzofuran) (**32**) are of the linearly linked as opposed to the stacked type, and arguments of section 2.2.2 again suggest that if singlet fission occurs at all, the mediated mechanism rather than the direct mechanism would be responsible. This would certainly be expected in the weakly coupled dimers **30** and **31**, although perhaps not in the directly conjugated dimer **32**, with its large overlap between the directly connected atoms of the link. Because in the case of **32** the two monomers are in direct conjugation, it is questionable whether the analysis of section 2.2.2 can be applied at all. Whereas the absorption and fluorescence spectra of **30** and **31** are very similar to those of monomeric **8**, the first transition of **32** is red-shifted by 2200 cm^{-1}.[82,86] Thus, the dimer **32** may well be past the borderline of what can still be considered a pair of chromophores as opposed to a single conjugated π system. However, it has the flexibility to twist around the central bond after excitation, permitting an effective uncoupling of the two units of **8**. In this regard, it is reminiscent of the carotenoids discussed in section 4.1.

In nonpolar solvents, the dimers **30** and **31** exhibit only fluorescence and no detectable triplet formation, presumably because the rates provided for singlet fission by both the direct and the mediated mechanisms are too slow. In strongly polar solvents, triplet formation occurs with temperature-dependent yields ranging up to ~9% (for **31** in DMF at 230 K), and the triplet formation action spectrum follows the ground-state absorption spectrum. The triplet is not formed directly from the initially excited singlet state but from a nonemissive charge-transfer intermediate that consists of a radical cation of one of the chromophores linked to the radical anion of the other chromophore, and whose absorption spectrum is a superposition of the known[81] spectra of these radical ions. This dipolar intermediate is in rapid equilibrium with the initially excited singlet state, and in a slower equilibrium with a species whose absorption spectrum is indistinguishable from that of the triplet of **8**. This cannot be the lowest triplet state of the dimer, which would be much lower in energy and could not return to the dipolar intermediate, and is assigned as a double-triplet state, in which both chromophores are excited. It is not known whether the two triplets are independent or coherently coupled into a quintet state of the dimer. The dependence of singlet fission in **30** and **31** on solvent polarity and the observation of a charge-transfer intermediate suggest that the mediated mechanism of section 2.2.2 is in operation, with the charge-transfer state occurring as a real rather than a virtual intermediate, making singlet fission a two-step process in this case.

For dimer **32**, the action spectrum of triplet formation is shifted by ~1/4 eV to the blue relative to the absorption spectrum of the ground state. This is approximately the amount by which the S_1 state excitation energy in this directly conjugated dimer is reduced relative to those in the monomer **8** and in the weakly coupled dimers **30** and **31**. It thus appears that the triplet is not stabilized by the conjugation and that in **32** singlet fission is endoergic by ~1/4 eV and proceeds from vibrationally excited singlet states above a threshold energy, in competition with vibrational relaxation. This is an example of a linearly linked dimer in which stronger coupling appears to accelerate singlet fission but also disfavors it by making it endoergic, in agreement with calculations.[31]

In **32**, singlet fission is observed in both polar and nonpolar solvents and the triplet yield varies from 1 to 3% in a manner that is not a simple function of solvent polarity. No intermediate is observed and the triplet forms directly from the initially excited singlet state. It is likely that in such a strongly coupled dimer the direct and the mediated mechanism cannot be disentangled, and further experimental and computational investigations are needed.

7. Conclusions and Outlook

7.1. Neat Materials

For some time, the process of singlet fission has been well established and some aspects of it quite well understood in molecular crystals and, to a lesser degree, in neat polymers and oligomers. It appears to be fast and important in neat materials whenever singlet excitation is present at energies comparable with twice the energy of the lowest triplet excitation. This occurs in two sets of circumstances.

(i) In ordinary materials, when $E(S_1) \ll 2E(T_1)$ (materials of type I), singlet fission is rarely important, and needs consideration only rarely, when a highly excited singlet is produced. This situation results from events such as the absorption of high-energy photons, electron−hole recombination, or high-intensity irradiation that permits significant singlet exciton fusion even when low-energy photons are used.

(ii) In the rare materials of type II, in which $E(S_1) \approx 2E(T_1)$ or $E(S_1) > 2E(T_1)$, singlet fission occurs whenever singlet excitation is present and it is an integral part of their photophysics. At present, the polyacenes **2** and **3**, the biradicaloid **8**, some carotenoids (**13**−**21**), and polydiacetylenes (**22**) are the only thoroughly studied representatives of this class of materials, and the behavior of **3** is not understood.

The triplet excitons produced by singlet fission in materials of type I are not formed in high yield under conditions relevant for photovoltaic applications since singlet fission has to compete with other fast processes that remove excess excitation energy. Moreover, they usually stand a good chance of re-fusion (annihilation) to yield S_1 in an exoergic process. Even in those materials of type II that do not satisfy the condition $E(T_2) > 2E(T_1)$ (type IIA), such as the carotenoids, triplet exciton re-fusion is likely to occur fast with the formation of vibrationally excited T_1 and release of vibrational energy, and this has been observed in **21**. If the multiplication of the number of excitons by the singlet fission process is to be made useful in a practical sense, for instance in a solar cell, it would be preferable to choose those materials of type II for which the condition $E(T_2) > 2E(T_1)$ is satisfied (type IIB). Structural guidelines for a search for suitable chromophores[30] are summarized in section 2.2.1, and considerations that provide some guidance with respect to the optimization of their mutual coupling are outlined in section 2.2.2. The presently least well understood part of the quest for practical singlet fission materials is assuring two independent charge separation events (section 2.3). It is not yet clear whether nanocrystals or thin layers of these materials would be best for the purpose. In either event, one has little control over the solid-state structure and little opportunity to manipulate interchromophore coupling. One

possibility would be to use solids composed of covalent dimers, whose molecular structure can be predictably controlled by chemical synthesis, even if the solid structure cannot. A prerequisite for advances in the handling of the triplets that result from singlet fission would appear to be a detailed understanding of the nature and behavior of transients that appear at ultrashort times when solids such as **2**, **3**, or **8** are excited, and this issue needs to be addressed urgently.

7.2. Isolated Molecules

The understanding of singlet fission in isolated molecules is much less well developed and very little has been published. Yet, for use as solar cell sensitizers, for instance in cells of the Grätzel type, small molecules might be advantageous. To accommodate two triplet excitations and thus make singlet fission possible, they need to contain at least two relatively weakly interacting electronic excitation sites, either already at the ground-state equilibrium geometry or upon suitable distortion. This condition is most simply fulfilled in covalent dimers or oligomers, but one needs to take care that the coupling of the chromophores does not reduce the excitation energy of the S_1 state much more than that of the T_1 state, in which case a type II crystal-forming chromophore would form a type I covalent dimer. This happened when **8** was dimerized to **32**.

In the very few cases studied, the process of singlet fission was absent or slow, and the efficiency was a few % at best. This is true even though the chromophores used, **2** and **8**, could be called type II since they form bulk molecular crystals of type II, in which singlet fission occurs rapidly. It appears that in the dimers studied in solvents of low polarity, the chromophores were not coupled strongly enough for the direct mechanism to be operative, and the mediated mechanism was too slow as well and permitted the initial excited state to follow other decay paths. In the two-step variant of singlet fission observed in **30** and **31** in highly polar solvents, most of the charge-separated intermediate returned to the ground state and only a small fraction proceeded to the double-triplet state.

Attempts to increase the strength of interchromophore coupling can focus on optimizing the direct or the mediated mechanism, which have different structural requirements. Attempts to optimize the latter run two risks: $E(S_1)$ may drop below $2E(T_1)$, and the two triplets, even if generated in a high yield, may not act independently. This problem is especially acute in dimers, in which the two triplets formed cannot diffuse apart at all, and it may be better to use nanocrystals or small aggregates, where they can. In a covalent dimer, electron injection into a semiconductor from the S_1 state must be slow enough to allow singlet fission to take place, yet injection from the T_1 state must be fast enough to avoid refusion of the.triplet pair, and this may be hard to engineer. Fusion of the triplet pair into S_1 would not be disastrous, but fusion into a triplet would be. Even if T_2 is energetically inaccessible, fusion into a vibrationally hot T_1 state, with a loss of one of the electronic excitations (and fusion into a very hot S_0 state, with a loss of both excitations) are a concern and must be slower than electron injection into the semiconductor.

If the two triplets cannot diffuse apart, one also needs to be concerned with the rate of quenching of the second triplet by the hole or the unpaired electron left behind after the first triplet undergoes charge separation. Either this quenching has to be made slower than the charge separation performed by the second triplet, or the hole or unpaired electron has to be transferred to a safe distance very fast.

Dimers of chromophores of type IIB offer the unprecedented prospect that electronically excited quintet states of organic molecules could be observed, because the spin dipole−dipole coupling operator that enters into the description of the singlet fission process is of rank two and its matrix elements connect pure singlets with pure quintets. Such an observation would represent a significant generalization of the usual Jablonski diagram (Figure 2), which explains molecular photophysics in terms of singlet and triplet states only. It would be interesting to explore the borderline between molecular quintet states and molecular states containing two uncorrelated triplets, analogous to the line between molecular triplets or singlets versus biradicals in which the radical centers interact so weakly that they are best described as a pair of doublets.

7.3. The Striking Difference

A generally accepted theoretical understanding of the difference between the fast singlet fission in neat materials and slow singlet fission in otherwise similar isolated molecules is currently missing. The difference is dramatic. In a thin layer of neat **8**, the triplet yield is fairly close to 200% and prompt fluorescence hardly has a chance to compete, even though the interchromophore interaction is provided merely by physical contact. In the solution of the weakly coupled covalent dimers of **8** in cyclohexane, triplet is not detectable and the fluorescence yield is close to 100%, even though it is slow (radiative lifetime of a few ns), in spite of the fact that the interchromophore interaction is provided by chemical bonds. A similar contrast exists between the properties of crystalline **2** and those of its covalent dimers **27**−**29**. The difference is not due simply to the fact that in a crystal the two newly born triplets can diffuse apart and live relatively long independent lives, whereas in the covalent dimer they are forced to remain close to each other and remain exposed to additional decay opportunities. In the dimer, they are formed much more slowly to start with.

Our favorite rationalization of the difference is based on the inspection of the form of integrals that enter eqs 7−15 and visualization of the charge distributions involved (Figure 10). We propose that the fast singlet fission in crystals that have been studied so far is a consequence of adequate direct coupling of the S_1 state to the $^1(TT)$ state through a matrix element of the two-electron part of the Hamiltonian (eq 12), and that this element is significantly smaller in the linearly linked covalent dimers, the only ones studied so far (a computational estimate for a model chromophore suggests a difference of 2 or 3 orders of magnitude). Because it enters into the rate expression in second power, even a small drop in size will have a large effect. In the linearly linked dimers, singlet fission then has to rely on the mediation of the interaction of the S_1 state with the $^1(TT)$ state by charge-transfer configurations, using both the one- and two-electron parts of the Hamiltonian. In linearly linked dimers, this mediation suffers from the relatively high energy of charge-transfer configurations in nonpolar media, related to fairly distant charge separation compared to stacked dimers. In polarizable media, the energy of the charge-transfer configurations will be reduced and the mediated mechanism becomes more plausible. In a sufficiently polar solvent, the energy required for the charge-transfer state can become

favorable enough for the charge-transfer state to become a minimum in the lowest excited singlet surface and to become observable as a real intermediate. Such an intermediate in what has become a two-step singlet fission has been observed, but the overall triplet yield was again small.

We realize that this rationalization is based on the very crude model described in section 2.2.2 and that a more explicit treatment of overlap, expected to intertwine the direct and mediated mechanisms, is badly needed. It is also true that many other differences between the linearly linked covalent dimers and the neat solids could play a role. These could be factors such as a different degree of singlet excitation delocalization, with its effect on the energies of virtual or real intermediate singlet states and on Franck−Condon factors (otherwise viewed, on potential energy barriers between starting and final geometries). Interactions other than those represented in eq 6, such as the spin dipole−dipole coupling tensor or the energy splitting among the singlet, triplet, and quintet sublevels of the double triplet state, could be quite different in the solids and the dimers. Hyperfine interactions with nuclear magnetic moments are also different in the two cases, since they are averaged out in a crystal by exciton motion, and they need not be in a covalent dimer. However, this is a weak effect and not likely to be important.

With regard to ultimate applicability of singlet fission to solar cells, the situation can be summarized as follows. Considerable advances have been made in understanding how to design optimal chromophores (type IIB, isoergic or slightly exoergic singlet fission, and T_2 above S_1). High triplet yields in crystals have been achieved and nothing fundamental seems to stand in the way of the use of such chromophores as neat solids, e.g., nanocrystals, if they happen to have a favorable crystal structure. In contrast, the use of the same chromophores in the form of covalent dimers, which offer the advantage of better controlled structural design, currently suffers from very low triplet yields.

Although we consider our explanation of the difference between neat solids and covalent dimers quite plausible, a definitive understanding of the difference in efficiency is lacking, and finding its origin is the most immediate problem to solve if covalent dimers are to find use in singlet fission based sensitized solar cells. The design, synthesis, and examination of suitable slip-stacked dimers, and an improvement of the theoretical model, seem to represent a logical path forward.

The most serious long-term problem is likely to lie elsewhere and has received almost no attention so far. Assuming that high yields of triplet can be obtained in a suitably designed dimer, oligomer, aggregate, or nanocrystal, how will one make sure that these triplets can be utilized independently, such that each one leads to a charge-separation event?

8. Acknowledgments

This project was supported by the U.S. Department of Energy, DE-FG36-08GO18017. M.S. was supported by the Hydrogen Fuel Initiative program of the U.S. Department of Energy, Office of Basic Energy Sciences, Division of Chemical Sciences, Geosciences, and Biosciences, Solar Photochemistry Program. The authors are grateful to Professors Mark Ratner and Michael Tauber and to Dr. Justin Johnson for a critical reading of the manuscript and valuable comments, to Professors Michael Tauber and Christopher Bardeen for providing preprints, and to Dr. Zdeněk Havlas and Mr. Eric Buchanan for calculations on the quintet state of **3**.

9. References

(1) Swenberg, C. E.; Geacintov, N. E. *Org. Mol. Photophysics* **1973**, *18*, 489.
(2) Pope, M.; Swenberg, C. E. *Electronic Processes in Organic Crystals and Polymers*, 2nd ed.; Oxford University Press: Oxford, U.K., 1999; pp 134−191.
(3) Ronda, C. *J. Lumin.* **2002**, *100*, 301.
(4) Wegh, R. T.; Donker, H.; Oskam, K. D.; Meijerink, A. *Science* **1999**, *283*, 663.
(5) Vergeer, P.; Vlugt, T. J. H.; Kox, M. H. F.; den Hertog, M. I.; van der Eerden, J. P. J. M.; Meijerink, A. *Phys. Rev. B* **2005**, *71*, 014119.
(6) Nozik, A.; Beard, M.; Luther, J.; Johnson, J.; Law, M.; Ellingson, R. J. *Chem. Rev.* **2010**, *110*, DOI: http://dx.doi.org/10.1021/cr900289f (in this issue).
(7) Shabaev, A.; Efros, Al. L.; Nozik, A. J. *Nano Lett.* **2006**, *6*, 2856.
(8) Periasamy, N.; Santhanam, K. S. V. *Chem. Phys. Lett.* **1977**, *51*, 442.
(9) Schulten, K.; Karplus, M. *Chem. Phys. Lett.* **1972**, *14*, 305.
(10) Dunning, T. H., Jr.; Hosteny, R. P.; Shavitt, I. *J. Am. Chem. Soc.* **1973**, *95*, 5067.
(11) Hosteny, R. P.; Dunning, T. H.; Gilman, R. R.; Pipano, A.; Shavitt, I. *J. Chem. Phys.* **1975**, *62*, 4764.
(12) Singh, S.; Jones, W. J.; Siebrand, W.; Stoicheff, B. P.; Schneider, W. G. *J. Chem. Phys.* **1965**, *42*, 330.
(13) Swenberg, C. E.; Stacy, W. T. *Chem. Phys. Lett.* **1968**, *2*, 327.
(14) Geacintov, N.; Pope, M.; Vogel, F. E., III. *Phys. Rev. Lett.* **1969**, *22*, 593.
(15) Merrifield, R. E.; Avakian, P.; Groff, R. P. *Chem. Phys. Lett.* **1969**, *3*, 386.
(16) Merrifield, R. E. *J. Chem. Phys.* **1968**, *48*, 4318.
(17) Johnson, R. C.; Merrifield, R. E. *Phys. Rev. B* **1970**, *1*, 896.
(18) Suna, A. *Phys. Rev. B* **1970**, *1*, 1716.
(19) Merrifield, R. E. *Pure Appl. Chem.* **1971**, *27*, 481.
(20) Klein, G.; Voltz, R. *Int. J. Radiat. Phys. Chem* **1975**, *7*, 155.
(21) Rademaker, H.; Hoff, A. J.; Van Grondelle, R.; Duysens, L. N. M. *Biochim. Biophys. Acta, Bioenerg.* **1980**, *592*, 240.
(22) Austin, R. H.; Baker, G. L.; Etemad, S.; Thompson, R. *J. Chem. Phys.* **1989**, *90*, 6642.
(23) Nozik, A. J.; Ellingson, R. J.; Micic, O. I.; Blackburn, J. L.; Yu, P.; Murphy, J. E.; Beard, M. C.; Rumbles, G. Proceedings of the 27th DOE Solar Photochemistry Research Conference, Airline Conference Center, Warrenton, VA, June 6−9, 2004; pp 63−66; Available on line: http://www.sc.doe.gov/BES/chm/Publications/Contractors%20Meetings/27th_DOE_Solar_Photochemistry_crop.pdf.
(24) Michl, J.; Chen, X.; Rana, G.; Popović, D. B.; Downing, J.; Nozik, A. J.; Johnson, J. C.; Ratner, M. A.; Paci, I. *Book of Abstracts, DOE Solar Program Review Meetings*, Denver, CO, October 24−28, 2004; U.S. Department of Energy: Washington, DC, 2004; p 5.
(25) Hanna, M. C.; Nozik, A. J. *J. Appl. Phys.* **2006**, *100*, 074510/1.
(26) Shockley, W.; Queisser, H. J. *J. Appl. Phys.* **1961**, *32*, 510.
(27) Ohkita, H.; Cook, S.; Astuti, Y.; Duffy, W.; Tierney, S.; Zhang, W.; Heeney, M.; McCulloch, I.; Nelson, J.; Bradley, D. D. C.; Durrant, J. R. *J. Am. Chem. Soc.* **2008**, *130*, 3030.
(28) O'Regan, B.; Grätzel, M. *Nature* **1991**, *353*, 737.
(29) Grätzel, M. *Nature* **2001**, *414*, 338.
(30) Paci, I.; Johnson, J. C.; Chen, X.; Rana, G.; Popović, D.; David, D. E.; Nozik, A. J.; Ratner, M. A.; Michl, J. *J. Am. Chem. Soc.* **2006**, *128*, 16546.
(31) Greyson, E. C.; Stepp, B. R.; Chen, X.; Schwerin, A. F.; Paci, I.; Smith, M. B.; Akdag, A.; Johnson, J. C.; Nozik, A. J.; Michl, J.; Ratner, M. A. *J. Phys. Chem. B* published online Dec. 21, 2009, http://dx.doi.org/10.1021/jp909002d.
(32) Johnson, J. C.; Nozik, A. J.; Michl, J. *J. Am. Chem. Soc.* in press.
(33) Greyson, E. C.; Vura-Weis, J.; Michl, J.; Ratner, M. A. *J. Phys. Chem. B.*, published online Feb. 25, 2010, http://dx.doi.org/10.1021/jp907392q.
(34) Merrifield, R. E.; Avakian, P.; Groff, R. P. *Chem. Phys. Lett.* **1969**, *3*, 155.
(35) Bouchriha, H.; Ern, V.; Fave, J. L.; Guthmann, C.; Schott, M. *Phys. Rev. B* **1978**, *18*, 525.
(36) Berk, N. F. *Phys. Rev. B* **1978**, *18*, 4535.
(37) Klein, G. *Chem. Phys. Lett.* **1978**, *57*, 202.
(38) Chabr, M.; Williams, D. F. *Phys. Rev. B* **1977**, *16*, 1685.
(39) Moller, W. M.; Pope, M. *J. Chem. Phys.* **1973**, *59*, 2760.
(40) Zimmerman, P.; Zhang, Z.; Musgrave, C. *Nature Chem.* **2010**, *2*, 648.
(41) Englman, R.; Jortner, J. *Mol. Phys.* **1970**, *18*, 145.
(42) Singh, J. *J. Phys. Chem. Solids* **1978**, *39*, 1207.

(43) Streitwieser, A. *Molecular Orbital Theory for Organic Chemists*, 1st ed.; John Wiley & Sons Inc.: New York, 1961.
(44) Pariser, R.; Parr, R. G. *J. Chem. Phys.* **1953**, *21*, 466.
(45) Pople, J. A. *Trans. Faraday Soc.* **1953**, *49*, 1375.
(46) Coulson, C. A.; Rushbrooke, G. S. *Proc. Cambridge Philos. Soc.* **1940**, *36*, 193.
(47) Pariser, R. *J. Chem. Phys.* **1956**, *24*, 250.
(48) Salem, L.; Rowland, C. *Angew. Chem., Int. Ed. Engl.* **1972**, *11*, 92.
(49) Borden, W. T. In *Diradicals*; Borden, W. T., Ed.; Wiley-Interscience: New York, 1982.
(50) Michl, J. *Mol. Photochem.* **1972**, *4*, 257.
(51) Bonačić-Koutecký, V.; Koutecký, J.; Michl, J. *Angew. Chem., Int. Ed.* **1987**, *26*, 170.
(52) Borden, W. T.; Davidson, E. R. *J. Am. Chem. Soc.* **1977**, *99*, 4587.
(53) Borden, W. T. In *Magnetic Properties of Organic Materials*; Lahti, P. M., Ed.; Marcel Dekker: New York, 1999; pp 61−102.
(54) Viehe, H. G.; Janoušek, Z.; Merenyi, R.; Stella, L. *Acc. Chem. Res.* **1985**, *18*, 148.
(55) Seixas de Melo, J. S. S.; Burrows, H. D.; Serpa, C.; Arnaut, L. G. *Angew. Chem., Int. Ed.* **2007**, *46*, 2094.
(56) Seixas de Melo, J. S.; Rondao, R.; Burrows, H. D.; Melo, M. J.; Navaratnam, S.; Edge, R.; Voss, G. *ChemPhysChem* **2006**, *7*, 2303.
(57) Trlifaj, M. *Czech J. Phys. B* **1972**, *22*, 832.
(58) Král, K. *Czech J. Phys. B* **1972**, *22*, 566.
(59) Förster, T. In *Modern Quantum Chemistry*; Sinanoglu, O., Ed.; Academic Press: New York, 1965; Vol. 3.
(60) Dexter, D. L. *J. Chem. Phys.* **1953**, *21*, 836.
(61) Jortner, J.; Rice, S. A.; Katz, J. L.; Choi, S.-I. *J. Chem. Phys.* **1965**, *42*, 309.
(62) Scholes, G. D.; Harcourt, R. D. *J. Chem. Phys.* **1996**, *104*, 5054.
(63) Platt, J. R. *J. Chem. Phys.* **1949**, *17*, 484.
(64) Moffitt, W. *J. Chem. Phys.* **1954**, *22*, 1820.
(65) Fleischhauer, J.; Michl, J. *J. Phys. Chem. A* **2000**, *104*, 7776.
(66) Fleischhauer, J.; Höweler, U.; Spanget-Larsen, J.; Raabe, G.; Michl, J. *J. Phys. Chem. A* **2004**, *108*, 3225.
(67) Allinger, N. L.; Tai, J. C. *J. Am. Chem. Soc.* **1965**, *87*, 2081.
(68) Koutecky, J. *J. Chem. Phys.* **1967**, *47*, 1501.
(69) Buenker, R. J.; Whitten, J. C. *J. Chem. Phys.* **1968**, *49*, 5381.
(70) Van der Lugt, W. Th. A. M.; Oosterhoff, L. J. *J. Am. Chem. Soc.* **1969**, *91*, 6042.
(71) Hudson, B. S.; Kohler, B. E. *Chem. Phys. Lett.* **1972**, *14*, 299.
(72) Frölich, W.; Dewey, H. J.; Deger, H.; Dick, B.; Klingensmith, K. A.; Püttmann, W.; Vogel, E.; Hohlneicher, G.; Michl, J. *J. Am. Chem. Soc.* **1983**, *105*, 6211.
(73) Hummer, K.; Ambrosch-Draxl, C. *Phys. Rev. B* **2005**, *71*, 081202.
(74) Schuster, R.; Knupfer, M.; Berger, H. *Phys. Rev. Lett.* **2007**, *98*, 037402.
(75) Tiago, M. L.; Northrup, J. E.; Louie, S. G. *Phys. Rev. B* **2003**, *67*, 115212.
(76) Marciniak, H.; Fiebig, M.; Huth, M.; Schiefer, S.; Nickel, B.; Selmaier, F.; Lochbrunner, S. *Phys. Rev. Lett.* **2007**, *99*, 176402.
(77) Marciniak, H.; Pugliesi, I.; Nickel, B.; Lochbrunner, S. *Phys. Rev. B* **2009**, *79*, 235318.
(78) Groff, R. P.; Avakian, P.; Merrifield, R. E. *Phys. Rev. B* **1970**, *1*, 815.
(79) Havlas, Z.; Michl, J. Unpublished calculations.
(80) Takeda, Y.; Katoh, R.; Kobayashi, H.; Kotani, M. *J. Electron Spectrosc. Relat. Phenom.* **1996**, *78*, 423.
(81) Schwerin, A. F.; Johnson, J. C.; Smith, M. B.; Sreearunothai, P.; Popović, D.; Černý, J.; Havlas, Z.; Paci, I.; Akdag, A.; MacLeod, M. K.; Chen, X.; David, D. E.; Ratner, M. A.; Miller, J. R.; Nozik, A. J.; Michl, J. *J. Phys. Chem. A* **2010**, *114*, 1457.
(82) Michl, J.; Nozik, A. J.; Chen, X.; Johnson, J. C.; Rana, G.; Akdag, A.; Schwerin, A. F. *Proc. SPIE Conf.* **2007**, *6656*, 66560E.
(83) Yarmus, L.; Rosenthal, J.; Chopp, M. *Chem. Phys. Lett.* **1972**, *16*, 477.
(84) Swenberg, C. E.; Van Metter, R.; Ratner, M. *Chem. Phys. Lett.* **1972**, *16*, 482.
(85) Bouchriha, H.; Ern, V.; Fave, J. L.; Guthmann, C.; Schott, M. *J. Phys. (Paris)* **1978**, *39*, 257.
(86) Johnson, J. C.; Akdag, A.; Chen, X.; Schwerin, A. F.; Paci, I.; Smith, M. B.; Ratner, M. A.; Nozik, A. J.; Michl, J. Unpublished results.
(87) Groff, R. P.; Merrifield, R. E.; Avakian, P. *Chem. Phys. Lett.* **1970**, *5*, 168.
(88) Frankevich, E. L.; Lesin, V. I.; Pristupa, A. I. *Chem. Phys. Lett.* **1978**, *58*, 127.
(89) Monge, J. L.; Mejatty, M.; Ern, V.; Bouchriha, H. *J. Phys. (Paris)* **1986**, *47*, 659.
(90) Monge, J. L.; Mejatty, M.; Ern, V.; Bouchriha, H. *J. Phys. (Paris)* **1988**, *49*, 643.
(91) Helfrich, W. *Phys. Rev. Lett.* **1966**, *16*, 401.
(92) Simpson, G. A.; Castellanos, J.; Cobas, A.; Weisz, S. Z. *Mol. Cryst.* **1968**, *5*, 165.
(93) Mehl, W. *Solid State Commun.* **1968**, *6*, 549.
(94) Levinson, J.; Weisz, S. Z.; Cobas, A.; Rolon, A. *J. Chem. Phys.* **1970**, *52*, 2794.
(95) Frankevich, E. L.; Sokolik, I. A. *Solid State Commun.* **1970**, *8*, 251.
(96) Ern, V.; McGhie, A. R. *Mol. Cryst. Liq. Cryst.* **1971**, *15*, 277.
(97) Ern, V.; Merrifield, R. E. *Phys. Rev. Lett.* **1968**, *21*, 609.
(98) Geacintov, N. E.; Pope, M.; Fox, S. J. *J. Phys. Chem. Solids* **1970**, *31*, 1375.
(99) Ern, V.; Bouchriha, H.; Fourny, J.; Delacote, G. *Solid State Commun.* **1971**, *9*, 1201.
(100) Chabr, M.; Wild, U. P.; Fuenfschilling, J.; Zschokke-Graenacher, I. *Chem. Phys.* **1981**, *57*, 425.
(101) Fuenfschilling, J.; Zschokke-Graenacher, I.; Canonica, S.; Wild, U. P. *Helv. Phys. Acta* **1985**, *58*, 347.
(102) Klein, G.; Voltz, R.; Schott, M. *Chem. Phys. Lett.* **1973**, *19*, 391.
(103) Tomkiewicz, Y.; Groff, R. P.; Avakian, P. *J. Chem. Phys.* **1971**, *54*, 4504.
(104) Vaubel, G.; Baessler, H. *Mol. Cryst. Liq. Cryst.* **1971**, *15*, 15.
(105) Kalinowski, J.; Jankowiak, R.; Baessler, H. *J. Lumin.* **1981**, *22*, 397.
(106) Sebastian, L.; Weiser, G.; Bässler, H. *Chem. Phys.* **1981**, *61*, 125.
(107) Geacintov, N. E.; Burgos, J.; Pope, M.; Strom, C. *Chem. Phys. Lett.* **1971**, *11*, 504.
(108) Frankevich, E. L.; Chaban, A. N.; Trebel, M. M.; Von Schuetz, J. U.; Wolf, H. C. *Chem. Phys. Lett.* **1991**, *177*, 283.
(109) Agostini, G.; Corvaja, C.; Giacometti, G.; Pasimeni, L. *Chem. Phys.* **1993**, *173*, 177.
(110) Wang, C.; Tauber, M. J. *J. Am. Chem. Soc.* **2010**, *132*, 13988.
(111) Kraabel, B.; Hulin, D.; Aslangul, C.; Lapersonne-Meyer, C.; Schott, M. *Chem. Phys.* **1998**, *227*, 83.
(112) Wohlgenannt, M.; Graupner, W.; Österbacka, R.; Leising, G.; Comoretto, D.; Vardeny, Z. V. *Synth. Met.* **1999**, *101*, 267.
(113) Comoretto, D.; Moggio, I.; Cuniberti, C.; Dellepiane, G.; Borghesi, A.; Lanzani, G.; Stagira, S.; Nisoli, M. *Proc. SPIE Conf.* **1997**, *3145*, 352.
(114) Wohlgenannt, M.; Graupner, W.; Leising, G.; Vardeny, Z. V. *Phys. Rev. Lett.* **1999**, *82*, 3344.
(115) Wohlgenannt, M.; Graupner, W.; Leising, G.; Vardeny, Z. V. *Phys. Rev. B* **1999**, *60*, 5321.
(116) Österbacka, R.; Wohlgenannt, M.; Chinn, D.; Vardeny, Z. V. *Phys. Rev. B* **1999**, *60*, R11253.
(117) Österbacka, R.; Wohlgenannt, M.; Shkunov, M.; Chinn, D.; Vardeny, Z. V. *J. Chem. Phys.* **2003**, *118*, 8905.
(118) Katoh, R.; Kotani, M. *Chem. Phys. Lett.* **1992**, *196*, 108.
(119) Von Burg, K.; Zschokke-Graenacher, I. *J. Chem. Phys.* **1979**, *70*, 3807.
(120) Burdett, J. J.; Müller, A. M.; Gosztola, D.; Bardeen, C. J. *J. Chem. Phys.* **2010**, *133*, 144506.
(121) Watanabe, S.; Furube, A.; Katoh, R. *J. Phys. Chem. A* **2006**, *110*, 10173.
(122) Gradinaru, C. C.; Kennis, J. T.; Papagiannakis, E.; van Stokkum, I. H.; Cogdell, R. J.; Fleming, G. R.; Niederman, R. A.; van Grondelle, R. *Proc. Natl. Acad. Sci. U.S.A.* **2001**, *98*, 2364.
(123) Kingma, H.; Van Grondelle, R.; Duysens, L. N. M. *Biochim. Biophys. Acta* **1985**, *808*, 383.
(124) Papagiannakis, E.; Das, S. K.; Gall, A.; Van Stokkum, I. H. M.; Robert, B.; VanGrondelle, R.; Frank, H. A.; Kennis, J. T. M. *J. Phys. Chem. B* **2003**, *107*, 5642.
(125) Jundt, C.; Klein, G.; Le Moigne, J. *Chem. Phys. Lett.* **1993**, *203*, 37.
(126) Müller, A. M.; Avlasevich, Y. S.; Muellen, K.; Bardeen, C. J. *Chem. Phys. Lett.* **2006**, *421*, 518.
(127) Müller, A. M.; Avlasevich, Y. S.; Schoeller, W. W.; Muellen, K.; Bardeen, C. J. *J. Am. Chem. Soc.* **2007**, *129*, 14240.
(128) Nijegorodov, N.; Ramachandran, V.; Winkoun, D. P. *Spectrochim. Acta, Part A* **1997**, *53*, 1813.
(129) Wolf, H. C. *Solid State Phys.* **1959**, *9*, 1.
(130) Avakian, P.; Abramson, E.; Kepler, R. G.; Caris, J. C. *J. Chem. Phys.* **1963**, *39*, 1127.
(131) Wright, G. T. *Proc. Phys. Soc.* **1955**, *B68*, 241.
(132) Fuenfschilling, J.; Von Burg, K.; Zschokke-Graenacher, I. *Chem. Phys. Lett.* **1978**, *55*, 344.
(133) Klein, G. *Chem. Phys. Lett.* **1983**, *97*, 114.
(134) Klein, G.; Voltz, R.; Schott, M. *Chem. Phys. Lett.* **1972**, *16*, 340.
(135) Martin, P.; Klein, J.; Voltz, R. *Phys. Scr.* **1987**, *35*, 575.
(136) Arnold, S. *J. Chem. Phys.* **1974**, *61*, 431.
(137) Swenberg, C. E.; Ratner, M. A.; Geacintov, N. E. *J. Chem. Phys.* **1974**, *60*, 2152.
(138) Albrecht, W. G.; Coufal, H.; Haberkorn, R.; Michel-Beyerle, M. E. *Phys. Status Solidi B* **1978**, *89*, 261.
(139) Schwob, H. P.; Williams, D. F. *Chem. Phys. Lett.* **1972**, *13*, 581.
(140) Schwob, H. P.; Williams, D. F. *J. Chem. Phys.* **1973**, *58*, 1542.
(141) Fuchs, C.; Klein, J.; Voltz, R. *Radiat. Phys. Chem.* **1983**, *21*, 67.
(142) Klein, J.; Martin, P.; Voltz, R. *J. Lumin.* **1981**, *24*−*25*, 99.
(143) Alfano, R. R.; Shapiro, S. L.; Pope, M. *Opt. Commun.* **1973**, *9*, 388.

(144) Pope, M.; Geacintov, N.; Vogel, F. *Mol. Cryst. Liq. Cryst.* **1969**, *6*, 83.
(145) Smith, A. W.; Weiss, C. *Chem. Phys. Lett.* **1972**, *14*, 507.
(146) Fleming, G. R.; Millar, D. P.; Morris, G. C.; Morris, J. M.; Robinson, G. W. *Aust. J. Chem.* **1977**, *30*, 2353.
(147) Thorsmølle, V. K.; Averitt, R. D.; Demsar, J.; Smith, D. L.; Tretiak, S.; Martin, R. L.; Chi, X.; Crone, B. K.; Ramirez, A. P.; Taylor, A. J. *Phys. Rev. Lett.* **2009**, *102*, 017401.
(148) Arnold, S.; Alfano, R. R.; Pope, M.; Yu, W.; Ho, P.; Selsby, R.; Tharrats, J.; Swenberg, C. E. *J. Chem. Phys.* **1976**, *64*, 5104.
(149) Johnson, J. C.; Reilly, T. H.; Kanarr, A. C.; van de Lagemaat, J. *J. Phys. Chem. C* **2009**, *113*, 6871.
(150) Jundt, C.; Klein, G.; Sipp, B.; Le Moigne, J.; Joucla, M.; Villaeys, A. A. *Chem. Phys. Lett.* **1995**, *241*, 84.
(151) Rao, A.; Wilson, M. W. B.; Hodgkiss, J. M.; Albert-Seifried, S.; Bässler, H.; Friend, R. H. *J. Am. Chem. Soc.* **2010**, *132*, 12698.
(152) Kazzaz, A. A.; Zahlan, A. B. *J. Chem. Phys.* **1968**, *48*, 1242.
(153) Frolov, S. V.; Kloc, Ch.; Schön, J. H.; Batlogg, G. *Chem. Phys. Lett.* **2001**, *334*, 65.
(154) Thorsmølle, V. K.; Averitt, R. D.; Demsar, J.; Chi, X.; Smith, D. L.; Ramirez, A. P.; Taylor, A. J. *Springer Ser. Chem. Phys.* **2005**, *79*, 269.
(155) Landolt-Börnstein *Structure Data of Organic Crystals, Part b*; Group III, Vol. 5; Springer Verlag: Berlin, 1971.
(156) Ferguson, J. *J. Mol. Spectrosc.* **1959**, *3*, 177.
(157) Donnini, J. M.; Abetino, F. *C. R. Ser. B* **1968**, *266*, 1618.
(158) Bowen, E. J.; Mikiewicz, E.; Smith, F. W. *Proc. Phys. Soc.* **1949**, *A62*, 26.
(159) Report of the Investigation Committee on the Possibility of Scientific Misconduct in the Work of Hendrik Schön and Coauthors, September 2002, Lucent Technologies, distributed by the American Physical Society.
(160) Lopez-Delgado, R.; Miehe, J. A.; Sipp, B. *Opt. Commun.* **1976**, *19*, 79.
(161) Aladekomo, J. B.; Arnold, S.; Pope, M. *Phys. Status Solidi B* **1977**, *80*, 333.
(162) Vaubel, G.; Baessler, H. *Mol. Cryst. Liq. Cryst.* **1970**, *12*, 47.
(163) Barhoumi, T.; Romdhane, S.; Fredj, A. B.; Henia, F.; Bouchriha, H. *Eur. Phys. J. B* **2003**, *34*, 143.
(164) Kalinowski, J.; Godlewski, J. *Chem. Phys. Lett.* **1975**, *36*, 345.
(165) Geacintov, N. E.; Binder, M.; Swenberg, C. E.; Pope, M. *Phys. Rev. B* **1975**, *12*, 4113.
(166) Porter, G.; Windsor, M. W. *Proc. R. Soc. A* **1958**, *245*, 238.
(167) Pavlopoulos, T. G. *J. Chem. Phys.* **1972**, *56*, 227.
(168) Arnold, S.; Whitten, W. B. *J. Chem. Phys.* **1981**, *75*, 1166.
(169) Schlotter, P.; Kalinowski, J.; Bässler, H. *Phys. Status Solidi B* **1977**, *81*, 521.
(170) Whitten, W. B.; Arnold, S. *Phys. Status Solidi B* **1976**, *74*, 401.
(171) Grätzel, M. *Prog. Photovoltaics* **2000**, *8*, 171.
(172) Arnold, S.; Swenberg, C. E.; Pope, M. *J. Chem. Phys.* **1976**, *64*, 5115.
(173) Prasad, J.; Kopelman, R. *J. Lumin.* **1990**, *45*, 258.
(174) Gershenson, M. E.; Podzorov, V.; Morpurgo, A. F. *Rev. Modern Phys.* **2006**, *78*, 973.
(175) Forrest, S. R. *Nature* **2004**, *428*, 911.
(176) Lee, K. O.; Gan, T. T. *Chem. Phys. Lett.* **1977**, *51*, 120.
(177) Burgos, J.; Pope, M.; Swenberg, C. E.; Alfano, R. R. *Phys. Status Solidi B* **1977**, *83*, 249.
(178) Vilar, M. R.; Heyman, M.; Schott, M. *Chem. Phys. Lett.* **1983**, *94*, 522.
(179) Thorsmølle, V. K.; Averitt, R. D.; Demsar, J.; Smith, D. L.; Tretiak, S.; Martin, R. L.; Chi, X.; Crone, B. K.; Ramirez, A. P.; Taylor, A. J. *Physica B* **2009**, *404*, 3127.
(180) Lee, J.; Jadhav, P.; Baldo, M. A. *Appl. Phys. Lett.* **2009**, *95*, 033301.
(181) Kuhlman, T. S.; Kongsted, J.; Mikkelsen, K. V.; Moller, K. B.; Solling, T. I. *J. Am. Chem. Soc.* **2010**, *132*, 3431.
(182) Pabst, M.; Köhn, A. *J. Chem. Phys.* **2008**, *129*, 214101.
(183) Amirav, A.; Even, U.; Jortner, J. *Chem. Phys. Lett.* **1980**, *72*, 21.
(184) Griffiths, A. M.; Friedman, P. A. *J. Chem. Soc., Faraday Trans. 2* **1982**, *78*, 391.
(185) Heinecke, E.; Hartmann, D.; Müller, R.; Hese, A. *J. Chem. Phys.* **1998**, *109*, 906.
(186) Orlowski, T. E.; Zewail, A. H. *J. Chem. Phys.* **1979**, *70*, 1390.
(187) De Vries, H.; Wiersma, D. *J. Chem. Phys.* **1979**, *70*, 5807.
(188) Halasinski, T. M.; Hudgins, D. M.; Salama, F.; Allamandola, L. J.; Bally, T. *J. Phys. Chem. A* **2000**, *104*, 7484.
(189) Ashpole, C. W.; Formosinho, S. J. *J. Mol. Spectrosc.* **1974**, *53*, 489.
(190) Schmidt, W. *J. Chem. Phys.* **1977**, *66*, 828.
(191) Crocker, L.; Wang, T.; Kebarle, P. *J. Am. Chem. Soc.* **1993**, *115*, 7818.
(192) Michl, J. *J. Chem. Phys.* **1974**, *61*, 4270, and references therein.
(193) Hellner, C.; Lindqvist, L.; Roberge, P. C. *J. Chem. Soc., Faraday Trans. 2* **1972**, *68*, 1928.
(194) Johnson, J. C.; Smith, M. B., Michl, J. Unpublished results.
(195) Porter, G.; Wilkinson, F. *Proc. R. Soc. A* **1961**, *264*, 1.
(196) Mattheus, C. C.; Dros, A. B.; Baas, J.; Oostergetel, G. T.; Meetsma, A.; de Boer, J. L.; Palstra, T. T. M. *Synth. Met.* **2003**, *138*, 475.
(197) Mattheus, C. C.; Dros, A. B.; Baas, J.; Meetsma, A.; de Boer, J. L.; Palstra, T. T. M. *Acta Crystallogr., Sect. C* **2001**, *57*, 939.
(198) Schiefer, S.; Huth, M.; Dobrinevski, A.; Nickel, B. *J. Am. Chem. Soc.* **2007**, *129*, 10316.
(199) Hesse, R.; Hofberger, W.; Bässler, H. *Chem. Phys.* **1980**, *49*, 201.
(200) He, R.; Tassi, N. G.; Blanchet, G. B.; Pinczuk, A. *Appl. Phys. Lett.* **2005**, *87*, 103107.
(201) Zanker, V.; Preuss, J. *Z. Angew. Phys.* **1969**, *27*, 363.
(202) Ostroverkhova, O.; Cooke, D. G.; Shcherbyna, S.; Egerton, R. F.; Hegmann, F. A.; Tykwinski, R. R.; Anthony, J. E. *Phys. Rev. B* **2005**, *71*, 035204.
(203) Jarrett, C. P.; Brown, A. R.; Friend, R. H.; Harrison, M. G.; de Leeuw, D. M.; Herwig, P.; Müllen, K. *Synth. Met.* **1997**, *85*, 1403.
(204) Hwang, J.; Wan, A.; Kahn, A. *Mater. Sci. Eng. Rep.* **2009**, *64*, 1.
(205) Kanai, K.; Akaike, K.; Koyasu, K.; Sakai, K.; Nishi, T.; Kamizuru, Y.; Nishi, T.; Ouchi, Y.; Seki, K. *Appl. Phys A: Mater. Sci. Process.* **2009**, *95*, 309.
(206) Hong, Z. R.; Lessmann, R.; Maenning, B.; Huang, Q.; Harada, K.; Riede, M.; Leo, K. *J. Appl. Phys.* **2009**, *106*, 064511.
(207) Saeki, A.; Seki, S.; Tagawa, S. *J. Appl. Phys.* **2006**, *100*, 023703.
(208) Kalinowski, J.; Godlewski, J. *Chem. Phys. Lett.* **1974**, *25*, 499.
(209) Brocklehurst, B.; Hipkirk, A.; Munro, I. H.; Sparrow, R. *J. Phys. Chem.* **1991**, *95*, 2662.
(210) Zenz, C.; Cerullo, G.; Lanzani, G.; Graupner, W.; Meghdadi, F.; Leising, G.; De Silvestri, S. *Phys. Rev. B* **1999**, *59*, 14336.
(211) Corvaja, C.; Franco, L.; Pasimeni, L.; Toffoletti, A. *Appl. Magn. Reson.* **1992**, *3*, 797.
(212) Albrecht, W. G.; Michel-Beyerle, M. E.; Yakhot, V. *Chem. Phys.* **1978**, *35*, 193.
(213) Albrecht, W. G.; Michel-Beyerle, M. E.; Yakhot, V. *J. Lumin.* **1979**, *20*, 147.
(214) Katoh, R.; Kotani, M.; Hirata, Y.; Okada, T. *Chem. Phys. Lett.* **1997**, *264*, 631.
(215) Zhang, J. P.; Inaba, T.; Koyama, Y. *J. Mol. Struct.* **2001**, *598*, 65.
(216) Rondonuwu, F. S.; Watanabe, Y.; Fujii, R.; Koyama, Y. *Chem. Phys. Lett.* **2003**, *376*, 292.
(217) Papagiannakis, E.; Kennis, J. T. M.; van Stokkum, I. H. M.; Cogdell, R. J.; van Grondelle, R. *Proc. Natl. Acad. Sci. U.S.A.* **2002**, *99*, 6017.
(218) Kingma, H.; Van Grondelle, R.; Duysens, L. N. M. *Biochim. Biophys. Acta, Bioenerg.* **1985**, *808*, 363.
(219) Nuijs, A. M.; Van Grondelle, R.; Joppe, H. L. P.; Van Bochove, A. C.; Duysens, L. N. M. *Biochim. Biophys. Acta, Bioenerg.* **1985**, *810*, 94.
(220) Frank, H. A.; McGann, W. J.; Macknicki, J.; Felber, M. *Biochem. Biophys. Res. Commun.* **1982**, *106*, 1310.
(221) Hayashi, H.; Kolaczkowski, S. V.; Noguchi, T.; Blanchard, D.; Atkinson, G. H. *J. Am. Chem. Soc.* **1990**, *112*, 4664.
(222) Alster, J.; Polívka, T.; Arellano, J. B.; Chábera, P.; Vácha, F.; Pšenčík, J. *Chem. Phys.* **2010**, *373*, 90.
(223) Tavan, P.; Schulten, K. *Phys. Rev. B* **1987**, *36*, 4337.
(224) Dellepiane, G.; Comoretto, D.; Cuniberti, C. *J. Mol. Struct.* **2000**, *521*, 157.
(225) Lanzani, G.; Cerullo, G.; Zavelani-Rossi, M.; De Silvestri, S.; Comoretto, D.; Musso, G.; Dellepiane, G. *Phys. Rev. Lett.* **2001**, *87*, 187402.
(226) Toussaint, D. *J. Chem. Phys.* **1983**, *78*, 2642.
(227) Lanzani, G.; Stagira, S.; Cerullo, G.; De Silvestri, S.; Comoretto, D.; Moggio, I.; Cuniberti, C.; Musso, G. F.; Dellepiane, G. *Chem. Phys. Lett.* **1999**, *313*, 525.
(228) Antognazza, M. R.; Lüer, L.; Polli, D.; Christensen, R. L.; Schrock, R. R.; Lanzani, G.; Cerullo, G. *Chem. Phys.* **2010**, *373*, 115.
(229) Gurunathan, K.; Vadivel, A.; Marimuthu, R.; Mulik, U.; Amalnerkar, D. *Mater. Chem. Phys.* **1999**, *61*, 173.
(230) Wohlgenannt, M.; Graupner, W.; Leising, G.; Vardeny, Z. V. *Phys. Rev. Lett.* **1999**, *83*, 1272.
(231) Clarke, T. M.; Durrant, J. R. *Chem. Rev.* **2010**, *110*, published online Jan. 11, 2010, http://dx.doi.org/10.1021/cr900271s (in this issue).
(232) Barbarella, G.; Melucci, M.; Sotgiu, G. *Adv. Mater.* **2005**, *17*, 1581.
(233) Günes, S.; Neugebauer, H.; Sariciftci, N. S. *Chem. Rev.* **2007**, *107*, 1324.
(234) Guo, J.; Ohkita, H.; Benten, H.; Ito, S. *J. Am. Chem. Soc.* **2009**, *131*, 16869.
(235) Najafov, H.; Lee, B.; Zhou, Q.; Feldman, L. C.; Podzorov, V. *Nature Mater.* **2010**, *9*, 938.

CR1002613